

NOVEL GRAFTING MATERIALS FOR SINUS FLOOR ELEVATION IN THE SHEEP MODEL

Yevgeny (Eugene) Sheftel

A thesis submitted in partial fulfilment of requirements

for the degree of Doctor of Clinical Dentistry

University of Otago,

Dunedin, New Zealand

2017

Abstract

Introduction

Sinus floor elevation (SFE) may be required for implant placement in the severely resorbed posterior maxilla. Although often successful, autologous bone grafting requires a donor site and may lose substantial volume while remodelling. Bone replacement grafting (BRG) materials were developed to overcome these limitations. This study investigated three novel grafting materials: 1) equine collagen cone (CN), 2) equine collagen cone filled with biphasic calcium phosphate particles (CO), 3) deproteinized bovine bone particles coated with polylactic acid and poly ϵ - caprolactone copolymer (SB). These were compared with the most commonly-used bovine bone BRG, Geistlich Bio-Oss® (BO).

Methods

The extra-oral access sinus grafting model from Haas et al. (1998) was used in 11 cross-bred female sheep. Two experimental sites on each side of the animal were prepared. CN, CO, SB, BO were each placed through separate 10 mm access window in the antral wall, under the elevated Schneiderian membrane. BO sites were covered with a porcine collagen membrane (Geistlich Bio-Gide®), while for CO, SB, BO sites the equine collagen membrane (RESORBA PARASORB®) from the manufacturer of these experimental materials was used.

The animals were euthanised after 16 weeks. New bone, residual graft particles and connective tissue areas were measured on un-demineralised resin-embedded sections.

Results

One sheep did not survive the surgery. All sites in remaining ten sheep healed uneventfully. The CN and SB grafting materials resorbed completely and failed to form new bone. BO and CO particles were bridged by the new bone, the new bone fraction was 10% ($\pm 9\%$) for BO and 4% ($\pm 5\%$) for CO. The differences were not statistically significant.

Conclusions

CN and SB cannot be recommended for sinus grafting, based on this model.

BO and CO demonstrated comparable histologic and histomorphometric outcomes.

Acknowledgements

I would like to thank the people whose support made accomplishing this work possible.

My principal supervisor, Professor Warwick Duncan, has contributed his time, skills knowledge and experience to this project. I am grateful for his guidance throughout my research and clinical journey.

I would like to thank my co-supervisors, Associate Professor Jonathan Leichter and Associate Professor Patrick Schmidlin, for their input and guidance through all the stages of the research and thesis writing.

I'm grateful to Dave Matthews for his assistance with the animal surgery, Andrew McNaughton for teaching me how to take and process microscopic images, Andrew Gray for helping with statistical analysis of the results Paul Hibbert for proofreading this manuscript, and Frances Ruddiman, my classmate with whom I shared frustrations and who kindly agreed to be an independent examiner for the histologic images.

I would also like to acknowledge Resorba® and ITI companies for funding this study and supplying the tested materials. I would like to thank Geistlich Pharma® for supplying their products for our experiment.

My most sincere gratitude goes to my wife and true love, Yulia, who crossed the globe with me to arrive in New Zealand. While I disappeared in the laboratory or in the library, she ran our life all by herself with endless devotion, care and love.

Table of contents

Abstract	I
Acknowledgements.....	III
Table of contents	IV
List of tables.....	X
List of figures.....	XI
List of abbreviations	XII
Chapter 1. Introduction and literature review	1
1.1 The need for sinus grafting.....	2
1.1.1 Sinus pneumatization	2
1.1.2 Alveolar ridge resorption	3
1.1.3 Inadequate quality of maxillary bone.....	3
1.1.4 Occlusal loading and stress distribution	6
1.1.5 Conclusion	7
1.2 Biology of bone repair and graft incorporation.....	9
1.2.1 Bone regeneration and remodelling	9
1.2.2 Graft incorporation and remodelling	14
1.2.3 Speed of consolidation	18
1.2.4 Conclusion	19
1.3 Grafting materials	21
1.3.1 Autologous bone grafts.....	21
1.3.2 Allografts	21

1.3.3	Xenografts	22
1.3.4	Alloplasts	24
1.3.5	Implants placed in the augmented sinus floor	25
1.3.6	Conclusions	27
1.4	Sinus grafting procedures.....	28
1.4.1	Maxillary sinus anatomy and its relevance to sinus grafting	28
1.4.2	Clinical procedures and variations in practice	30
1.4.3	Alternatives to augmentation	34
1.4.4	Conclusions	35
1.5	Animal models	37
1.5.1	Small animals	38
1.5.2	Large animals	38
1.5.3	Conclusions	41
1.6	Analytical techniques for graft consolidation.....	42
1.6.1	Demineralized sections.....	42
1.6.2	Undemineralized sections	43
1.6.3	Measurements	43
1.6.4	Conclusions	44
1.7	Aims of study	45
1.7.1	Research question	45
Chapter 2.	Materials and Methods	46
2.1	Experimental animals.....	46
2.1.1	Inclusion criteria	46

2.1.2	Exclusion criteria	46
2.1.3	Pre-intervention management	47
2.1.4	Statistics and power	47
2.2	Grafting materials	48
2.2.1	IBI SmartBone® (Industrie Biomediche Insubri SA CH-6805 Mezzovico-Vira, Ticino, Switzerland)	48
2.2.2	PARASORB Cone® (Resorba Wundversorgung GmbH, Nürnberg, Germany)	49
2.2.3	PARASORB Cone Oss® (Resorba Wundversorgung GmbH, Nürnberg, Germany)	49
2.2.4	PARASORB Resodont® (Resorba Wundversorgung GmbH, Nürnberg, Germany)	50
2.2.5	Bio-Oss® (Geistlich Pharma AG, Wolhusen, Switzerland)	51
2.2.6	Bio-Gide® (Geistlich Pharma AG, Wolhusen, Switzerland)	52
2.2.7	Allocation and randomization	53
2.3	Surgical protocols	55
2.3.1	Surgical grafting procedure	55
2.3.2	Sacrifice	60
2.4	Histologic sections preparation	63
2.4.1	Trimming	63
2.4.2	Resin embedding	64
2.4.3	Slide preparation	66
2.4.4	Staining	66
2.5	Histomorphometric analysis	68

2.5.1	Imaging of histologic sections.....	68
2.5.2	Histomorphometric analysis.....	68
2.5.3	Statistical analysis	71
Chapter 3.	Results.....	72
3.1	Handling properties of grafting materials	72
3.1.1	PARASORB Cone®	72
3.1.2	PARASORB Cone Oss®.....	72
3.1.3	SmartBone®.....	72
3.1.4	PARASORB RESODONT® membrane vs Bio-Gide®	73
3.2	Post-operative healing.....	74
3.3	Descriptive histology.....	75
3.3.1	Dermis and mucosa.....	75
3.3.2	Access window	77
3.3.3	Augmented sites	79
3.3.4	Histological artefacts.....	88
3.3.5	Summary of findings in descriptive histology	91
3.4	Histomorphometric analysis	92
3.4.1	New bone, residual graft and connective tissue fractions.....	92
3.4.2	Augmentation height	95
3.4.3	Reliability and consistency.....	96
3.4.4	Summary of findings in histomorphometric analysis.....	99
Chapter 4.	Discussion	100
4.1	Introduction	100

4.2	Discussion of study outcomes.....	100
4.2.1	Summary of primary outcomes.....	100
4.2.2	Histologic picture	101
4.2.3	Histomorphometric outcomes.....	106
4.3	Discussion of the model and the method.....	108
4.3.1	Animal model.....	108
4.3.2	Surgical procedure.....	110
4.3.3	Sources of bias.....	113
4.3.4	Study limitations.....	114
4.4	Conclusions.....	117
4.5	Recommendations for future research.....	119
	References.....	121
	Appendices.....	137
	Appendix I.....	137
	Chemical reagents used	137
	Equipment used	137
	Materials and medications used in sheep surgery.....	138
	Appendix II	140
	Resin for embedding	140
	MMA Embedding protocol	141
	Staining with MacNeal’s Tetrachrome / Toluidine Blue solution	141
	Appendix III – Histologic slides.....	143
	Appendix IV – Histological data.....	147
	Histomorphometric data	147

Inter-examiner agreement	151
Appendix V – Radiograph of the resin-embedded specimens	154

List of tables

Table 1-1 Lekholm and Zarb classification	5
Table 1-2 Similarity between human and animal bone characteristics	38
Table 1-3 Sheep vs human bone healing	40
Table 2-1 Allocation of experimental materials.....	53
Table 2-2 Summary of grafting materials and membranes	59
Table 2-3 Use of membranes in surgical sites.....	60
Table 3-1 Schneiderian membrane perforations and outcomes.....	77
Table 3-2 Repair of surgical defect in the wall of the sinus	79
Table 3-3 Mean fractions of hard tissue in the ROI by treatment modality	92
Table 3-4 Mean fractions of hard tissue in the ROIs with more than zero new bone..	94
Table 3-5 Augmentation height	96
Table 3-6 Inter-examiner agreement	96
Table 3-7 Intra-examiner correlation.....	97
Table 3-8 Inter-examiner agreement, successfully augmented sites only	98
Table 3-9 Intra-examiner agreement, successfully augmented sites only	98

List of figures

Figure 2-1 SmartBone® (courtesy of IBI).....	48
Figure 2-2 PARASORB Cone Oss® and Cone®.....	50
Figure 2-3. PARASORB Resodont®. Courtesy of RESORBA®.....	51
Figure 2-4. Geistlich Bio-Oss® (A) and Bio-Gide® (B). Courtesy of Geistlich Pharma	51
Figure 2-5 Study design diagram	54
Figure 2-6 Surgical procedure.....	57
Figure 2-7 Exposure and cannulation of external carotid arteries	61
Figure 2-8 Trimming and labelling of specimens	63
Figure 2-9 Sectioning and staining of the specimens	65
Figure 2-10 Histomorphometric analysis.....	70
Figure 3-1 Schneiderian membrane and submucosa (CO site, specimen 409).....	76
Figure 3-2 Healing of the surgical access window (BO grafted site, specimen 419)....	78
Figure 3-3 Bio-Oss® augmented site (specimen 414).....	81
Figure 3-4 Cone Oss ® augmented site (specimen 419).....	83
Figure 3-5 SmartBone® augmented sites	84
Figure 3-6 SmartBone ® residual grafting material (specimen 418)	85
Figure 3-7 Cone® augmented sites	87
Figure 3-8 Histologic artefacts – stained debris. SB grafted site.....	89
Figure 3-9 Gas bubbles artefacts.....	90
Figure 3-10 Hard and soft tissue fractions for Bio-Oss® (BO) and Cone Oss® (CO)..	93
Figure 3-11 Tissue fractions for Bio-Oss® (BO) and Cone Oss® (CO) with more than zero new bone formation.....	95

List of abbreviations

ABG	Autologous bone graft
BCP	Biphasic calcium phosphate
BIC	Bone-to-implant contact
BMP	Bone morphogenic protein
BMU	Bone modelling unit
BO	Bio-Oss®
CN	Cone®
CO	Cone Oss®
CT	Connective tissue
DBBM	Deproteinised bovine bone mineral
DBM	Demineralized bone matrix
DFDBA	Demineralized freeze-dried bone allograft
ECM	Extra-cellular matrix
FDDBA	Freeze-dried bone allograft
H&E	Haematoxylin and eosin
HA	Hydroxyapatite
ISQ	Implant stability quotients
MS	Maxillary sinus
NB	New bone
NBF	Neutral buffered formalin
PCL	Polycaprolactone
PLA	Poly-lactic acid
PMN	Polymorphonuclear (cells)
PRP	Platelet-rich plasma

RAP	Regional activation phenomenon
RG	Residual graft
ROI	Region of interest
SB	SmartBone®
SD	Standard deviation
SFE	Sinus floor elevation
SM	Schneiderian membrane
TCP	Tricalcium phosphate

Chapter 1. Introduction and literature review

Implant-supported prostheses have revolutionized dentistry by providing a predictable and functional fixed treatment option for missing teeth. Implants require an adequate volume and quality of bone to be successfully placed and integrated. The posterior maxilla was demonstrated to be the most challenging site for implant survival¹⁻⁵. The reasons for reduced survival of implants in posterior maxilla may be related to the macroscopic and microscopic anatomy of posterior maxilla, namely: reduced quantity of bone due to maxillary sinus pneumatization and edentulous ridge resorption, inadequate quality of bone, and greater occlusal loading upon the implants. Sinus floor elevation (SFE) procedures were developed to overcome these challenges.

SFE are usually making use of grafting materials to guide bone repair and produce new living extra-skeletal bone in the site of future implant placement. Extensive body of research has been accumulated for different types of grafting materials and surgical techniques. New grafting materials are expected to be cheaper, more effective in guiding new bone formation or to have superior handling properties.

Histomorphometry is the gold standard to assess bone healing in the grafted sinus. The fractions of residual graft, new bone and soft tissue can only be reliably assessed by histomorphometry. Human and animal studies concerning the healing of graft materials within the maxillary sinus have been carried out using histomorphometric analysis⁶⁻⁸.

This study was designed to evaluate performance of three novel grafting materials against a positive control in a sheep model. The histologic and histomorphometric analysis of the results was done.

1.1 The need for sinus grafting

1.1.1 Sinus pneumatization

The maxillary sinus of an infant is occupied by crypts of developing teeth and has little “free” space. Sinus air space growth accompanies the eruption of maxillary teeth. At 12-13 years, the sinus floor is level with the nasal floor, and at the age of 20, after completion of tooth eruption, the sinus floor reaches an average of 5 mm inferior to the nasal floor⁹. Maxillary sinuses demonstrate remarkable variability in size and wall thickness¹⁰, yet in some individuals, “physiologic” pneumatization leaves the roots of maxillary teeth with nothing but lamina dura and a thin layer of mucosa within the sinus¹⁰. The reasons for the differences in pneumatization are poorly understood. Heredity¹¹, positive air pressure¹², pneumatizing drive of the mucus membrane¹², craniofacial configuration¹³, growth hormones¹³, and sinus surgery¹⁰ were identified as factors that may influence maxillary sinus pneumatization.

Multiple studies describe late recommencement of the pneumatization in adults that have lost posterior maxillary teeth¹⁴⁻¹⁷. This late pneumatization was related to “disuse atrophy” of supporting bone after posterior tooth loss^{15,16}. Wolff’s law¹⁸ is a hypothesis which is used to describe the mechanism behind the change. According to Wolff, the bone tissue will continuously adapt itself to withstand mechanical stress. Teeth in function conduct stress onto supporting bone which responds by maintaining sufficient volume and orientation of trabeculae. Frost (1994)¹⁹ has further developed Wolff’s hypothesis: below the specified threshold of stress, the bone tissue remodelling leads to a decrease in mass to adjust to lower function levels. Sinus pneumatization in edentulous sites can be an example of such re-adjustment.

Sharan and Madjar (2008)¹⁵ have inspected panoramic radiographs to measure post-extraction sinus pneumatization and found that on an average 1.8-2.2 mm of sinus floor

resorption is expected after the extraction of maxillary teeth. However, in some cases, almost all bone in the sinus floor is lost, leaving only a paper-thin bony shell which is unable to support implants^{15, 20, 21}.

1.1.2 Alveolar ridge resorption

The vertical dimension in the posterior maxillary area is lost not only to receding sinus floor but also to the resorbing alveolar ridge. The alveolar bone is functionally dependent on teeth and consists of bundle bone. Wolff's law that applies to the sinus floor can similarly be used for alveolar ridges. When the teeth are removed, the bundle bone is lost to remodelling. The alveolar ridge resorption occurs at a faster pace during the first 3-4 months after tooth extraction^{22, 23} and then slows significantly²⁴; however, the resorption may continue for a prolonged period of time.

The combination of sinus pneumatization and alveolar ridge resorption may lead to the insufficient bone quantity to support implants in the posterior maxilla. A minimum of 3-5 mm of vertical dimension was recommended to achieve primary implant stability²⁵⁻²⁷. However, Peleg et al. (2006) reported cumulative survival of 97.9% of 2,091 implants placed in 1-2 mm residual bone²⁸. These implants were placed concomitant with sinus grafting by a very experienced practitioner using strict placement protocol. The need for primary stability was addressed by the authors, who stated that "...initial stability was obtained by meticulous condensation of the particulated bone graft around the implants. This condensation was possible due to direct visualization of the entire grafted compartment. The wide window opening was essential"²⁸.




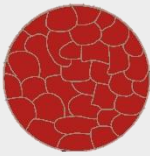
Thus, sinus grafting can be used to manage insufficient bone volume by expanding the vertical and horizontal dimensions of the supporting bone prior to or at the time of implant placement²⁹.

1.1.3 Inadequate quality of maxillary bone

While the volume of bone is essential to support an implant, the biomechanical properties of the recipient site play an important role as well³⁰.

Various classifications were developed to describe the biomechanical properties or bone quality of the recipient site³¹. The first classification of bone quality still in extensive use today was developed by Lekholm and Zarb in 1985³². The authors used radiography to describe the bone quality and quantity (Table 1-1). This classification was validated in multiple studies: for correlation with CT Hounsfield units³³⁻³⁵, for mineral content^{36, 37}, and for implant primary stability and osseointegration³⁷.

Table 1-1 Lekholm and Zarb classification

Bone type	Description	Illustration
Type I	Almost the entire bone is composed of homogenous compact bone	
Type II	Thick layer of compact bone surrounds a core of dense trabecular bone	
Type III	Thin layer of cortical bone surrounds a core of dense trabecular bone	
Type IV	A thin layer of cortical bone surrounding a core of low-density trabecular bone of poor strength.	

Adapted from Lekholm and Zarb (1985)³²

Lekholm and Zarb³² distinguished the types of bone by using Roman numerals, but some studies³⁶ refer to them using D (for density) and Arabic numerals, for example, Type I may be referenced as D1 bone quality and type IV – D4.

Multiple studies^{1, 30, 38, 39} reported higher chances of failure for the implants that are placed in poor-quality bone with the thin cortex and low-density trabeculae (Type IV bone). Histomorphometric and CT analysis showed that the posterior maxilla has a lower mineralized content, reduced trabecular thickness and density⁴⁰⁻⁴³. The poor quality of bone is thought to impact the survival rate of the implants placed in posterior maxilla, which is the lowest among all the oral implantation sites^{1, 38, 44, 45}.

While mineralized bone content in type IV quality natural bone has been demonstrated to be 28%⁴⁶, the mineralized bone content in grafted sites varied between 28.3% (grafted with CaCO₃) and 40.1% (grafted with autologous bone), or in Lekholm and Zarb's classification, type IV to type III bone quality³⁶.

Thus, after grafting, the bone quality remains poor or may improve only slightly. However, as the bone remodels around implants, the bone-to-implant contact can increase – figures of 60-80% have been reported^{47,48}. The remaining particles of the graft don't seem to affect bone-to-implant contact formation⁴⁹⁻⁵⁴.

1.1.4 Occlusal loading and stress distribution

Reduced quantity and quality of bone in posterior maxilla can be detrimental to both primary osseointegration of the implant and long-term survival under occlusal loading.

Post-insertion stability of the implant is required for osseointegration to occur. Cameron et al. (1973)⁵⁵ introduced the concept of threshold micromovement of the implant using porous Vitalium staples in an unstable osteotomy sites in. The researchers stated that displacements of 150 µm and more should be considered as excessive and will cause fibrous implant encapsulation. Hence, mechanical loading was thought to be a critical factor determining the long-term survival of implants^{5, 56}. In engineering terms, the implant acts as a bar elastically supported by the surrounding bone. According to finite element analysis, when the physical stresses exceed a certain physiologic threshold, the bone-implant interface could fail⁵⁷. Clinically, the excessive local stress around an implant was associated with marginal bone loss and histologically – with pressure necrosis of the host bone and microfractures of trabeculae^{58, 59}. Some earlier studies stated that overloading an implant may result in complete loss of osseointegration of implants, even after a long time of service^{5, 60}.

However, since the earlier days of dental implantology, a considerable body of evidence has accumulated⁶¹⁻⁶⁴, linking the peri-implant tissues' inflammation and progressive marginal bone loss that may lead to implant failure. Most bone loss around teeth (*periodontitis*) is regarded as a biofilm-mediated infection and, analogously, some researchers believe that bone loss around an implant also constitutes an infectious process (*peri-implantitis*)⁶⁵⁻⁶⁷. The term peri-implantitis has been firmly based in the theory and practice of implant therapy, albeit its clinical definition is still disputed^{62, 63, 68, 69}.

Stress applied to the implant is concentrated around its neck as demonstrated with mathematical models and finite element analysis^{70, 71}. However, in posterior maxilla the cortical plates can be very thin or non-existent, thus larger forces may be propagated to the apical areas⁷². In addition to that, the occlusal forces are increased five- to ten-fold in posterior regions of maxilla as opposed to anterior regions²⁹.

While unable to improve the bone quality, sinus grafting aims may improve stress distribution by providing a larger volume of bone to place longer and wider implants in positions more suitable for the prosthesis. Finite element analysis study has revealed that even though the maximum stress is applied to the cervical area of the implant, sinus grafting in the apical regions reduces intra-bony stress by 30%; displacements of the implant tip during loading can be reduced by up to 32%⁷³.

1.1.5 Conclusion

Insufficient bone volume is a frequent problem encountered in the rehabilitation of the edentulous posterior maxilla. The bone available for implant placement may be limited by pneumatization of the maxillary sinus, together with the loss of alveolar bone height. Posterior maxilla consists of sparsely trabeculated bone with mediocre mechanical properties and limited repair capacity. Increased occlusal forces are

applied to the posterior maxilla compared to the anterior portion, placing primary implant stability and initial osseointegration of the implants in posterior maxilla at risk.

While sinus grafting cannot improve the bone quality by a great margin³⁶, it can provide more bone volume to support implants. Systematic reviews of the relevant literature have demonstrated that the sinus floor augmentation procedure is highly successful and well-documented; the use of modern moderately-rough implants provides cumulative implant survival rate above 90% in the augmented sites ⁷⁴⁻⁷⁷.

1.2 Biology of bone repair and graft incorporation

The desired outcome for sinus grafting procedures is graft incorporation into and replacement by the vital bone while maintaining the volume. The process whereby the grafted material is incorporated into the surrounding natural bone has been described as *consolidation*. During graft consolidation, the host blood vessels sprout into the grafted area, and osteogenic cells form the new bone. This process is a variation of normal bone repair and remodelling. Certain properties of the grafting material can facilitate graft consolidation. Among these properties, osteoconduction, osteoinduction and osteogenesis are commonly cited⁷⁸.

1.2.1 Bone regeneration and remodelling

To accurately describe the graft consolidation in the sinus floor, the normal bone repair and remodelling process is to be explained. The bone forms and repairs via two principal routes: intra-membranous and endochondral.

1.2.1.1 Intramembranous and endochondral bone formation

When the word “bone” is used, it is important to distinguish whether it describes the bone as an organ (with specific location, anatomy, cartilage, marrow and periosteum) or as tissue type. Bones as organs develop embryonically using two distinct mechanisms:

- a) **The intramembranous bone formation** is mediated by the inner periosteal osteogenic layer with bone synthesized initially without the mediation of a cartilage phase. Bones of the skull are formed by the intramembranous mechanism.
- b) **The endochondral bone formation** describes the synthesis of bone on a mineralized cartilage scaffold after epiphyseal and physeal cartilage have

shaped and elongated the developing organ. Long bones (including ileum) are formed by the endochondral mechanism.

The repair of fractured or injured adult bones can also be intramembranous or endochondral. The subcutaneous demineralized bone matrix (DBM) grafts sourced from femoral bone (formed by endochondral ossification) induce endochondral ossification⁷⁹, while DBM sourced from calvarium (formed by intramembranous ossification) ossify by the intramembranous mechanism⁸⁰. The endochondral bone repair can also occur when the site is not mechanically stable⁸¹.

The difference in these mechanisms of bone formation may play a significant role when developing the experimental model. The rabbit femur and tibia have been widely used as the animal model in implantology⁸²⁻⁸⁴. However, the difference in bone formation and physiology may have an impact on the applicability of the results to intramembranous maxilla and mandible⁸⁵.

Autologous grafts retain the mechanisms of healing and repair of the bones they were harvested from^{80, 86}. The endochondral grafts (tibia, iliac crest) lost more volume postoperatively, compared to intra-membranous grafts (calvarium, intraoral sites)^{86, 87}.

1.2.1.2 Stages of bone repair

After an injury, the bone repair starts with blood clot formation and platelet aggregation. The platelets and endothelial cells produce cytokines, including TGF- β , vascular endothelial growth factor (VEGF), and platelet-derived growth factor (PDGF)⁸⁸. The cytokines set off a rigorously controlled multi-stage inflammatory response, during which the neutrophil, the macrophage and, finally, the lymphocyte-predominant cell populations migrate into the area, subdue the invading microorganisms, phagocytose the debris and induce bone repair⁸⁹.

Stimulated by angiogenic signal molecules, blood vessels sprout into granulated tissue. These signal molecules are released earlier from the platelets and later from osteogenic cells and macrophages⁹⁰. Hypoxia in the grafted area is by itself a potent stimulating factor for angiogenesis^{91, 92}.

After the vascularization of the repairing site, the osteogenic cells start to form new bone. The exact origin of osteogenic cells in maxillary bone repair is unknown. They may migrate via the blood supply or proliferate from locally present stem cells, or both⁹³⁻⁹⁶. The Schneiderian membrane (SM) may also contain osteoprogenitor cells: in a series of in-vitro and in-vivo studies in human subjects, Srouji et al. (2009,2010)^{97, 98} successfully retrieved osteoprogenitor cells from the sinus membrane samples. These cells produced histologically evident bone at ectopic sites following transplantation into mice. However, it's not clear whether sinus membrane-derived osteoprogenitor cells play a significant role in the new bone formation after sinus floor elevation. For example, after SFE and implant placement in monkeys, no new bone formed underneath SM around apical implant surfaces⁹⁹.

The formation of bone can be divided into three stages¹⁰⁰:

1. **Woven bone formation:** In an environment where no pre-existing bone (*intramembranous mechanism*) or cartilage matrix (*endochondral mechanism*) is present, undifferentiated mesenchymal cells differentiate into pre-osteoblasts and then to osteoblasts that secrete bone matrix in all directions in a random array. The disorganized osseous tissue that forms is called woven bone due to its characteristic histologic appearance.
2. **Adaptation of bone mass to load:** When a sufficient amount of woven bone has been synthesized to serve as a structural scaffold, osteoblasts array themselves in well-polarized fashion along the woven bone surface. Unlike the first stage, they start to secrete collagen fibrils only onto the pre-existing bone surface, not

circumferentially. The bone matrix that forms is organized in a parallel or lamellar orientation, and this type of bone is called lamellar bone. The lamellar bone resistance to stress is superior to that of the woven bone⁸⁹. The rate of lamellar bone deposition in humans is 1-1.5 $\mu\text{m}/\text{day}$ ¹⁰⁰.

3. **Adaptation of bone structure to load** (bone remodelling): During the third stage, after the lamellar bone is formed, the bone remodelling adapts the bone trabecular structure to stress. The remodelling is done by organized resorption and apposition in a conglomerate of cells, which Frost in his book named the basic multicellular unit (BMU)¹⁰¹. In BMU the cutting cone of osteoclasts advances with a speed of about 50 μm per day and is followed by a vascular loop, accompanied by perivascular osteoprogenitor cells¹⁰¹. About 100 μm behind the osteoclasts, the osteoblasts line up on the wall of the resorption canal and begin to deposit concentric layers of lamellar bone¹⁰¹. The unit of bone, formed by BMU, is called *osteon*.

1.2.1.3 Regulation of bone remodelling and repair

In the 1960s the prevalent concept of bone regulation was the metabolic one. A variety of metabolic factors, vitamins and hormones indeed influence the bone formation and remodelling. For example, the thyroid hormone, vitamin D, and calcitonin all serve as regulators¹⁰². This view, however, can't explain the adaptation to stress, a unique bone property. Harold Frost, in a series of publications, hypothesized that the adaptation to stress is the primary regulatory factor in bone formation, remodelling and resorption^{103, 104}. This hypothesis, which Frost named the 'Mechanostat Theory', explains that the mechanical load which is applied to the bone matrix and cells causes them to generate signals which they and other cells can respond to. The signalling depends on the load magnitude, and the stress thresholds for changes in signals are genetically determined. The key concept in bone adaptation to stress is the repair of the microfractures in

trabeculae by new osteons. Thus, the adaptation of the bone structure to load is regulated by the very load which is applied, according to the Mechanostat model. While the biological mechanism of this model is not entirely understood^{105, 106}, it offers a convenient framework to understand the bone repair, remodelling and graft consolidation.

The normal rate of bone remodelling wouldn't allow for the efficient bone regeneration. However, after the bone is wounded, the bone forming and remodelling processes experience a transient burst which may last for more than two years²⁹. This burst was named by Frost 'Regional Acceleration Phenomenon' (RAP)^{107, 108}. The increased rate of remodelling helps in volumetric bone regeneration and adapting the newly formed bone to stress via trabecular orientation¹⁰⁹.

1.2.1.4 Critical size defects

The bone repair process depends on the size of the defect and the stability of the wound. Smaller defects can repair by direct bridging with Haversian channels, while larger defects require more complex staged repair as described in the section 1.2.1.2. Defects which cannot be fully regenerated with bone, but instead are filled with fibrous connective tissue, are called *critical size defects*. The critical size varies between species and bone sites¹¹⁰. For the rat skull, the critical defect size was identified as 5 mm, while for the sheep, cranial defects were 22 mm¹¹¹.

The critical size defect models have been used extensively in the orthopaedic research of bone regenerative materials. The tested materials in orthopaedic research are required to prove their effectiveness by bringing the critical size defects to osseous healing¹¹². In sinus grafting, however, the role of grafting material is mostly the maintaining of space and providing the surface for the formation of the new *extra-skeletal* bone (explained in more detail in section 1.2.2). The size of the surgical access

window in a lateral approach for sinus grafting is usually less than 20 mm. The healing of the access window is not considered to be a primary outcome, therefore it is not assessed in depth; however, full healing was observed at 6 months in monkeys ¹¹³.

1.2.1.5 Osteogenesis in non-grafted sinus sites

The elevation of the Schneiderian membrane (SM) creates a space which is immediately filled by a blood clot. Experimental animal data¹¹³⁻¹¹⁶ and clinical reports in humans^{117, 118} have clearly demonstrated that new extra-skeletal bone formation occurred underneath the elevated SM without the use of a filler material.

However, without a space-maintaining device, the blood clot will quickly resorb, the elevated SM will collapse and no new bone formation will happen¹¹⁹. Implants serving as space-maintainers may fail to prevent the SM collapse^{120, 121}. Sinus grafting may offer a more predictable treatment modality if the grafting material poses no interference to normal formation of the new bone in the augmented site. Ideally, the grafting material will become incorporated and replaced by the recipient bone.

1.2.2 Graft incorporation and remodelling

Graft incorporation includes the in-growth of new vasculature (angiogenesis), the formation of woven bone-graft complex, and remodelling of the integrated graft material and surrounding bone by BMUs²⁹.

The graft is a foreign body. It can be encapsulated in the connective tissue, rather than incorporated into the bone of the recipient site. To be incorporated, the grafting material needs not only to be biocompatible (non-toxic to cells) but also to allow

adherence of osteogenic cells and bone deposition directly onto the surface of the grafting material.

1.2.2.1 Osteoconduction, osteoinduction, osteogenesis

Originally, the term *osteoconduction* was coined in orthopaedic literature and was not related to bone grafting materials but rather to various orthopaedic implants. For example, osteoconduction is not possible in certain materials such as copper and silver¹²², but well documented on titanium implants^{69, 78}. The difference between the materials lies in the ability of osteoblasts to adhere to their surface. Osteoblasts adhere to the grafting material not directly, but via proteins such as vitronectin, fibronectin and albumin that are adsorbed to the surface of the material from blood and extracellular matrix^{123, 124}. The graft-cell adhesion biochemistry is a complex and not entirely understood process, where surface topography, charge, wettability, pH and ionic composition of the graft all play a role¹²⁵.

The osteogenic cells are recruited to the site by biochemical factors. This recruitment process is sometimes called *osteoinduction*. The autologous bone grafts and demineralized bone grafts, such as DFDBA, are considered osteoinductive due to the presence of biochemical factors such as bone morphogenic proteins (BMPs). The surgical injury and normal bone repair produce sufficient amounts of osteoinductive factors to recruit previously undifferentiated bone cells⁷⁸. However, agents, such as BMPs and platelet-rich plasma (PRP), have been added to grafting materials in an attempt to enhance bone formation within grafts with variable success¹²⁶⁻¹²⁸. Several reviews concerning the use of osteoinductive factors¹²⁹⁻¹³¹ concluded that while demonstrating promising results in some studies, the addition of osteoinductive factors still lacks unequivocal evidence.

Osteoconduction and osteoinduction are sometimes used interchangeably to describe bone formation in the grafted area. It was indeed established that the topology of the surface of some grafting materials might induce osteogenic cell differentiation and proliferation, although the biological mechanism is not fully understood^{124, 132, 133}.

If the graft itself contains bone-forming cells which may produce new bone it may be argued that such a graft possesses *osteogenic* properties. It was established that some osteoprogenitor cells from autologous bone graft might survive the intraoperative manipulation and retain osteogenic potential^{134, 135}. The origin of osteogenic cells at the sites of bone regeneration is not entirely clear. In the seminal work on a rat model, Ray (1972)¹³⁵ demonstrated that autologous bone transplants might re-vascularize by anastomose creation to the blood vessels of the recipient bed as early as 2 days post-transplantation. This reperfusion doesn't prevent the necrosis of the existing osteocytes¹³⁶, but some osteogenic cells survive and retain their osteogenic potential¹³⁵. The surviving multipotential cells of the autologous graft and the migrating multipotential cells from the recipient site populate the necrotic marrow spaces; osteoblasts line the edges of the dead trabeculae and lay down a seam of osteoid, which eventually surrounds a central core of necrotic bone¹³⁷. As the graft incorporation and fracture repair involve recruitment of progenitor cells from the blood stream^{81, 138}, we may only speculate about the extent of the contribution of the surviving cells from the graft to the new bone formation and graft incorporation.

1.2.2.2 Graft incorporation into viable bone

1.2.2.2.1 Angiogenesis

The incorporation of the graft into the recipient bone starts on the day of the procedure and depends on sufficient blood supply¹³⁹. Bone is a metabolically active tissue supplied by an intrasosseous vasculature with osteocytes positioned no more than 200 μm from a capillary^{140, 141}. The hypoxic necrosis of the central part of the graft happens

to stem cell grafts on engineered scaffolds⁹⁰ as well as autologous bone transplants¹⁴². Driven by hypoxia and inflammation, the sprouting of new vessels starts within days from surgery^{92, 139}.

The vascularization of autologous grafts is different from the vascularization of non-vital xenografts or alloplasts. The non-vital xenografts and alloplasts simply become incorporated into the granular tissue which has abundant vasculature. Capillaries serve not only as oxygen and nutrient suppliers but also as the pathway and the promoter for the pluripotential osteogenic cells. Osteogenesis is thought to happen along the vascular structures of the tissue⁹².

The grafting material should possess interconnecting pores of sufficient size to allow for the ingrowth and interconnection of the capillary bed^{143, 144}. The porosity of the material is even more important for the ingrowth of bone. A pore size of 100 µm is often cited as a minimum requirement for bone ingrowth¹⁴⁵⁻¹⁴⁷. Some studies report that volume and rate of integration depend on the pore size^{148, 149}. Other researchers promote the importance of additional structural parameters, such as pore morphology, percent porosity, and pore connectivity^{150, 151}. The ideal porosity and the crystalline microstructure of the grafting material remain to be identified.

1.2.2.2.2 Osteogenesis

By stabilizing the blood clot and by providing a cell-adhesive osteoconductive surface, even the non-vital grafting material can guide new bone into a grafted area¹⁵². The osteoconduction by the grafting material may result in bone regeneration of a non-healing, critical size defect, when woven bone sprouts into the vascularized space between the particles of bone substitute^{153, 154}. As a result of graft incorporation, the particles of grafting material become connected by the newly formed bone⁷⁴. As bone-graft complex gains some structural durability, the stress which is applied to it can theoretically control the remodelling, according to Frost's Mechanostat theory¹⁰⁴.

A series of animal experiments have demonstrated that after sinus grafting, the new bone is more abundant near the bony walls of the sinus than on the 'far side' of the grafted area, in the proximity of the SM^{7, 155-157}. Some authors have used the term '*consolidation gradient*' to explain the differences¹⁵⁵. The consolidation gradient may suggest that after sinus grafting, osteogenic cells migrate from the existing bone wall and are guided by osteoconductive properties of the grafting material towards the SM.

1.2.2.3 Graft remodelling

Depending on the chemical and physical structure, the grafting material may degrade after the implantation. In general, two pathways exist for resorption of the material:

1. **Haversian remodelling:** Materials containing crystalline hydroxyapatite may be resorbed in the same manner as the bone, by osteoclasts. Histologically, osteoclastic resorption is characterised by the presence of multi-nuclear cells in lacunae on the surface of the material¹⁵⁸. Haversian remodelling results in creeping substitution by natural bone.
2. **Non-osteoclastic chemical breakdown:** This mechanism leads to loss of mineralized tissue in the grafted area. The chemical breakdown mechanism depends on the acidity of the environment, and the chemical composition and the porosity of the material^{159, 160}.

Ideal grafting material will be completely substituted by the natural bone while retaining the mineralized tissue volume. These appear to be contradictory demands: the materials which are easily replaced by bone tend to lose a significant portion of their volume¹⁶¹, while space-maintaining materials tend to remain indefinitely in the grafted area¹⁶².

1.2.3 Speed of consolidation

As in the normal bone repair, the sinus floor elevation (SFE) will activate the regional acceleration phenomenon (RAP) manifesting in rapid vascularization, bone-graft complex formation, and maturation of the grafted area¹⁶³. The graft maturation time is significant for implant treatment planning. The woven bone starts to form under elevated sinus as early as 4 days post-op¹⁶⁴. The initial speed of bone ingrowth into the graft may be as fast as 1 mm per week²⁹. However, calculations based on histomorphometric analysis of samples taken at four time-points from human grafted sinuses suggested the average rate of 1 mm bone ingrowth per month¹⁶⁵. A review of histological studies in humans¹⁶⁶ has concluded that mineralized bone volume changes insignificantly between 6 months and 12 months of healing. Kohal et al. (2015)¹⁶⁷ in a recent publication state that even after 3 months of healing, there is only minor addition of new bone.

In the systematic review of clinical outcomes⁷⁶, the healing periods ranged between 3-10 months after grafting, prior to implant placement, and up to 10 months after implant placement. The healing periods did not affect implant survival for any of the grafting material, which suggests that either: 1) Healing is by-and-large is finished by 3 months post-grafting or 2) Bone mineralization after 3 months is sufficient to support implant stability and osseointegration.

1.2.4 Conclusion

Grafting alters the natural repair of bone by stabilizing the blood clot, maintaining the space for the new bone ingrowth, and by providing osteoconductive surfaces for osteogenic cells' adherence. Osteoconductive, osteoinductive and osteogenic properties of the graft may all influence the outcome of grafting. The porosity and crystallinity of the graft are important to allow the vascularization of the area.

The osteogenic cells in SFE arrive from the direction of antral walls, and the new bone formation creates a gradient of consolidation towards the Schneiderian membrane. With time, the particles of the graft become part of graft-bone complex. This complex undergoes remodelling, and the graft may be substituted by the recipient bone. The graft resorption and substitution depends on the chemical and physical structure of the grafting material.

1.3 Grafting materials

1.3.1 Autologous bone grafts

Autogenous bone is harvested directly from the patient. Common harvesting sites are the retromolar region, the chin, or the iliac crest¹⁶⁸. The harvested bone may be cancellous, cortical or mixed morphology and in block or particulate form depending on the harvesting technique.

Autologous bone grafts (ABG) possess osteoconductive, osteoinductive and osteogenic properties. As result of consolidation, the autologous grafts are replaced by the viable new bone; the process is known as creeping substitution¹³⁷.

There are, however, serious drawbacks with ABG. First, ABGs are harvested from the additional surgical site, which leads to increased site morbidity, patient discomfort, and sometimes, additional complications¹⁶⁹⁻¹⁷¹. Second, when used for sinus floor elevation (SFE), ABG may lose 20-50% of its initial volume during the first year^{74, 172-174}.

The unpredictable graft resorption and the donor site morbidity have led the industry to develop an array of bone substitution materials.

1.3.2 Allografts

Allografting is the process by which bone is transferred between two genetically dissimilar individuals of the same species. Several methods are used to process human bone, including irradiation, physical debridement, ultrasonic or pulsatile water washes, ethanol treatment, and antibiotic soaking¹⁷⁵. Freeze-dried bone allograft (FDBA) and demineralized freeze-dried bone allograft (DFDBA) are the most commonly used allografts for SFE. Both FDBA and DFDBA are considered to be osteoconductive and osteoinductive¹⁴³; however, the osteoinductive potential was inferior to that of ABG¹³⁷.

Histologically, allografts demonstrated creeping substitution by the bone, with the histomorphometric outcomes similar to those of xenografts (discussed in the section 1.3.3) in terms of new bone formation and the residual graft resorption¹⁷⁶. Similarly to ABG, a substantial loss of volume was reported for allografts¹⁷⁷.

The principal concern with allografts is viral disease transmission, including hepatitis C, hepatitis B, and human immunodeficiency virus (HIV). The Sinus Conference in 1996 concluded that DFDBA is not an appropriate bone substitute because of the risk of disease transmission and pronounced resorption¹⁷⁸. Allografts enjoy popularity in the United States of America, where strict donor screening programs were employed¹³⁷, but their use is restricted in Europe by regulation¹⁴³.

1.3.3 Xenografts

Xenografts for sinus floor elevation consist of mineral derived from animals (usually from cows or pigs) or calcified exoskeletons of marine coral or algae. The organic components of the xenografts are removed by processing, leaving the macro- and microporous structure, which closely resembles human cancellous bone and supports vascularization and new bone ingrowth. The exact process of manufacturing for each material is a commercial secret and is not published in detail. The osteoconductive and resorptive properties of xenografts that were produced using different protocols may vary¹⁷⁹.

For the animal-derived products, the concerns have been raised about the possibility of transmitting prion diseases¹⁸⁰; however, no cases of such a transmission were recorded. In contrast, two cases of HIV transmission through allografts were reported¹⁴³.

Xenografts were found to be osteoconductive in the one-wall calvarial defect animal model¹⁵², critical size defect repair model¹⁸¹, and in human sinus floor augmentations¹⁸².

Unlike the ABGs, the xenografts do not necessarily undergo complete resorption and substitution by the host bone. Although some algae-derived products will completely biodegrade as early as 8 weeks¹⁷⁹, the bovine-derived xenograft was present years after implantation^{162, 183-185}. Histologic long-term investigations of biomaterial degradation in human participants are scarce and mostly confined to case series^{162, 185-187}, which show partial resorption of the biomaterial. In a recent longitudinal trial in humans, the fraction of DBBM decreased from 37% down to 20% between 5 to 11 months of healing reaching statistical significance¹⁸⁸.

As described in section 1.3.1, the loss of volume by the graft is a primary concern when using the autologous bone for SFE^{172, 189}. Thus, slow- or non-resorbing grafts may be especially suited for SFE where long-term space maintenance is required^{190, 191}. In a recent systematic review¹⁷³ authors have calculated a cumulative volumetric reduction of slow-resorbing xenografts and alloplasts placed in the sinus to be 18-23%, if used alone or in combination with ABG. This is a considerable improvement compared to 45% of volume loss by pure AB grafts¹⁷³. Some authors advocate the use of a combination of osteoinductive autologous bone graft and osteoconductive non-resorbing xenograft to achieve grafting site stability together with higher new bone formation¹⁹²⁻¹⁹⁴. However, authors of a systematic review¹⁹⁰ could not accept, nor reject this claim.

The extent of replacement of the xenograft by the bone may depend on the way the material was manufactured – specifically, high-temperature deproteinization. Temperatures which exceed 1000°C cause sintering of the crystalline structure of hydroxyapatite and reduction of its porosity and micro-roughness¹⁹⁵. The effect of sintering is well-known for synthetic alloplastic materials – it delays the resorption of the synthetic hydroxyapatite¹⁹⁶. In contrast, recent randomized controlled studies with

human participants have failed to demonstrate a statistically significant difference of replacement-resorption between sintered and non-sintered xenografts^{197, 198}.

1.3.4 Alloplasts

Alloplasts are a diverse group of completely synthetic grafting materials. Like xenografts, they stabilize the wound and provide an osteoconductive scaffold for the new bone formation. Their main advantage is safety, in terms of disease transmission. Also, for patients who are concerned with human-derived or animal-derived products, alloplasts may be the only acceptable grafting material.

The other reason for the development of alloplastic materials is the theoretical possibility of adjusting their chemical and physical characteristics to suit a specific clinical demand. For example, the manufacturers of calcium phosphate ceramics are able to control macro- and microporosity as well as inter-connectedness of their products¹⁹⁹. While biomaterial science has made considerable advances, ideal characteristics for the alloplastic material are yet to be identified¹⁶¹. As for physical properties, although faster ingrowth is favoured by a more porous, interconnected structure, denser ceramics have better mechanical integrity²⁰⁰.

Alloplasts for sinus grafting in humans were investigated in case studies²⁰¹⁻²⁰³, controlled trials²⁰⁴⁻²⁰⁷ and systematic reviews²⁰⁸⁻²¹⁰. It appears that histologic and clinical outcomes of SFE using some alloplasts are comparable to those of xenografts.

Calcium phosphate alloplasts received the most attention in research: non-resorbing hydroxyapatite (HA) and quickly-resorbing tricalcium phosphate (TCP) and their combination, biphasic calcium phosphate²¹⁰. In a seminal work, Jensen et al. (2009) examined different HA/TCP ratios in the minipig mandibular defect model¹⁶¹. The 80% / 20% and 60% / 40% HA/TCP ratios have demonstrated residual graft and new bone

formation comparable to that of DBBM (Bio-Oss®), while 20% / 80% HA/TCP ratio lost volume similar to ABG. All bone substitutes demonstrated less new bone than ABG.

The concept of space-maintaining synthetic osteoconductive material for sinus grafting received support from a recent pilot study¹⁴⁷. Two human participants received sinus augmentation with porous titanium granules in one sinus and DBBM in the contralateral sinus. The implants were placed after 9 months, and trephine biopsies were taken from the sites. The new bone formation was similar for both sinuses after 9 months of healing¹⁴⁷. In another case series with five human participants, the operators used a 0.3 mm poly-L-lactic acid (PLA) mesh reinforced with resorbable HA to suspend the SM in the elevated position²¹¹. At 6-9 months post-operation, the newly formed bone enabled insertion of implants 8.5-11.5 mm long. Trephine biopsies confirmed new bone formation histologically²¹¹.

Reports of SFE using tissue-engineered constructs, either combined with growth factors or cultured cells, appear more and more in the literature. For a review see Larsson et al. (2016)²¹². The development of these conceptually novel materials began 30 years ago. It was hindered by the complexity of the procedures, the costs and concerns over the neoplastic potential of growth factors and stem cells²¹³; the engineered tissues are still unavailable for wider professional use today.

1.3.5 Implants placed in the augmented sinus floor

Sinus grafting aims to create more viable bone for implant placement. As it was stated in section 1.1.3, after graft consolidation the quality of the created bone corresponds to type IV bone, based on the Lekholm and Zarb classification³⁶. Despite the seemingly inferior quality of augmented bone, the cumulative survival rate of moderately rough surface implants placed in the grafted sinus is more than 90%, similar to that of

implants placed in non-grafted posterior maxilla²¹⁴. The implant osseointegration was shown to be independent of the grafting material that was used¹⁷².

Implant osseointegration can be measured histologically as the percentage of bone-to-implant contact (BIC) out of the total surface of the implant. BIC around implants in grafted sites was reported to be between 40% and 80%^{47, 48, 53, 215}. Thus, the bone contacting implants was denser than the poor-quality bone present in the rest of the augmented site. In one study, implants were shown to have successfully osseointegrated in sites with NB content as low as 24%²¹⁶.

However, if bone coating forming over implants is thin and not contributing to mechanical support, the BIC figure may be misleading. In a canine study, 50 µm lamellar bone coating was formed over titanium implant threads that contacted bone marrow of the cancellous bone²¹⁷. This mechanically non-important layer may amplify the value of bone-to-implant contact to levels higher than those achieved in a cortical bone.

On the other hand, BIC was positively correlated with implant torque-out tests⁸² and non-destructive stability tests such as ISQ²¹⁸. According to Frost's Mechanostat hypothesis¹⁹, the implant under occlusal loading will apply stress to the supporting bone; in this case, the increased BIC might be a result of adaptive bone remodelling.

While histology provides an invaluable tool for research, the exact correlation between histologic parameters (new bone fraction, BIC), and implant success is yet to be elucidated. Esposito et al. (2010)²¹⁹ in the systematic review stated that reporting histomorphometric bone-mineralised content alone is insufficient to draw clinically relevant conclusions and should not be done in human subjects.

1.3.6 Conclusions

Autologous bone is the only grafting material possessing osteoinductive, osteoconductive and osteogenic properties. However, it is not the ideal for sinus floor elevation, as autologous bone requires an additional surgical site for harvesting and may lose substantial volume during consolidation.

An array of biomaterials has been developed and tested. Currently, there is little evidence of the superiority of one type of biomaterial over another in terms of histologic outcomes or implant survival. The reason to develop new biomaterials for sinus grafting is to make them cheaper, easier to handle and more acceptable by the patient.

1.4 Sinus grafting procedures

Boyne & James (1980)²²⁰ and then Tatum (1986)²²¹ reported on their attempts at SFE. Since these early reports, a variety of SFE procedures have been developed. These procedures may differ by surgical protocol, timing, equipment, access and the use of grafting materials and barrier membranes. In this section, the principles of sinus grafting, along with variations in practice and alternatives to sinus floor elevation for implant placement, will be discussed.

1.4.1 Maxillary sinus anatomy and its relevance to sinus grafting

The maxillary sinus (MS) is an epithelium-lined space in the maxillary bone. In adults, it has a reverse pyramidal shape with a wider base being the roof of the orbit and the apex situated close to the roots of the first bicuspid tooth.

The physiologic purpose for paranasal spaces in humans is not entirely understood; however, they may perform various functions. In his review, Drettner (1980)²²² lists the following roles the MS might play in humans:

1. Phonetic (sound resonance and transmission)
2. Respiratory (air conditioning and pressure equalizing)
3. Olfactory (reservoir of air may be utilized as reference to new olfactory stimuli)
4. Static (reduced weight of the facial bones)
5. Mechanical (shock absorbing in traumatic injuries)
6. Thermal (heat insulating of the skull base)

The sinus space anatomy varies between individuals. It can form either a singular space or several spaces, divided by septae²²³. Maxillary sinus septae were first described by Underwood in 1910²²⁴. It was speculated that septum gradually forms between two zones of alveolar bone resorption²²⁵. The presence of septae can pose

difficulty for surgical access, Schneiderian membrane elevation and grafting material placement^{220, 226}. According to computerized tomography analysis, the septae is present in 29% of humans²²⁵. To date, there were no published reports about the frequency and morphology of MS septae in animals. Pre-surgical screening of sinus anatomy may be employed in animal SFE research to account for the possible septae, constrictions, vasculature or other unusual anatomical features of MS.

The sinus floor in humans consists of dense lamellar bone. It can be smooth or uneven, depending on the position of the roots of maxillary teeth. With time, the teeth roots which protrude into the sinus space may become attached to only a paper-thin layer of cortical bone via the PDL¹⁵.

The sinus space is lined with Schneiderian membrane (SM), which consists of a single layer of ciliated, columnar, respiratory epithelium covering lamina propria²²⁷. The lamina propria fuses with the underlying periosteum to form the mucoperiosteum, which is 0.13-0.5 mm thick in a healthy sinus²²⁷. After SFE, a transient swelling and inflammation of the membrane may be observed²²⁸. Using computerized tomography investigation, Makary et al. (2016)²²⁹ demonstrated that this swelling might reach up to 7 mm after the first week, but then gradually decreases over the course of 12 months, dropping below 1 mm after 6 months of healing. Interestingly enough, the average thickness at 12 months post-op was lower than pre-op; the difference was statistically significant²²⁹.

The average thickness of SM in goats and sheep is 2.03 mm and in pigs – 2.80 mm²³⁰; thicker membrane suggests less chance of perforations during SFE.

The vascular supply of the sinus is provided by the posterior superior alveolar artery, inferior orbital artery, greater palatine artery, and sphenopalatine artery (branches of the maxillary artery, which is a continuation of the external carotid artery). The

vasculature exhibits multiple anastomoses between the supplying branches²³¹. This abundant vascular architecture can be beneficial for post-operative healing after sinus interventions²³². On the other hand, because severing 2.5 - 3 mm arteries can complicate surgery, a thorough pre-op investigation may be warranted²³³. In posterior maxilla, 70-100% of blood supply originates from the periosteum²³⁴. Therefore, care must be taken not to compromise the blood supply when raising flaps for the lateral access.

Innervation of the sinus is supplied by the superior, middle and anterior alveolar nerves, greater palatine nerve and infraorbital nerve²³⁵. The nerves accompany the veins and lymphatics of the sinus. Severing or damaging the nerves of MS during SFE was not reported in the literature; however, care must be taken to avoid compression of the infra-orbital nerve bundle while performing blunt dissection of the tissues²⁹.

The lateral walls of the sinus in humans consist of relatively thin bone, which may become even thinner (reaching 1.71 – 1.57 mm) when the maxillary teeth are lost²³⁶. Thus, care must be taken not to unintentionally perforate the bone and the underlying SM when gaining access to the MS through its lateral wall. In animals, the lateral walls of the sinus may be thicker or thinner than human ones, depending on the animal²³⁰

1.4.2 Clinical procedures and variations in practice

The aim of the first reported SFE was to reduce the size of posterior maxilla for denture placement, as the paper-thin bone did not allow for the alveoplasty²²⁰. Today, the sinus space is entered routinely to increase the bony support for dental implants. A variety of techniques have been developed for sinus grafting. As my study employs one specific protocol, it's worth outlining the main variations in clinical practice of SFE.

1.4.2.1 Access

Boyne & James (1980)²²⁰ described the lateral access to MS using a modified Caldwell-Luc procedure. In 1986, Tatum²²¹ reported on his early results with a crestal approach to the maxillary sinus and simultaneous placement of implants. The need for the lateral approach can be dictated by the residual bone height. Less than 5 mm of residual bone height is commonly stated as the indication for the lateral access sinus grafting procedure²⁹; however, this figure is rather arbitrary²³⁷. The lateral SFE is advocated for severely resorbed posterior maxillary sites to place big volume grafts in a controlled manner, combined whether with delayed or immediate implant placement²⁹. While the lateral approach provides vision and better control of the surgical site, it is also more invasive.

1.4.2.2 Maintaining augmented space

A variety of biomaterials (reviewed in section 1.3 of this chapter) have been developed for SFE. In general, the biomaterials in SFE serve as wound stabilizers and space maintainers that prevent SM collapse. If the augmented space is maintained for sufficient time by means other than placing autologous bone or its substitutes, the de-novo formation of bone is thought to occur²³⁸. In a case report, Lundgren et al. (2004)¹¹⁷ claimed that the creation of space between the antral bone and the Schneiderian membrane could result in new bone formation around implants in the maxillary sinus, even without the use of bone graft materials. These findings were confirmed histologically in an experimental animal model¹¹⁴. Multiple reports were published concerning radiographic and histologic evidence of no-graft SFE in animals and humans²³⁹.

However, maintaining augmented space without grafting can be a challenging task. In an experimental study in primates, a resorbable polylactide device was used, but the new extra-skeletal bone failed to form, probably due to the quicker-than-needed resorption of polylactide²⁴⁰. In another primate study, a titanium space-maintainer was

employed, and new bone formation was observed. However, the augmented tissue was greatly reduced in volume between 3 and 6 months and, in most cases, the space-maintainers perforated SM¹¹³. A recent systematic review²⁴¹ included five randomized clinical trials and one cohort study; it concluded that non-grafted SFE is a viable cost-reducing technique, resulting in a high implant success rate. The authors stressed the need for studies with a longer follow-up.

1.4.2.3 Piezo-electric devices

Traditionally, to gain access through the sinus walls, burs or trephines have been used. However, concerns were raised about heat damage to the bone while drilling and SM perforations^{242, 243}. Piezo-electric devices were introduced to provide a solution to these concerns²⁴⁴. In these devices, a high-frequency alternating electrical current is transmitted to the piezo crystals, causing their expansion and contraction. These mechanical oscillations are transferred to the working tip of the piezo-electric device, which is able to disrupt and fragment solid bone tissue but leaves soft tissues intact²⁴⁵. The main disadvantage of piezo-electric devices is operation time, which can be increased as much as five-fold compared to the rotary instruments²⁴⁶.

Trisi et al. (2011)²⁴⁷ investigated early osseointegration of implants placed in the osteotomies, which had been prepared by piezo-electric and rotary devices using a sheep mandible model. The piezo-electric group demonstrated less peri-implant bone resorption. Similar findings were reported in mini-pigs²⁴⁸.

Quality data concerning use of piezo-electric devices for SFE in humans is scarce. A recent systematic review included only four studies, three of them with a high risk of bias²⁴⁹. The authors failed to find a statistically significant difference between rotary and piezo-electric devices for prevention of SM perforations but confirmed the prolonged operation time with piezo-electric devices. Also, they discuss the

importance of operator experience for prevention of SM perforation with any of the devices.

1.4.2.4 Use of membranes

When using lateral access for sinus grafting, the access window can be covered with the barrier membrane. The barrier is thought to prevent the migration of connective tissue and epithelial cells according to the principles of guided bone regeneration²⁵⁰.

Histomorphometric evidence of enhanced bone formation, following membrane placement over the lateral window, is available. In a randomized controlled clinical trial with a split-mouth design²¹⁴, bilateral sinus grafts were performed for twelve patients with or without covering the lateral window using a non-resorbable membrane. At re-entry after 12 months, biopsies were taken. The mean new bone fraction was 25.5% with and 11.9% without a covering barrier. Similar results were obtained in a controlled clinical trial²⁵¹ measuring bone formation in 113 sinuses. The mean new bone fraction was 27.6% when a membrane was used, compared to 16% without. However, a recent systematic review of histomorphometric outcomes²⁵² failed to find any statistically significant difference in new bone formation when the membrane was placed over the surgical window.

Clinical outcomes of placing barriers over the access window were also investigated. The earlier systematic reviews^{74,77} supported the use of barriers over the access window and reported higher implant success rate in membrane-covered sites. However, a more recent review done by the Cochrane Collaboration²⁵³ included only one trial at a high risk of bias with 106 patients, which investigated implants in covered and uncovered sites. After one year of loading, no statistically significant difference was reported for implant failure.

In this systematic review, Esposito et al. (2014)²⁵³ compared the impact of different protocols of SFE on implant failure:

1. Lateral versus trans-crestal access to the sinus (one trial).
2. Rotary instruments versus piezo-surgery to open lateral sinus window (one trial).
3. One-stage (implant placement at the time of SFE) versus two-stage (delayed implant placement) lateral sinus lift (one trial).
4. Using or not using the barrier membrane to seal the lateral window (one trial).
5. Different bone substitutes and autologous bone grafts (two trials).
6. Rotary versus hand malleting for the trans-crestal approach (two trials).

No statistical difference in terms of implant survival was observed for any of the tested protocols. The number of included studies and the quality of evidence was relatively low.

1.4.3 Alternatives to augmentation

When the bone height is inadequate to support a long implant, a short implant can be used instead (just what distinguishes a “long” or “short” implant is somewhat arbitrary). Earlier studies have reported reduced success rates for shorter implants²⁵⁴; thus, longer, 13-18 mm implants were recommended in clinical practice. To be consistent with the current literature, we will address implants less than 10 mm in length as short implants. More recent reports and several systematic reviews demonstrate that implant survival and success seems to be similar for both short and long implant groups²⁵⁵⁻²⁵⁷. Despite having similar failure rates, peak failure incidence for shorter, <10 mm implants was reported to be 2.5 years earlier than longer implants²⁵⁶. None of the prosthetic factors influenced short implant failure^{258, 259}: crown-to-implant ratio, splinting, occlusal table, cantilever length, implant system, opposing

dentition, and bruxism. Tawil et al. (2006)²⁵⁹ followed implants shorter than 10 mm for 53 months on average and found no statistically significant correlation between peri-implant bone loss and the crown-to-implant ratio or cantilever length.

However, short implants placed in posterior maxilla demonstrated lower survival rates compared to long implants^{4, 260, 261}. The possible reasons for implant failure in posterior maxilla were discussed in section 1.1 of this chapter. In brief, lack of primary stability, reduced bone quality, increased mastication forces and unfavourable stress distribution in this anatomical site are thought to impact the survival rates of the implants. Also, in cases of the extremely resorbed posterior maxilla, even 4-6 mm implants may not have the required bone support, indicating the need for SFE prior to implant placement.

Other alternatives to SFE were reported in the literature: zygomatic implants²⁶², all-on-four rehabilitations²⁶³, and angulated abutments²⁶⁴, to name a few. These alternative treatments may provide viable options in certain clinical situations. However, they are too case-specific and dependent on operator technique and experience to fully replace SFE in clinical practice.

1.4.4 Conclusions

SFE procedures for implant placement are considered predictable and safe. A variety of modifications of the original surgical protocols have been introduced. Maintaining the augmented space is paramount for the extra-skeletal bone formation to occur. This may be achieved by grafting the sinus with autologous bone or bone substitute. Other methods of maintaining space have also been shown to be successful and cost-effective; however, they can be less predictable and more operator-demanding. The use of piezoelectric devices to prevent heat damage to the bone and SM perforation, and use

of barrier membranes to cover the access window, have been advocated and supported by some authors and systematic reviews.

Alternatives to implant placement in the grafted sinus have also been reported in the literature; however, they cannot fully eliminate the need for SFE in clinical practice.

1.5 Animal models

Due to ethical considerations, newly developed materials for implantation should be tested in non-human models prior to clinical tests in humans. While the in-vitro testing may provide valuable information about cell-material interaction and possible toxicity in an easily standardized and controlled medium (and prevent the non-suitable materials from being needlessly tested on animals), the cultured cells cannot represent the response of an entire tissue or the organism itself. The animals can provide the complex environments which are needed to assess the behaviour of implanted biomaterials fully.

Several animal models were developed in orthopaedic and dental implant research. The key factor to consider when choosing an animal model is the level of physiological similarity of the experimental site in the animal to the corresponding anatomical site in humans.

Pearce et al. (2007)²⁶⁵ summarised the biologic similarity of animal bone to the human bone for dental implantology; the summary is reproduced in Table 1-2. The authors have compared the animal bone tissue to that of humans in terms of macrostructure (dimensions, weight, stiffness, resistance to fracture), microstructure (trabecular density, porosity, lamellar and Haversian structure), bone composition (chemical composition, bone ash density) and bone remodelling (mechanics of bone repair and remodelling, rate of regeneration and remodelling)²⁶⁵. Other considerations in choosing the model may include the animal's ability to withstand and recover from surgery, costs of handling and housing, the availability of the animals, and acceptability to society²⁶⁶.

Table 1-2 Similarity between human and animal bone characteristics

	Dog	Sheep/Goat	Pig	Rabbit
Macrostructure	++	+++	++	+
Microstructure	++	+	++	+
Bone composition	+++	++	+++	++
Bone remodeling	++	++	+++	+

Adapted from Pearce et al. (2007) ²⁶⁵

Similarity to human bone: + least similar, ++ moderately similar, +++ most similar.

1.5.1 Small animals

Small animals, such as rabbits and rats, are extensively used in orthopaedic and dental research. Despite the differences in bone biology (healing and remodelling are much slower in humans) and the need to adapt the implantable devices to the animal size, the small animals are relatively cheap, easy to handle and reach maturity earlier than the large ones²⁶⁵.

Rats were not used as an SFE model due to them being too small. Rabbit SFE models, however, were reported^{119, 267, 268}. Rabbits' maxillary sinus anatomy bears enough similarity to that of humans²⁶⁹. Like humans, the air pressure through the ostium can lead to the collapse of the rabbit's maxillary sinus membrane and affect the augmented bone structure²⁷⁰, which provides a viable physiologic model for SFE.

1.5.2 Large animals

Large animal models' advantages are the ability to use 'human-size' implantable devices, and the bone healing rate, which is closer to that of humans. For SFE modelling, the size of the sinus is important, therefore, in this process, large animals are preferable to the small ones. SFE was reported in dogs, pigs, sheep, goats and primates.

1.5.2.1 Dogs

Dogs have been extensively used in dental implantology research. A study by Aerssens et al. (1998)²⁷¹ examined the differences in bone composition, density and quality between various species (human, dog, sheep, pig, cow and chicken). The authors stated that the canine bone tissue had most similarity to the human one.

Using dogs for SFE research, was, however, criticized by Haas et al. (1998)²⁷². The authors stated that the dog model is not comparable to humans for the lack of Schneiderian membrane and lack of pneumatization. In contrast, Rosen and Sarnat (1955)¹⁴ have demonstrated sinus pneumatization in dogs after tooth extraction on one side. Perhaps the most important consideration is the dog being a companion animal, which raises additional ethical questions and reduces the willingness of ethical committees to approve dog-based experiments²⁶⁶.

1.5.2.2 Pigs and minipigs

The anatomy of pig sinus is suitable for grafting and similar in size to human sinus^{156, 273}. Commercially available breeds of pigs grow to excessively large sizes, and their handling may be difficult and even dangerous. The development of mini-pigs overcame this problem to some extent and multiple SFE studies in porcine models are using mini-pigs^{116, 156, 161, 274}. The intra-oral approach to the antral wall in a porcine model requires a wide surgical extension of the vestibule²³⁰. Also, unlike the human edentulous maxilla, the antral wall in pigs is relatively thick, dense and difficult to trephine²³⁰.

1.5.2.3 Sheep and goats

Sheep and goats are analogous animals for the purpose of SFE research²⁶⁵. Their bone shows considerable resemblance to human bone in terms of macrostructure^{265, 275} and

chemical composition²⁷¹. Both sheep and goats were used in SFE research^{121, 126, 276, 277}. In New Zealand, the domestic sheep (*Ovis aries*) are commercially available in large numbers, their handling is easy, and the cost is relatively low. Being an industrially farmed animal, their use in scientific research tends to be more acceptable by society. Our institution accumulated considerable knowledge about the sheep model in implant²⁷⁸⁻²⁸⁰ and SFE²⁸¹⁻²⁸³ research.

After a post-mortem study, Brumund et al. (2004)²⁸⁴ stated that general nasal anatomy and the paranasal sinus anatomy in sheep are similar to humans in appearance and orientation. A different study²³⁰ demonstrated that the antral wall in sheep is thin enough to resemble the antral wall of the human posterior edentulous maxilla. Like in pigs, the intra-oral approach to the antral wall in sheep requires vestibular enlargement prior to the actual SFE procedure²³⁰. An alternative, extra-oral approach was developed by Haas et al. (1998)²⁷².

Table 1-3 Sheep vs human bone healing

Healing time									
Sheep	6	5	1	2	4	6	8	12	16
	hours	days	week	weeks	weeks	weeks	weeks	weeks	weeks
Humans	8	1	9	3	5	8	11	16	21
	hours	week	days	weeks	weeks	weeks	weeks	weeks	weeks

When researching consolidation of grafting materials, the rate of healing and repair of the animal is to be taken into account. Bone defect repair was used by Duncan (2005)²⁷⁸ to estimate the difference between human and sheep healing rate and found that sheep bone repairs approximately 30% faster (Table 1-3).

The trabecular bone of skeletally immature sheep is weaker, more elastic, has higher shock absorptive qualities, contains more collagen, is less dense and more porous than that of skeletally mature sheep²⁸⁵. Hence, for more coherent results it is important to choose animals of similar age for the study.

1.5.2.4 Primates

Nonhuman primates, though closest to humans from the point of view of bone biology, are rarely considered as models for bone repair because of their high cost, low availability, handling difficulty and ethical concerns²⁸⁶.

While SFE research was reported in primates^{114, 287, 288}, the number of studies is relatively low. The increasing resistance of the ethical committees to approve primate-based research throws into question future reproducibility of outcomes of the primate-based studies.

1.5.3 Conclusions

Animal testing is a necessary step in developing implanted materials for clinical use in humans. A variety of animal models have been developed for sinus floor elevation (SFE) research. When considering the degree of physiologic similarity to humans, together with the animal availability, cost, ease of handling and ethical concerns, sheep and goats seem to be well-suited for SFE research.

There is a growing body of work using the ovine sinus model, in part by our institution. The results from the ovine sinus model should be both relevant to humans and easily reproducible by other groups.

1.6 Analytical techniques for graft consolidation

Graft consolidation in clinical practice is usually assessed either by direct observation at re-entry or indirectly by radiography. In research, the histologic analysis provides the basis of knowledge about graft consolidation, osseous healing, foreign body reactions and graft decomposition on tissue and cellular levels. The histomorphometric analysis is done by sectioning the histologic image into portions occupied by different tissues. For SFE, the newly formed bone (NB), the residual graft (RG), and the connective tissue (CT) are commonly measured^{210, 289}.

In humans, the histologic analysis is restricted to partial biopsies at the time of implant placement^{185, 202, 290}. A meta-analysis by Corbella et al. (2016)²⁸⁹ included 84 human studies reporting histomorphometric outcomes of SFE with different grafting materials. These analyses were mainly carried out to evaluate the material resorption and the presence of new bone tissue using haematoxylin & eosin or toluidine blue staining, alone or in combination with tri-chromic staining, the latter to reveal collagen fibres.

Animal studies routinely report histologic and histomorphometric outcomes of SFE^{268, 273, 276}. In animals, whole grafted areas can be sectioned and analyzed at multiple time-points.

1.6.1 Demineralized sections

Direct histologic preparation of osseous tissues is impossible as the specimens are destroyed during sectioning. While prone to artefacts and tears²⁹¹, demineralization allows for specimen preparation from the ossified tissues. The specimens are demineralized (usually using ethylenediaminetetraacetic acid (EDTA)), embedded, typically, in paraffin and cut into thin, 4 - 7 μm sections. The basic histological staining with haematoxylin and eosin (H&E) allows for visualization of the cells and non-

mineralized extracellular structures²⁹¹. Staining with immunohistochemical markers is used to identify specific cells types or cellular activity.

Paraffin-embedded demineralized sections were used in both animal^{116, 119, 270} and human SFE studies^{292, 293}.

1.6.2 Undemineralized sections

Mineralized bone is very stiff; it yields histological sections with less destruction and chatter when the surrounding embedding material is also stiff. Since the 1940s, histological examination of undemineralized bone tissue has been facilitated by embedding the bone tissue in one of several plastic formulations²⁹⁴. The resin block with embedded specimens are sectioned, and the sections are then ground to the microscope-suitable thickness (5-100 μm). Unlike the demineralized sections, undemineralized specimens allow for comparison between more mineralized, mature bone and less mineralized, woven or laminar bone. Distinguishing between osseous structures is important for histomorphometric analysis, where areas occupied by the newly formed bone, the grafting material and the connective tissue are determined.

Multiple groups use undemineralized sections in human^{204, 295, 296} and animal-based^{7, 297, 298} SFE research, ensuring the relevance and reproducibility of results using this method.

1.6.3 Measurements

Selection of the region of interest (ROI) for performing the histomorphometric analysis is a debatable subject, and no consensus has been reached between the various research groups. Some authors^{185, 186, 298} include the whole augmented site in the analyzed ROI. Others attempt to analyze the gradient of graft consolidation by dividing the ROI into zones – from the area closer to the floor or wall of the sinus, towards the elevated SM.

Busenlechner et al. (2009)¹⁵⁵ defined three ROIs: R1 – bridging distance to the sinus walls; R2 – intermediate distance; R3 – distant bone formation.

De Lange et al. (2014)²⁰⁴ specified three square areas of interest, each of 625 μm^2 starting at 500 μm distance from the sinus floor.

Alayan et al. (2015)⁷ divided the specimen into three equal-area zones by proximity to the sinus wall.

While the consolidation gradient of the graft was demonstrated in these studies, the reproducibility and clinical relevance of the gradient is questionable. In my study, the whole augmented site was analyzed for histomorphometric parameters.

1.6.4 Conclusions

Histologic and histomorphometric analysis remain the mainstay of animal-based research of sinus floor elevation. Undemineralized sections are widely used and are a reproducible method for producing histomorphometric outcomes. Although the choice of the region of interest varies between groups, attempts should always be made to provide a reproducible outcome.

1.7 Aims of study

The aim of this study was to prove non-inferiority of three novel and commercially available bone substitutes to a commonly used xenograft (control) for sinus floor elevation in, a well-known sheep maxillary grafting model using an extra-oral approach. The experimental materials (the alloplast and the xenograft) are not principally different from the materials that are already in clinical use. However, the intra-surgical handling of the experimental materials is thought to be superior. Also, the equine source of two of the experimental materials may be more readily accepted by some religious patients.

1.7.1 Research question

There is no data available concerning the outcomes of sinus grafting with the exact formulation of two of the tested products. A third product (IBI SmartBone®) was used in a recent case series in humans and demonstrated favourable histomorphometric outcomes, being replaced by viable bone. The small sample size of this report did not allow us to draw a quantitative hypothesis.

In my study, two hypotheses were tested:

1. The histologic and histomorphometric outcomes of sinus floor elevation in sheep using three novel bone substitute products (equine collagen cone, equine collagen cone filled with biphasic calcium phosphate particles, and deproteinized bovine bone particles coated with polylactic acid and poly ϵ - caprolactone copolymer) are not statistically different to the commonly-used xenograft (Bio-Oss®)
2. The handling properties of the experimental bone substitute products are superior to those of the commonly-used xenograft (Bio-Oss®)

Chapter 2. Materials and Methods

The study population, the intervention, and the measurements will be described in this section. This study followed the ARRIVE guidelines²⁹⁹ for the reporting of *in vivo* experiments. This study was performed in accordance with the New Zealand Animal Welfare Act (1999). The Otago Animal Ethics Committee approved the study under protocol number AEC 78-14. The animals in this study were also used by another group for alveolar ridge preservation research. The results of this study were reported elsewhere³⁰⁰.

2.1 Experimental animals

Eleven female cross-bred ewes from the Hercus Taeri Research Unit Breeding Station were selected for the study according to the following criteria:

2.1.1 Inclusion criteria

1. Age 3-4 years
2. Weight 70 kg or more. Underweight animals are more prone to surgery complications and have slower recovery overall.
3. Complete dentition. Missing teeth are thought to be a sign of broken-mouth periodontitis³⁰¹.

2.1.2 Exclusion criteria

1. Infectious pododermatitis (footrot). This condition requires antibiotic therapy. Otherwise it can cause lameness, loss of weight, and poor recovery after surgical procedures³⁰².
2. Pregnant or lamb at foot.

2.1.3 Pre-intervention management

All included animals were tagged, treated for parasites, immunized and relocated to a secure pasture before the intervention.

They were held in a separate paddock for 48-72 hours prior to the surgery and were not allowed oral intake of food and fluids for 24 hours prior to general anaesthesia.

2.1.4 Statistics and power

A number of studies using xenografts, allografts and combination grafts for SFE in sheep were published using various sample sizes^{121, 126, 276, 297, 298}. In studies where the sample size was larger than ten animals, the authors discovered statistically significant histomorphometric outcomes. An additional consideration comes from our collaboration with another group that used the same animals for alveolar ridge preservation research³⁰⁰. The previous study of alveolar ridge preservation in sheep sampled eight animals and did not reach statistical significance³⁰³. By increasing the number of animals to eleven, they aimed to increase the statistical power of their study.

2.2 Grafting materials

2.2.1 IBI SmartBone® (Industrie Biomediche Insubri SA CH-6805 Mezzovico-Vira, Ticino, Switzerland)

SmartBone® (SB) is a commercially available novel xenograft of bovine origin. While the bovine bone xenograft is not an innovation on its own, SmartBone® bovine xenograft matrix is coated with degradable synthetic poly (L-lactide-co-ε-caprolactone) (PLA-PCL) and gelatin. The manufacturer states this coating should improve the mechanical properties of otherwise brittle xenograft and provide better cell adhesion. The addition of gelatine increases the graft's wettability by blood. Unlike particulate grafting materials, the PLA-PCL coating allows SmartBone® to withstand stress, such as shaping it with files or pliers for better adaptation, drilling holes into the material, or securing it with screws to the recipient site (Figure 2-1). The material is porous, with 27% of its volume occupied by air, to allow for quicker tissue ingrowth and vascularization³⁰⁴. SB used in this study comes in a shape of a porous rigid cube 10 x 10 x 10 mm.

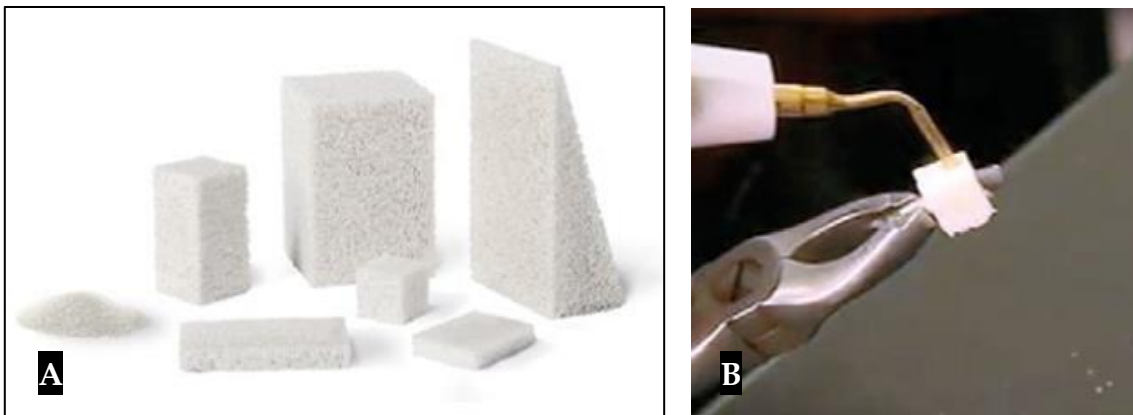


Figure 2-1 SmartBone® (courtesy of IBI)

- A. The material is available in shaped rigid porous blocks*
- B. The blocks can be further shaped by cutting or drilling*

2.2.2 PARASORB Cone® (Resorba Wundversorgung GmbH, Nürnberg, Germany)

PARASORB Cone® (CN) is a commercially available resorbable type I collagen cone (Figure 2-2). One cone, diameter 1.2 cm, height 1.6 cm, contains 22.4 mg of equine collagen. The collagen fibrils are not cross-linked, they are reconstituted using a proprietary technology³⁰⁵. The recommended use of this product is wound stabilization and haemostasis after tooth extractions. Off-label uses have also been reported, mainly as a scaffold and vehicle for biologic agents^{306, 307}.

2.2.3 PARASORB Cone Oss® (Resorba Wundversorgung GmbH, Nürnberg, Germany)

Cone Oss® (CO) is a novel and not yet commercially available product consisting of an equine collagen cone (identical to CN) with suspended biphasic calcium phosphate (BCP) granules. The BCP used for this product is a combination of 60% hydroxyapatite (HA) and 40% beta-tricalcium phosphate (β -TCP). The β -TCP portion is thought to be resorbable while the HA should remain in the grafted site as a scaffold for long-term volume preservation³⁰⁸. This product concept resembles that of Bio-Oss Collagen®: a combination of osteoconductive mineralized graft in a collagen scaffold. The scaffold holds the graft particles together, allowing for easier handling and special orientation in the grafted site. It is soaked in blood and replaced by invading granular tissue and newly forming vasculature. Unlike Bio-Oss Collagen®, the CO graft particles are synthetic; their composition resembles the biphasic Straumann Bone Ceramic ® grafting material.

The composition of CO is demonstrated in the cross-section in Figure 2-2 The collagen component is white, and the BCP phase is stained with methylene blue for demonstration purposes. The periphery and the apical portion of CO are mouldable to

allow better adaptation to various defect sizes. The collagen content also provides primary haemostasis.

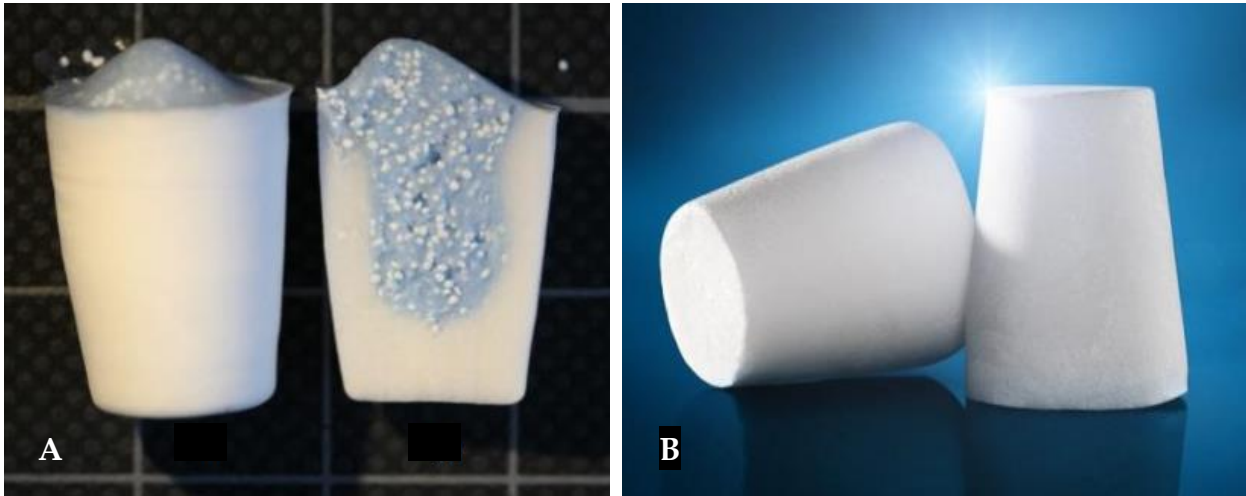


Figure 2-2 PARASORB Cone Oss® and Cone®

Both materials have conical shape; Cone Oss® is essentially a Cone® filled with biphasic calcium phosphate (BCP) granules

A. Cone Oss®. The BCP phase is stained with methylene blue for demonstration purposes.

B. Cone®

2.2.4 PARASORB Resodent® (Resorba Wundversorgung GmbH, Nürnberg, Germany)

PARASORB Resodent® is a commercially available resorbable type I collagen membrane (Figure 2-3). The collagen is non-cross linked and manufactured by the complete reconstitution of equine collagen. Unlike porcine or bovine collagens, the equine origin does not give rise to religious concerns, such as in Muslim or Hindu populations. PARASORB Resodent® collagen membrane contains 2.8 mg native collagen fibrils per 1 cm². According to the manufacturer, unlike Geistlich Bio-Gide®, both sides of the PARASORB Resodent® membrane can be applied to the surgical site.

A new package of 22x25mm of PARASORB Resodont® was opened for each animal and trimmed to the size of the defect, prior to placement over sites grafted with CO.



Figure 2-3. PARASORB Resodont®. Courtesy of RESORBA®

2.2.5 Bio-Oss® (Geistlich Pharma AG, Wolhusen, Switzerland)

Geistlich Bio-Oss® (BO) is a xenograft from bovine origin. BO is probably the most extensively studied bone substitute material in dentistry^{309, 310}. Multiple groups use this material as a positive control to test novel products in humans and animals ^{161, 201, 203, 206, 281}.



Figure 2-4. Geistlich Bio-Oss® (A) and Bio-Gide® (B). Courtesy of Geistlich Pharma

Commercially available 0.5 g packages of BO were used in the experiment (Figure 2-4). For every surgical site, a new package was opened, a standardized measured amount of BO was dispensed in a 0.8 ml Dappen dish, then mixed with the saline and used for grafting.

2.2.6 Bio-Gide® (Geistlich Pharma AG, Wolhusen, Switzerland)

The Bio-Gide® membrane is a resorbable collagen membrane of porcine origin. The membrane is produced without chemical additives or further cross-linking. Bio-Gide® has a bilayer structure with the smooth, cell-occlusive side, and the rough, cell-permeable side which should be facing the graft. Bio-Gide was used in a single layer over the sites grafted with BO. A new package of 25x25mm of Bio-Gide® was opened for each animal and trimmed to fit the surgical site prior to placement.

2.2.7 Allocation and randomization

Each animal received all four treatment modalities: one positive control with BO and Bio-Gide®, and three test modalities with CN, CO and SB as described above.

The sites for grafting in all animals were allocated prior to the intervention. To eliminate a possible bias from the consistent placement of specific grafting material in specific sites, the allocations were rotated for every subsequent animal as presented in the Table 2-1.

Table 2-1 Allocation of experimental materials

Sheep	Left anterior	Left posterior	Right anterior	Right posterior
412	CO†	BO†	SB†	CN†
413	CN	BO	CO	SB
414	SB	CN	BO	CO
415	CO	SB	CN	BO
416	SB‡	CO	BO‡	CN
417	CN	BO	CO	SB
418	SB	CN	BO	CO
419	CO	SB	CN	BO
420	BO	CO	SB	CN
421	CN	BO	CO	SB
409	SB	CN	BO	CO

CO – PARASORB Cone Oss®; **BO** – Geistlich Bio-Oss®; **CN** – PARASORB Cone®; **SB** – IBI SmartBone®

† - The allocation for the first operated animal was arbitrarily chosen. We decided to use more organised allocation scheme for the subsequent animals.

‡ - Due to operator error, the grafting materials placed in two sites were different from the pre-defined scheme

The study design is summarized in Figure 2-5

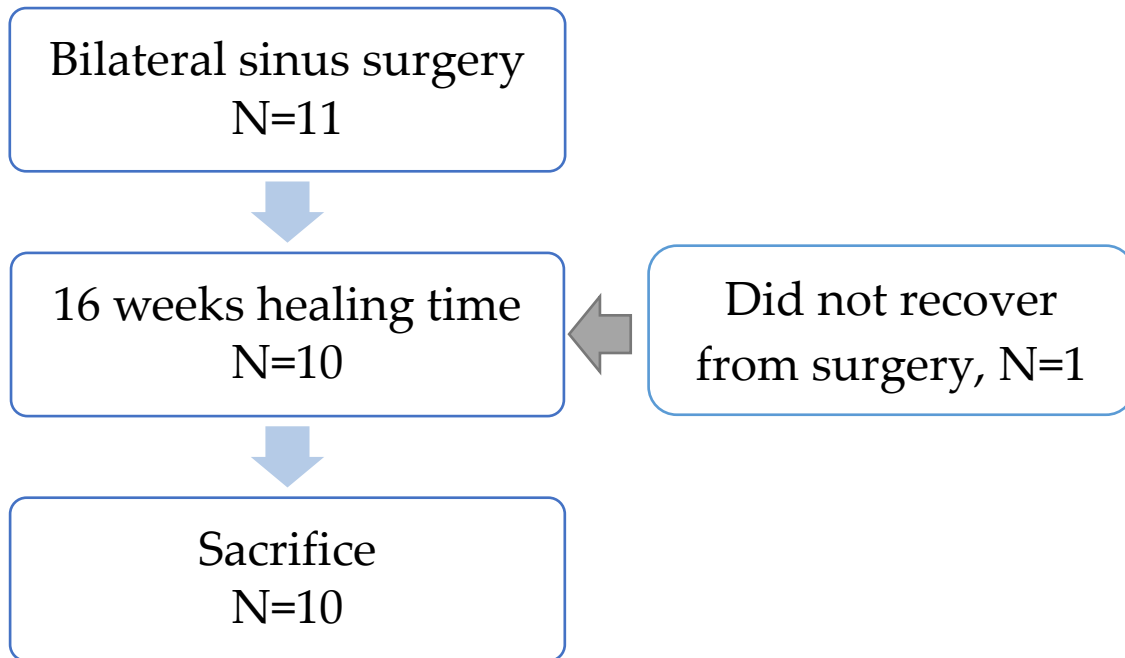


Figure 2-5 Study design diagram

2.3 Surgical protocols

2.3.1 Surgical grafting procedure

All grafting procedures were performed in Invermay Agricultural Research facilities between 3rd and 13th of February 2015.

2.3.1.1 General Anaesthesia

We pre-medicated all experimental animals with antibiotics (trimethoprim, Amphoprim® injection 1ml/15kg, Virbac New Zealand Ltd., East Tamaki, Auckland) prior to the intervention. We induced the general anaesthesia by means of intravenous infusion of thiopentone 20mg/kg (Bomac Laboratories Ltd., Manukau City, Auckland). After placement of the sheep on a mobile operating table, an endotracheal tube was inserted via the oral route, an endotracheal balloon was inflated, and the tube was secured to prevent displacement. Anaesthesia was maintained with 1-2% halothane. We placed a gastric tube to decompress the stomach, and the gastric content was left to drain freely into a container placed beneath the surgical table. We used a pulse oximeter to monitor the vital signs of the experimental animal during the surgical procedure.

2.3.1.2 Pain control

Prior to intervention, we infiltrated the dedicated surgical site with local anaesthetic: 2 X 2.2ml of mepivacaine 2%, with adrenaline concentration 1:100000 (Scandonest®, Septodont, Ivoclar Vivadent Ltd., Auckland New Zealand). This prolongs the action of local anaesthetic and helps to control bleeding during the surgery.

After closing the surgical access wound with sutures, we administered 1 ml of Bupivacaine hydrochloride 0.5%, with adrenaline 1:200000 by local infiltration (Marcaine®; AstraZeneca, North Ryde, Australia) for post-operative pain relief.

2.3.1.3 Surgical procedure

After rotating the head of the animal onto the side, we shaved the wool over the surgical site, exposed the skin, then cleaned and disinfected the site with Betadine® solution (Alcon Laboratories, Inc. Rockville Pike, Bethesda, MD, USA). We used disposable sterile draping to cover the animal, except for the surgical site.

We adopted the surgical approach from Haas et al. (1998)¹²¹. We accessed the antral wall extra-orally. First, a para-median oblique sagittal skin incision about 6 cm in length was done to the subdermal level inferior to the lower eyelid, using the electro-surgical unit (NeoMed™ 3000A ESU, Solid State Electrosurgery Unit, USA).

After that, by using a combination of sharp and blunt dissection with electrocautery to control the bleeding, we exposed the masseter muscle and then separated about 1 cm of this muscle from its origin. Soft tissues were retracted. By gentle percussion on the antral wall, we verified the presence of the sinus space prior to outlining the osteotomy location with the trephine.

We created two osteotomies on each side of the animal, meaning a total of four experimental sites per animal (Figure 2-6). A circular bone window was demarcated in the anterior part of the exposed maxilla, using a cup-shaped trephine 10 mm in diameter, with saline cooling, without perforating the full thickness of the bone. The central part of the window was finally separated with a piezo-surgical device – Mectron® Piezosurgery 2 ultrasonic unit (Henry Schein Shalfoon™, Auckland NZ) – using the OT5 round diamond-coated tip.

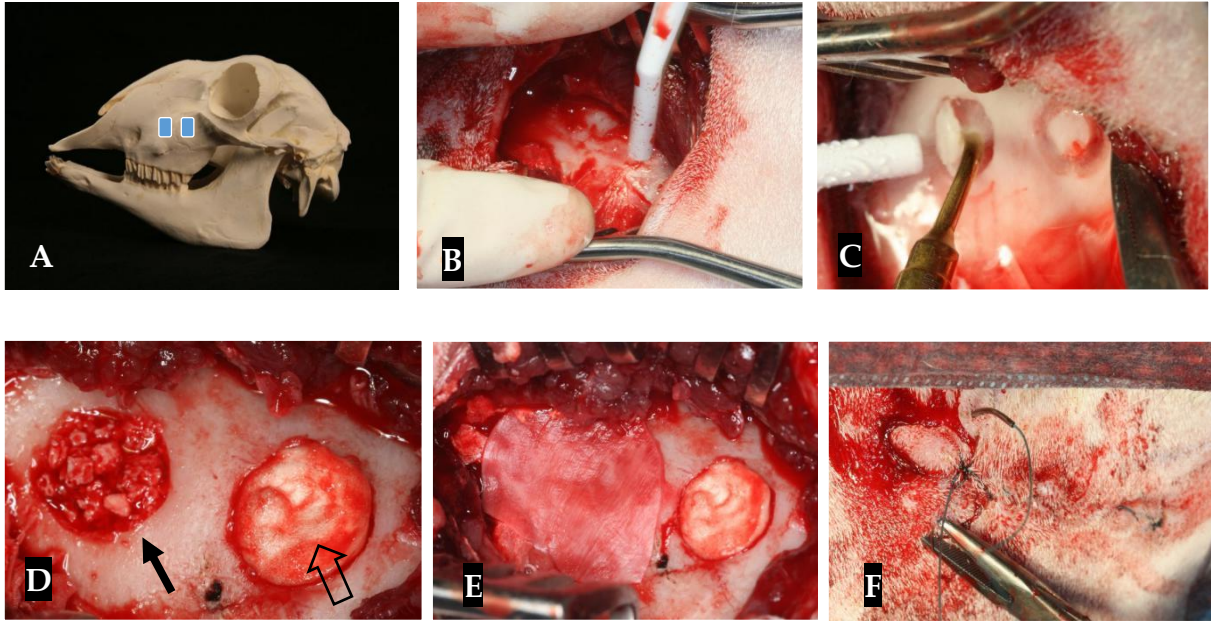


Figure 2-6 Surgical procedure

A – Surgical sites location. B – Soft tissue dissection. C- Osteotomy preparation. D – Grafting materials in place (black arrow – Bio-Oss®, empty arrow – Cone Oss®). E – Bio-Gide® membrane to cover the Bio-Oss®. F – Primary closure of the soft tissues.

The bone from the central portion of the osteotomy was detached from the Schneiderian membrane (SM), removed and discarded. The SM was elevated superiorly and distally using sinus membrane dissectors (Sinus Kit, Osstem™, Korea) and checked for perforations. We positioned the second osteotomy 8 mm posteriorly to the first one, and the Schneiderian membrane was also elevated and checked for perforations. If an SM perforation was identified, we used a barrier membrane to line the defect and prevent the grafting material from penetrating into the maxillary sinus according to the Loma-Linda pouch technique³¹¹. We used PARASORB Resodont® membrane, for the repair. Where sinus anatomy resulted in a limited available space due to a presence of septae or sinus hypoplasia, an alternative osteotomy was prepared in the same surgical site.

The pre-allocated material was placed under the elevated SM in the following manner: BO was mixed with saline prior to grafting. SB block was also mixed with saline and pounded in a Dappen dish to a particulated form, using a blunt hand instrument. CN and CO were transferred into the surgical site straight out of their sterile package. We took care not to deform the CN and CO. The grafting materials were described in the previous chapter, and are summarized in Table 2-2

Table 2-2 Summary of grafting materials and membranes

Name	Ingredients	Manufacturer
PARASORB Cone® (CN)	Resorbable equine collagen	RESORBA Medical GmbH (Germany)
PARASORB Cone Oss® (CO)	Resorbable equine collagen filled with biphasic (60% HA : 40% TCP) calcium phosphate granules	RESORBA Medical GmbH (Germany)
SmartBone® (SB)	Composite bone substitute made of deproteinized cancellous bovine bone coated with poly(L-lactide-co-ε-caprolactone) and gelatin	Industrie Biomediche Insubri SA (Switzerland)
Bio-Oss® (BO)	Deproteinized bovine cancellous bone	Geistlich Biopharma AG (Switzerland)
Bio-Gide®	Porcine collagen resorbable membrane	Geistlich Biopharma AG (Switzerland)
PARASORB RESODONT®	Equine collagen resorbable membrane	RESORBA Medical GmbH (Germany)

We placed a barrier membrane (Table 2-3) over the access window so that all membrane edges were supported by at least 5 mm of a sound bone. The muscle and fascia layers were repositioned and sutured using resorbable 3/0 polyglycolic acid sutures (PGA Resorba®, catalogue number PA1117, RESORBA Medical GmbH, Nürnberg, Germany). The dermis was sutured with synthetic resorbable monofilament Maxon® sutures (Medtronic™, Minneapolis, US).

Table 2-3 Use of membranes in surgical sites

Type of grafting material	Membrane to cover the access window
Bio-Oss®	Bio-Gide®
PARASORB Cone Oss®	PARASORB RESODONT®
PARASORB Cone®	PARASORB RESODONT®
SmartBone®	PARASORB RESODONT®

2.3.1.4 Post-surgical management

Halothane was stopped, and the animal was extubated and moved to a separate individual recovery area for a few hours under the monitoring of the veterinary technician.

For three days following the surgery, the sheep were kept in a designated paddock, where they were monitored and received postoperative regimen. During this period each animal received:

- Mouth-rinse once a day with 30ml of 0.2% w/v chlorhexidine gluconate solution (Savacol®, Colgate-Palmolive, NZ)
- Subcutaneous injection of anti-inflammatory medications, 5ml carprofen (Rimadyl® injection 50mg/ml, Zoetis, Mt Eden, New Zealand) once a day
- Subcutaneous injection of antibiotics (Trimethoprim 1ml/15kg) once a day.

After three days of intensive postoperative care, the experimental animals were returned to pasture and were allowed to graze freely for the duration of the healing period. Sequential weight measurements were taken to confirm normal recovery.

2.3.2 Sacrifice

After 16 weeks of healing, the experimental animals were brought to the AgResearch Invermay facilities to be euthanised.

General anaesthesia was induced in the same way as during the initial surgical procedure. The animals were placed on an operating table in a Trendelenburg position (supine position, with the legs being higher than the head) with the neck overextended. The skin was incised along both sternocleidomastoid muscles, and the external carotid arteries were exposed by blunt dissection. Each artery was cannulated with a 14G catheter (Optiva TM, Smiths Medical, UK) and the catheters perfused with normal saline (0.9% Sodium chloride, Baxter Healthcare Ply Ltd., NSW Australia) to prevent obstruction.

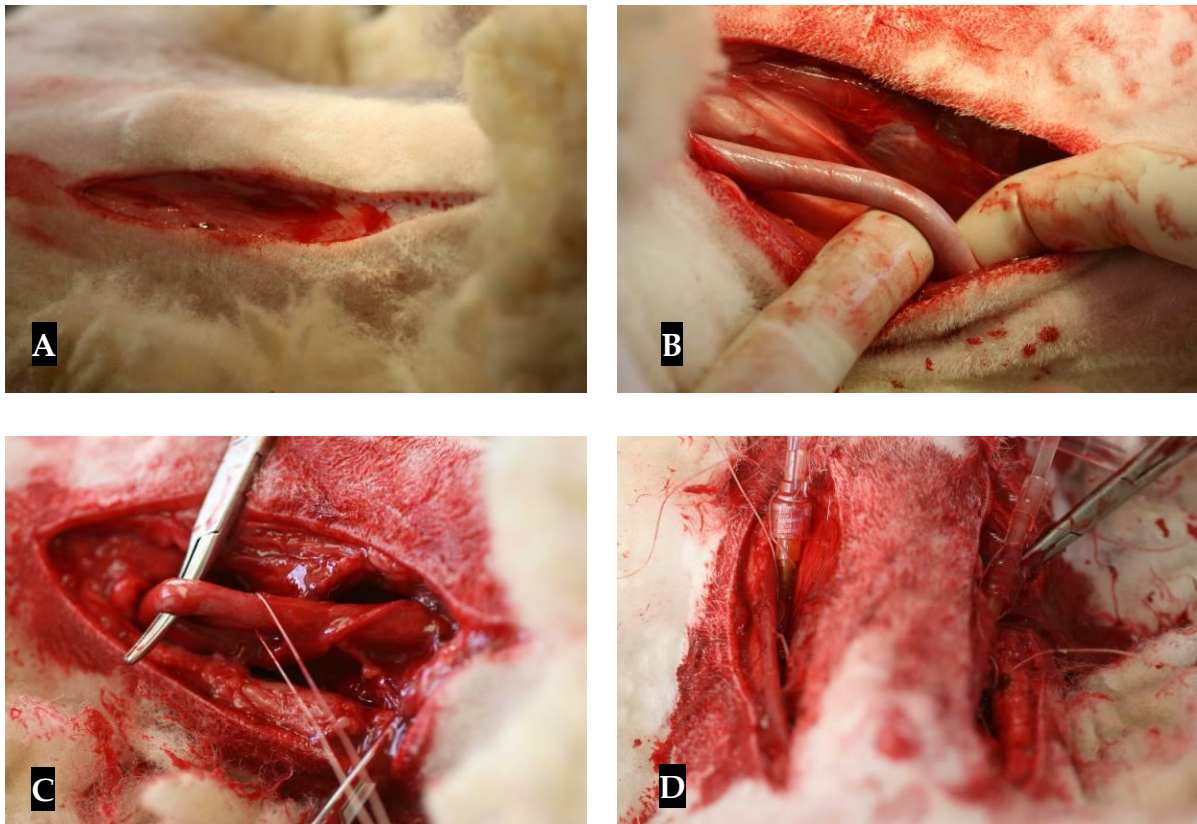


Figure 2-7 Exposure and cannulation of external carotid arteries

A – initial incision; B – external carotid artery exposed; C – external carotid artery ligated; D – both external carotid arteries cannulated

Both catheters were secured with silk sutures to prevent their displacement. The external carotid arteries were ligated around the catheters to prevent the back-flow of the perfusing solution (Figure 2-7).

After the catheterization was finished, each catheter was perfused with 1 L of normal saline (0.9% Sodium chloride, Baxter Healthcare Pty Ltd., NSW Australia) and 1.5 ml of 5000 IU heparin. After heparin perfusion, the animals were killed by an overdose of halothane for 2 minutes. The animals were then extubated, the carotid arteries were perfused with 1 L chilled formalin fixative per side, using 10% neutral buffered formalin (NBF) (BioLab Ltd., New Zealand). Both jugular veins were severed with a scalpel blade, and the heparinized blood was allowed to drain into a container on the floor.

Once the operated sites were identified, maxillary sinus specimens were retrieved by en-bloc resections, rinsed with water, and placed into individual plastic containers. The containers were filled with 10% NBF, sealed and labelled.

2.4 Histologic sections preparation

2.4.1 Trimming

The anatomical orientation of the specimens was marked by inserting a silk suture in the anteroinferior position. The blocks were trimmed to a roughly rectangular shape and fitted into the perforated plastic cassettes 5 x 10 x 1.5 cm.

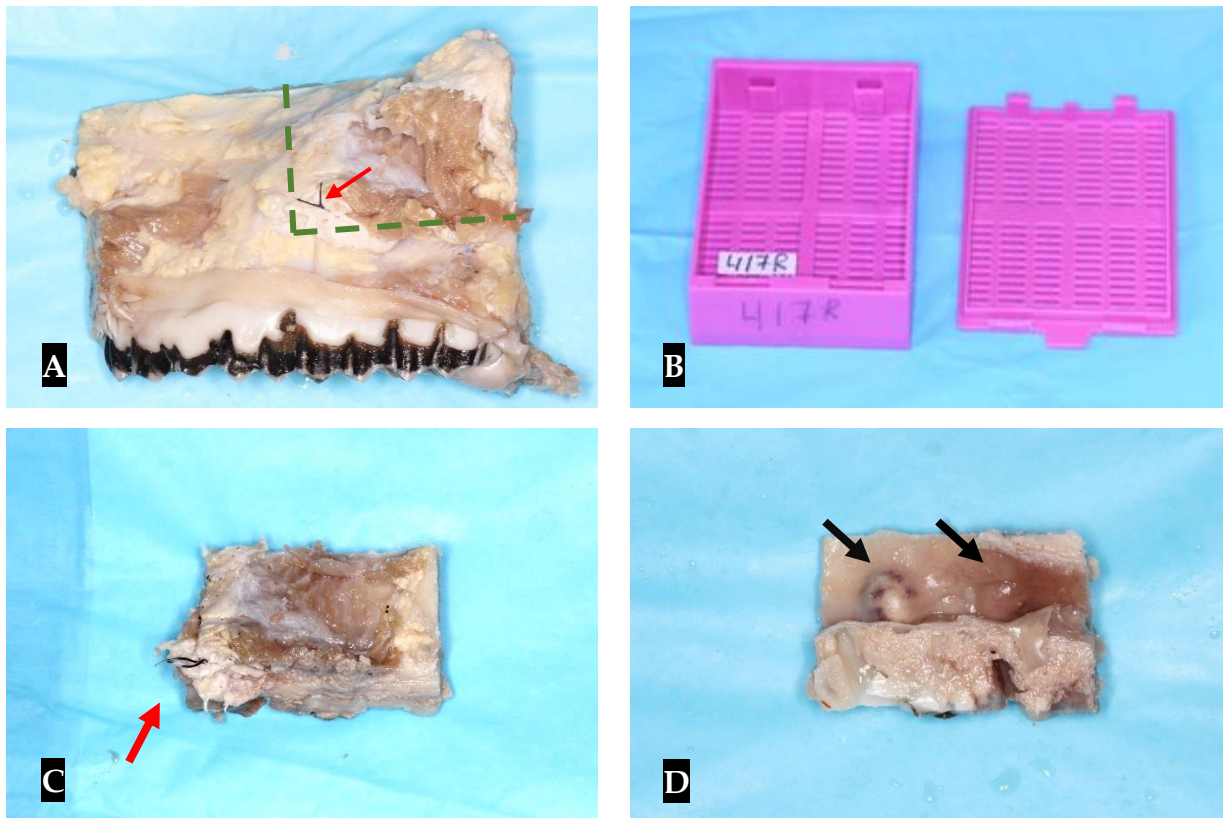


Figure 2-8 Trimming and labelling of specimens

A – Untrimmed specimen. (green dashed line – trimming outline; red arrow – silk suture indicating the anteroinferior corner of the trimmed specimen)

B – The labelled specimen cassette with a pencil-marked paper label

C – Trimmed specimen (red arrow – silk suture indicating the anteroinferior corner of the trimmed specimen)

D – Antral surface of the specimen from C. Black arrows – grafted sites

These cassettes were chemically stable and non-dissolvable in any of the solutions which were used during processing. They also served as label holders for specimens during processing. The cassettes were labelled with pencil writing on the outside (Figure 2-8).

2.4.2 Resin embedding

In order to perform non-demineralized histology, the tissues must be resin-embedded. The protocol for resin-embedding was initially described by Donath and Breuner³¹². It was further modified and refined by Duncan²⁷⁸. A recent project by our institution³⁰³ followed this modified version, which was fully adopted for this study, and is attached as Appendix II. The labelled cassettes, each containing one specimen, were placed in a covered glass container under a fume hood. The tissues were dehydrated, cleaned, and embedded using the following steps:

1. 20 % ethanol-water solution. The ethanol solution was changed after 2 days and then after 2 more days changed for 40% ethanol
2. 40% ethanol-water solution for 2 days
3. 75% ethanol-water solution for 2 days
4. 95% ethanol for 6 days; the solution was replaced after 2 and 4 days
5. 100% isopropanol for 6 days on an oscillating platform; the solution was replaced after 2 and 4 days
6. Xylene (Ajax Finechem Pty Ltd, New Zealand) for 6 days on an oscillating platform; the solution was replaced after 2 and 4 days
7. Washed with methyl meta-acrylate (MMA) monomer (Sigma Aldrich, USA), then put in activated MMA II solution (four parts MMA monomer, one part dibutyl phthalate and 0.5% benzoyl peroxide) for 2 days on an oscillating platform.

The cassettes with the specimens were washed again with MMA I monomer, after which the specimens were retrieved and placed into hermetically closing individual jars with a pre-set MMA-III (4 parts MMA monomer, 1part dibutyl phthalate and 1% benzoyl peroxide) base. These jars were filled with MMA-III to a depth of 8-10mm one week prior to the embedding process, to allow the MMA-III base to set. The paper label was transferred from the cassette to the jar, together with each specimen.

The jars with the specimens were then fully filled with MMA-III solution. They were left to set in a cold-water bath and covered from light to slow down the exothermic polymerization reaction. If too fast, the polymerization may produce gas bubbles which may damage the specimen.

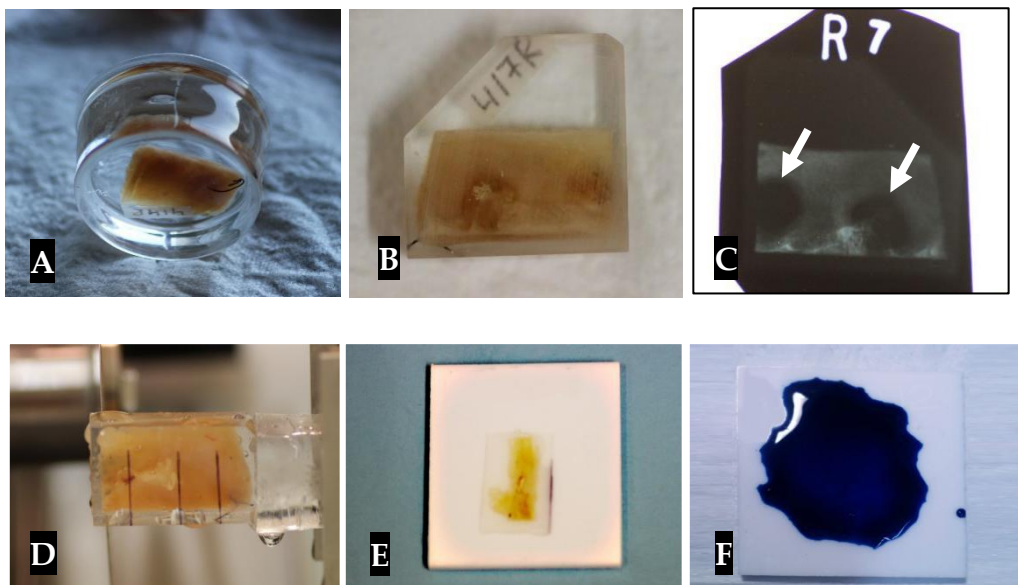


Figure 2-9 Sectioning and staining of the specimens

A – MMA-embedded specimen retrieved from the glass jar. B – specimen trimmed to a shape. C – orientation radiograph indicating two surgical sites (white arrows). D – slicing of the specimen into coronal sections using a precision microtome with a diamond wheel. E – the sliced coronal section is mounted onto a white opaque acrylic slide using cyanoacrylate glue. F – ground section is stained with McNeal's tetrachrome solution.

When the setting process was completed, the glass jars were broken to retrieve the acrylic resin blocks containing the tissue specimens (Figure 2-9). To simplify the slicing of the specimens, these blocks were trimmed down and polished to a rectangular shape with at least 2-3 mm of acrylic resin surrounding the embedded specimen. The trimmed blocks were marked with the specimen's identification code, using a permanent marker.

2.4.3 Slide preparation

The radiograph of all the trimmed acrylic blocks was done to outline the area of interest for sectioning (see Appendix V). The sectioning of the acrylic resin blocks (Figure 2-9) was done using Struers Accutom precision table-top microtome (Ballerup, Denmark) fitted with a diamond cutting wheel (MOD 13 127x0.4x12.7mm): Sequential sections 700 µm wide were sliced; each section was mounted onto a white opaque acrylic slide using cyanoacrylate glue (MDS Adhesive QX-4, MDS Products Inc, Laguna Hills, CA, USA); the slides were then engraved with the specimen identifier using a straight dental hand-piece with a round bur.

Between six and twelve coronal sections were cut from each specimen, depending on graft area anteroposterior width. Two coronal sections representing the central area of the grafted site were chosen for further processing.

The selected sections were ground and polished from an initial 700 µm to microscope-suited 80-100 µm using a Tegra-Pol rotary grinding machine (Struers, Ballerup, Denmark) and Silicon Carbide Paper (grit size #180 to #4000). The width of the sections was verified with a digital micrometre (Digital Indicator, Mitutoyo, Japan).

2.4.4 Staining

The mounted slides were immersed in 20% ethanol in the ultrasonic bath for five minutes to remove the debris and clean the surface. The specimens were immersed in

1% formic acid in an ultrasonic bath for five minutes to allow for the stain penetration into mineralized tissues. The sections were then stained with a mixture of one-part MacNeal's tetrachrome (methylene blue, azure II and methyl violet) and two-parts toluidine blue. MacNeal's tetrachrome stain was originally developed to stain blood films³¹³; it is classified as a neutral dye in which one of the components is acid and colours cytoplasm, the other is basic and colours nuclei, cartilage, mast cells, and acid mucins³¹⁴. The modification of MacNeal's stain with toluidine blue was described by Schenk in 1984³¹⁵. The resulting stain colours the calcified bone and its components in shades from dark to light blue³¹⁶.

The staining protocol is described in further detail in Appendix III. The stained slides were then rinsed with distilled water and left to be air-dried overnight on a bench-top.

2.5 Histomorphometric analysis

2.5.1 Imaging of histologic sections

For histological analysis, high-resolution images were obtained using a light microscope (Olympus AX70, Olympus Optical Co. Ltd, Japan) and an imaging system (Micropublisher 5.0 RTV, Qimaging) at 10x magnification. Only a small portion of a full section is visible at this magnification; therefore, to obtain a complete scan of a section, a montaging technique was employed.

Each section was scanned as a series of 20-80 images (depending on the size of the section) with a 10% overlap between the adjacent areas, using the Volocity 5.2.0 (Improvision, MA, USA) montaging software. The image series was then stitched together into a single panoramic scan in Autopano Pro 2.5.2 (Kolor, USA), which automatically detects the matching points in the overlapping areas of the individual images.

2.5.2 Histomorphometric analysis

2.5.2.1 Region of interest

The present study aimed to investigate the graft consolidation and a new bone formation in the augmented sinus. Therefore, the area between the sinus wall to the Schneiderian membrane was included in the region of interest (ROI) for analysis. For reproducibility of results, the following guidelines were implemented when outlining ROI for each specimen:

1. A straight-line tangent to medial margins of repairing sinus walls was drawn.
2. Two perpendicular lines tangent to the most distal hard tissue formations (graft or new bone) in the augmented area were marked.

3. A third line following the Schneiderian membrane connected the previously charted perpendicular lines.

A representative slide with ROI is shown in Figure 2-10

2.5.2.2 Histomorphometry

The percentage of area within the ROI occupied by hard tissue was determined for each slide. McNeal's tetrachrome stains the newly forming bone with greater intensity than the mature bone due to a higher glycosaminoglycan content in the newly forming bone. The differences in staining were used to digitally section images into areas occupied by graft, new bone and connective tissue.

The image was sectioned into the graft, new bone and connective tissue sections (Figure 2-10) using a combination of:

1. Automatic selection with colour threshold plugin (version 1.16 by Gabriel Landini, visit <http://www.mecourse.com/landinig/software/software.html> for details) of image analysis computer software, ImageJ (version 1.51n, National Institute of Health, USA), and
2. The tracing tool of ImageJ software.

The colour threshold plugin automatically selects all pixels specified by their colour. By manually adjusting the colour thresholds the graft and the new bone were selected separately. Due to variability in staining of the specimens and difference in the thickness of various parts of histologic slides it was not possible to fully rely on this automatic selection. The integrated tracing tool of ImageJ was used to add areas missed by automatic thresholding manually. This tool selects adjacent pixels within a certain predetermined range in colour. Connective tissue area was calculated by subtracting the graft and the new bone areas from the total area of the region of interest.

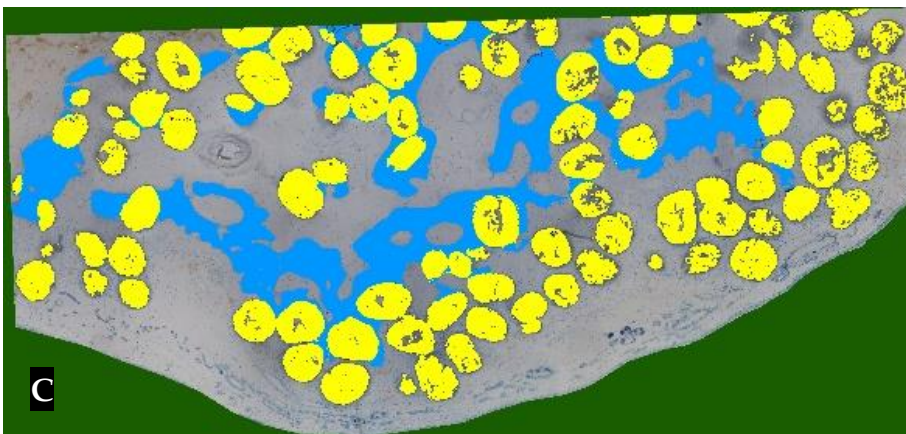
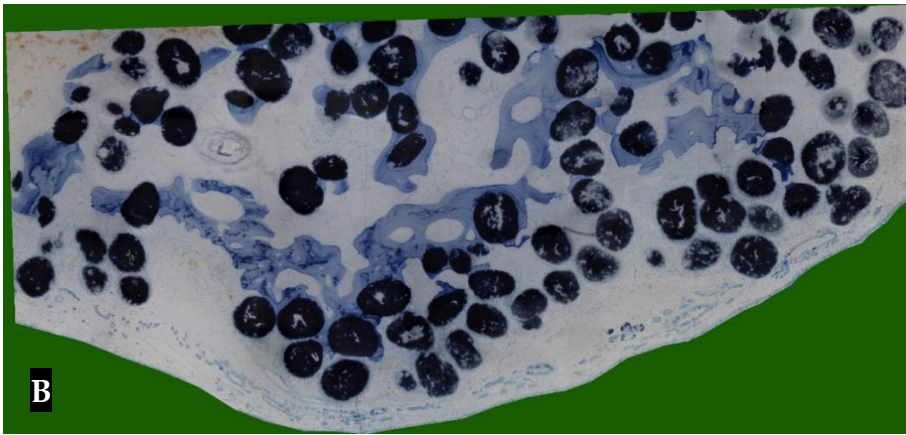
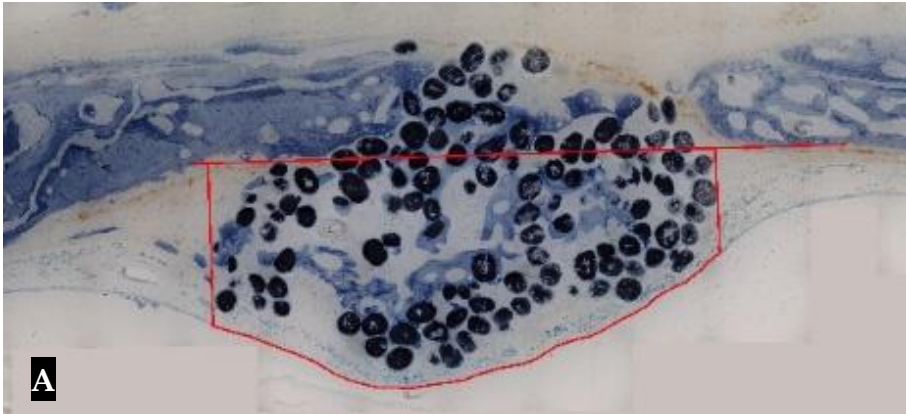


Figure 2-10 Histomorphometric analysis

A – the overview of the specimen with ROI outlined by red lines. B – magnified view of the ROI. C – image sectioned into residual graft (yellow), new bone (blue) and connective tissue (uncoloured)

2.5.3 Statistical analysis

Two sections per surgical site were chosen to reduce a possible bias of having a mal-positioned section. The average between the two sections was used for statistical analysis as the representative value for the respective grafted site.

Mean values and standard deviations were calculated for all outcome variables. Non-normal distribution was observed within groups, and the Wilcoxon signed rank test was planned to compare between groups. Differences were considered statistically significant when two-sided p was <0.05 . The statistical analysis was performed with IBM® SPSS® software (version 23, International Business Machines Corp., Armonk, New York, United States).

Chapter 3. Results

3.1 Handling properties of grafting materials

3.1.1 PARASORB Cone®

Cone® (CN) can be easily removed from its packaging using tweezers. The material is spongy with high plasticity. It can easily be moulded into the desired shape and inserted into the dedicated surgical site. CN should be handled with dry gloves and instruments, as premature contact with blood will cause it to lose rigidity, thus making the insertion into the dedicated site more challenging.

Compared to particulate grafts, the sub-membrane space created by CN is more defined by its conical shape. While it was easier to insert CN than BO, the operator had only limited control of the augmentation.

3.1.2 PARASORB Cone Oss®

PARASORB ConeOss® (CO) is essentially CN with alloplastic filler. The handling properties of CO was similar to those of CN.

3.1.3 SmartBone®

SmartBone® (SB) used in the study came in the shape of a porous cube 10 x 10 x 10 mm. It was easily retrieved from its packaging and manipulated. The material was porous but rigid. By grinding or cutting it could be adapted to a desired shape, however, it was impossible to pre-shape the cube to fit the sinus space due to the complex and unclear morphology of the recipient site. Therefore, the cube was soaked in saline and crushed into a gel-like state with a blunt instrument prior to being grafted.

3.1.4 PARASORB RESODONT® membrane vs Bio-Gide®

PARASORB RESODONT® is made of reconstituted equine type I collagen, whereas Bio-Gide® is composed of porcine type I collagen. Bio-Gide® membranes have two distinct surfaces: cell occlusive and cell permeable, which determines the correct placement - the rough, cell permeable surface is placed towards the graft. PARASORB RESODONT® has two identical surfaces, and applying a specific surface towards the bone is irrelevant. Compared to Bio-Gide ®, RESODONT® was more rigid and less adhesive to the bone, soft tissues, and itself, and therefore it was easier to handle under the wet conditions of a surgical site.

3.2 Post-operative healing

The first animal that received the surgical intervention (number 412) failed to recover from the procedure. Despite recovering from general anaesthesia, it could not get up on its feet, feed or drink. It was assessed by the veterinarian and diagnosed with gastrointestinal complications due to a protracted surgery (about 6 hours). This animal was euthanized to prevent further suffering. The grafted sites from the euthanized animal were excluded from the analysis, thus reducing the study sample to a total of 10 animals.

We shortened the time on the operating table for all subsequent animals. These animals recovered from the procedure with no complications. They were medicated and closely monitored before their release to pasture. All surgical sites healed uneventfully for 16 weeks following the grafting procedure. The soft tissue healing was complete for all the surviving animals.

3.3 Descriptive histology

3.3.1 Dermis and mucosa

The healing of soft tissues was similar for all the grafting materials and experimental sites.

3.3.1.1 Epidermis

The layers of epidermis, dermis, muscle and fascia covering the antral wall were macroscopically intact. The cells and the extra-cellular matrix of the dermis were only lightly stained with McNeal's tetrachrome solution. Therefore more in-depth descriptive analysis was not performed.

3.3.1.2 Mucosa and submucosa

The mucosal lining of the sinus wall, the Schneiderian membrane, presented as a single layer of pseudostratified columnar ciliated epithelium with multiple goblet cells. In proximity to the basal membrane, the submucosa was highly vascular. The vascularity was gradually diminished towards the deeper layers of lamina propria. Multiple mucinous glands in the immediate submucosa were well-stained and easily identified (Figure 3-1).

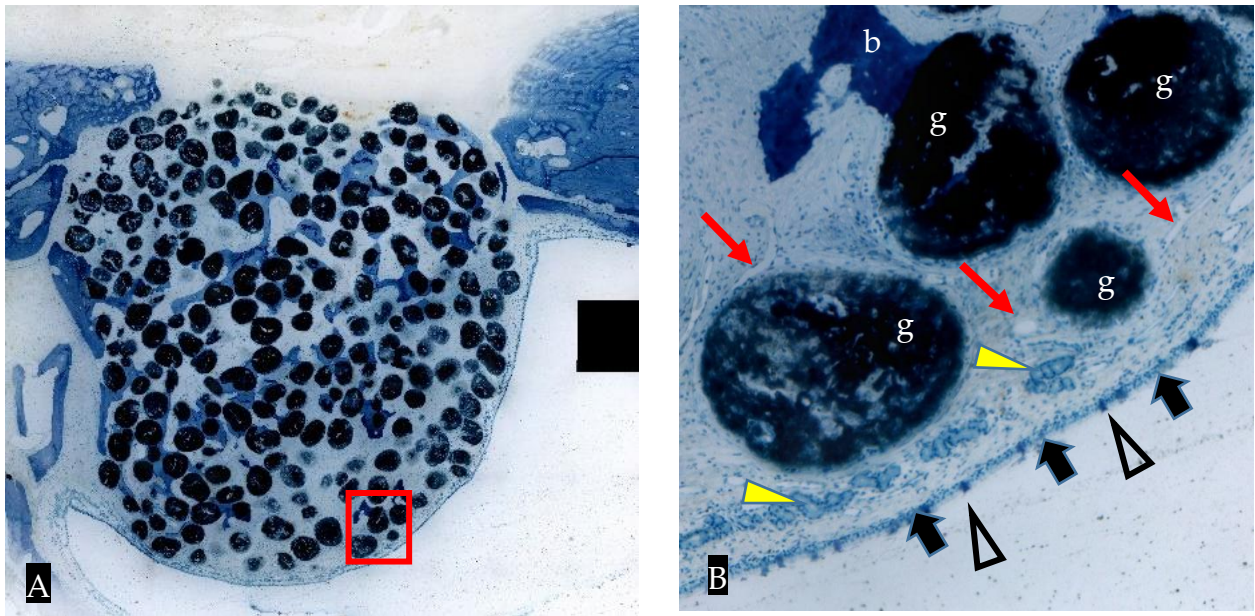


Figure 3-1 Schneiderian membrane and submucosa (CO site, specimen 409)

A. Overview of the specimen. Red rectangle outlining the position of B

*B. Mucosa and submucosa (x4 magnification). **b** – new bone; **g** – graft; **black arrows** – Schneiderian membrane; **empty arrowheads** – goblet cells; **yellow arrowheads**– mucous glands; **red arrows** - capillaries*

The epithelial lining of the sinus was uninterrupted in all specimens, but there was one CO site (from the animal 414) where the membrane appeared to be disrupted, and the particles of graft were seen outside the boundaries of SM. During the grafting surgery, no perforations were detected at that site.

Four SM perforations less than 5 mm were detected during the surgery in two animals. They were repaired as described in section 2.3.1.3 using barrier membrane (Table 3-1). We discovered that the grafting material disappeared completely from three of these sites and no extra-skeletal bone formed.

Table 3-1 Schneiderian membrane perforations and outcomes

Sheep	Site	Materials for repair	Histologic outcome
413	Bio-Oss®	RESODONT®	Successful augmentation, irregular SM.
417	Bio-Oss®	RESODONT®	Failed augmentation
417	Cone Oss®	RESODONT®	Failed augmentation
417	SmartBone®	RESODONT®	Failed augmentation

In several specimens, the epithelium lining appears to be irregular, containing multiple invaginations and evaginations. These specimens also presented with higher vascularity, and denser infiltrate of PMNs in the submucosa. The inflammation was not quantified as the McNeal’s tetrachrome staining is not optimal for immune cell identification and counting.

3.3.2 Access window

New bone formation between edges of the surgical wound in the bony walls of the sinus was evident in all specimens. For all treatment modalities, the newly formed bone (NB) was evident on both antral and facial sides of the original cortical bone plates. NB could be identified by darker staining, less regular structure, thin elongated trabeculae, and large marrow spaces. In 8 out of 10 BO grafted sites, 7 out of 10 CO sites, 8 out of 10 CN sites, and 2 out of 10 SB sites the surgically cut edges were impossible to locate with confidence due to remodelling and replacement by the new bone structures (Figure 3-2).

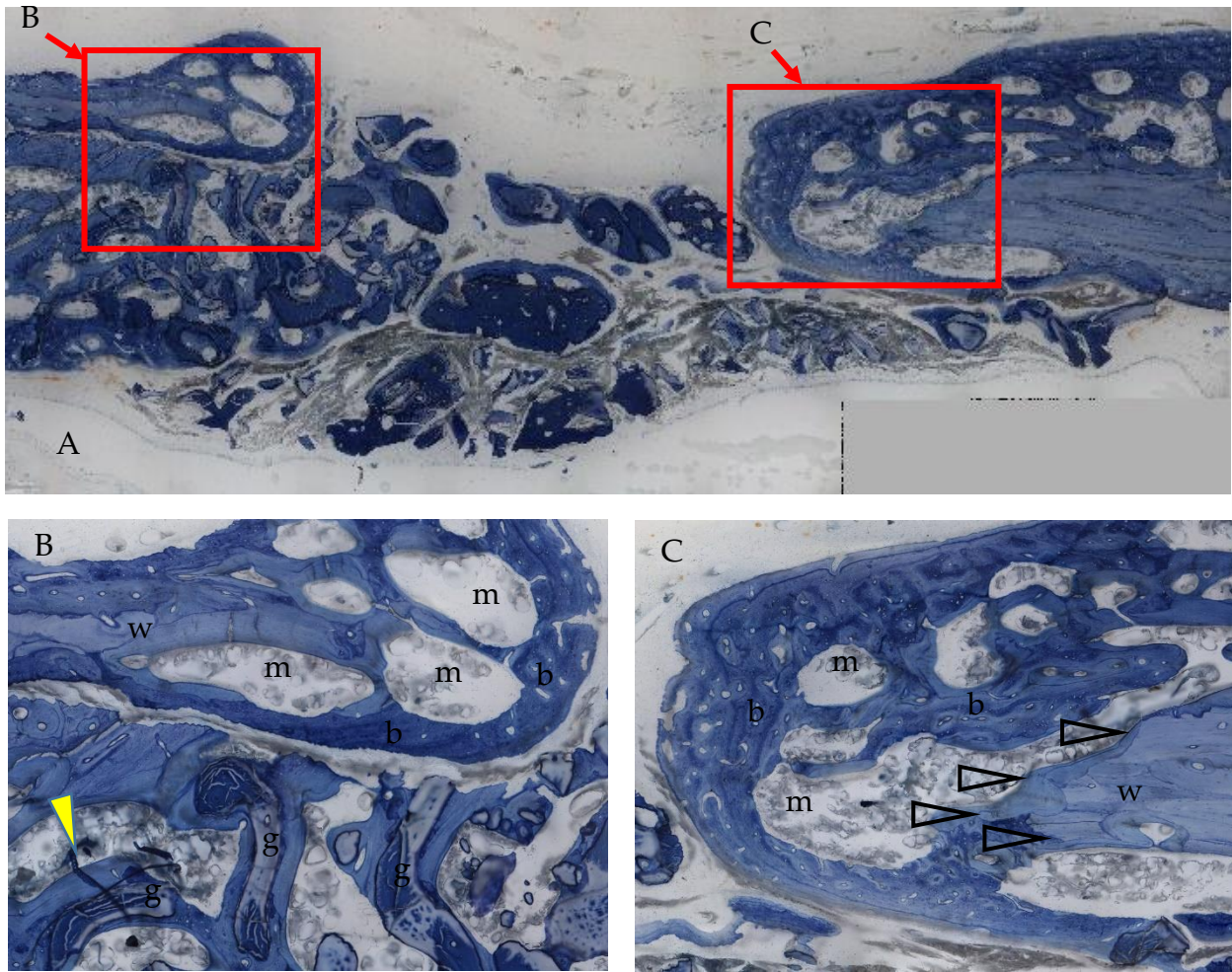


Figure 3-2 Healing of the surgical access window (BO grafted site, specimen 419)

- A. Overview. Red rectangles represent the positions of magnified B and C slides
- B. Exuberant healing and remodelling of the sinus wall. The original bone plate margins are difficult to identify (*w* – original sinus wall under remodelling; *b* – new bone; *m* – marrow spaces; *g* – xenograft particles; **yellow arrow** – artefact).
- C. Exuberant healing and remodelling of the sinus wall. The original bone plate margins are easy to identify (**empty arrowheads** - original sinus wall under remodelling; *b* – new bone; *m* – marrow spaces).

The initial access size was outlined with a 9-mm round cup-shaped trephine bur; however, this wasn't standardized between all sites due to the use of a piezosurgical device to finalize the access window separation. Hence, for multiple specimens the

initial size of the defect was difficult to determine; the statistical inter-group analysis was not performed for initial defect size and healing (Table 3-2).

Complete repair of the access window was evident in two specimens (1 BO, 1 CO). The mean residual gap was 3.7 mm; the differences between groups were not statistically significant (Table 3-2).

Table 3-2 Repair of surgical defect in the wall of the sinus

	BO (SD)	CO (SD)	CN (SD)	SB (SD)
Initial defect size, mm †	8.5 (1.7) n=7	7.9 (1.7) n=3	10.4 (2.7) n=5	10.1 (1.5) n=8
Residual defect size, mm *	4.0 (2.3) n=10	2.9 (2.1) n=10	4.5 (1.3) n=10	3.47 (2.5) n=10
Healing of the defect, percentage †	57% (22%) n=8 ‡	63% (29%) n=4 ‡	45% (22%) n=6 ‡	59% (20%) n=8

SD – standard deviation

† - statistical analysis not performed

‡ -in one sample a complete repair was observed, although the initial defect was not determined.

** - $p>0.05$ between all groups*

3.3.3 Augmented sites

In all specimens, the space between the mucosal lining and the bone wall of the sinus contained the submucosal connective tissue and the vasculature. In nine out of ten BO specimens and seven out of ten CO specimens an additional submucosal space was created by the grafting procedure, i.e. successful augmentation. This space contained the residual grafting material and the newly formed bone. In CN sites, no such additional space was found, and no residual grafting material was present. Among SB specimens, only one demonstrated additional submucosal space formation with residual grafting material and newly formed bone, i.e. successful augmentation.

Specific features were evident for sites augmented with CO, CN and SB.

3.3.3.1 Bio-Oss® sites

The sites grafted with BO presented as bell-shaped areas outlined by sinus membrane, under which the loosely packed residual graft particles were evident. In most cases, the residual Bio-Oss® particles were also found to be integrated within the newly formed bone of the sinus walls. In eight out of ten Bio-Oss® specimens woven and lamellar bone was found in direct contact with residual graft particles within the defined region of interest (Figure 3-2, Figure 3-3).

Upon closer examination at X10 magnification, multi-nuclear, osteoclast-like cells in formations resembling resorption lacunae were evident at the periphery and directly on the surface of the graft particles, suggesting osteoclastic resorption of the xenograft (Figure 3-3).

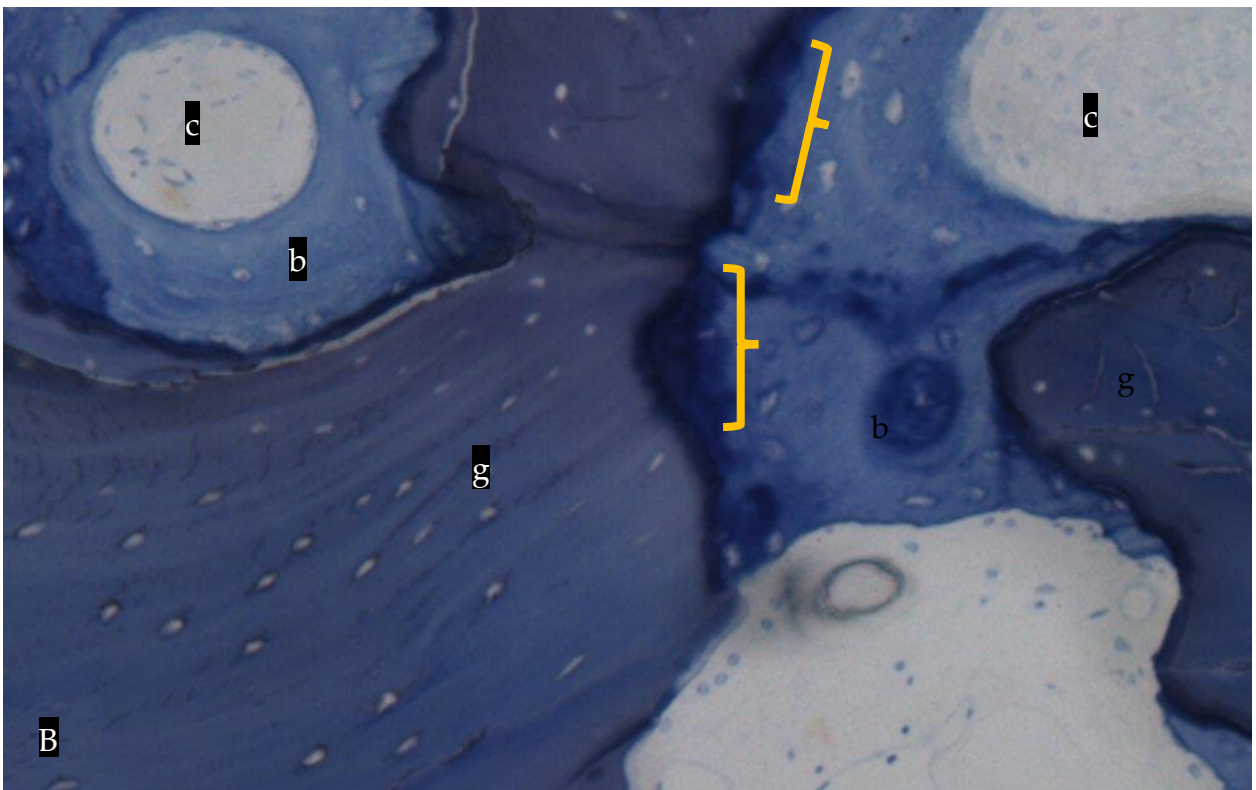
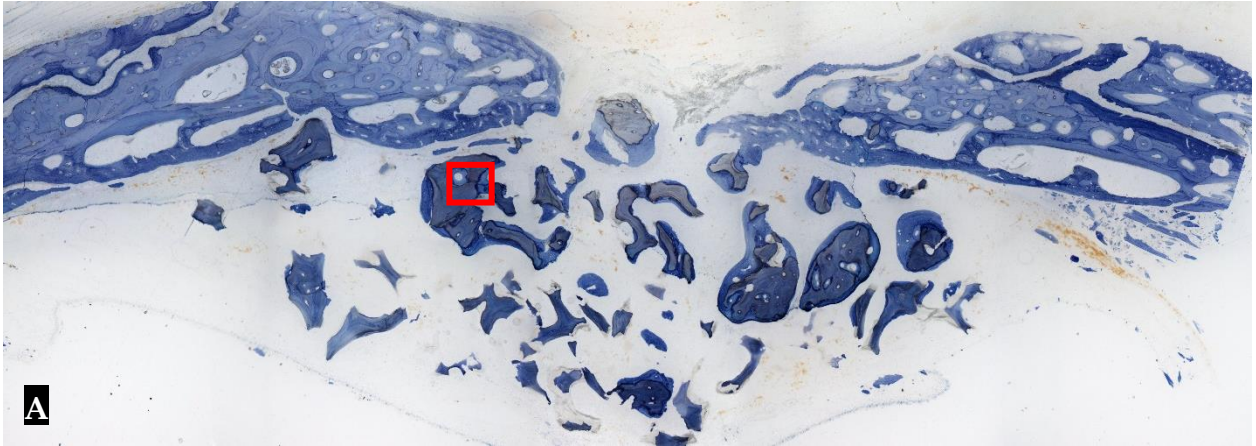


Figure 3-3 Bio-Oss® augmented site (specimen 414)

- A. Overview. Red rectangle represents the positions of magnified image in (B)
- B. Magnified X10 image of residual graft-new bone complex with resorption lacunae (**yellow braces** – resorption lacunae; **b** – new bone; **c** – connective tissue; **g** – xenograft particles)

3.3.3.2 PARASORB Cone Oss® sites

Similar to BO sites, the CO sites presented as bell-shaped areas outlined by sinus membrane. The residual graft particles in CO augmented sites were found to be tightly packed underneath SM, but the collagen matrix was completely resorbed and replaced by dense, cellular connective tissue. Newly formed bone appeared in five out of ten specimens of CO sites. Most of the new bone appeared in direct contact with the residual graft particles, both proximal and distant to the walls of the sinus. Due to the alloplastic particles' innate surface irregularity, it was impossible to determine whether osteoclastic resorption happened on the surface of the particles (Figure 3-4).

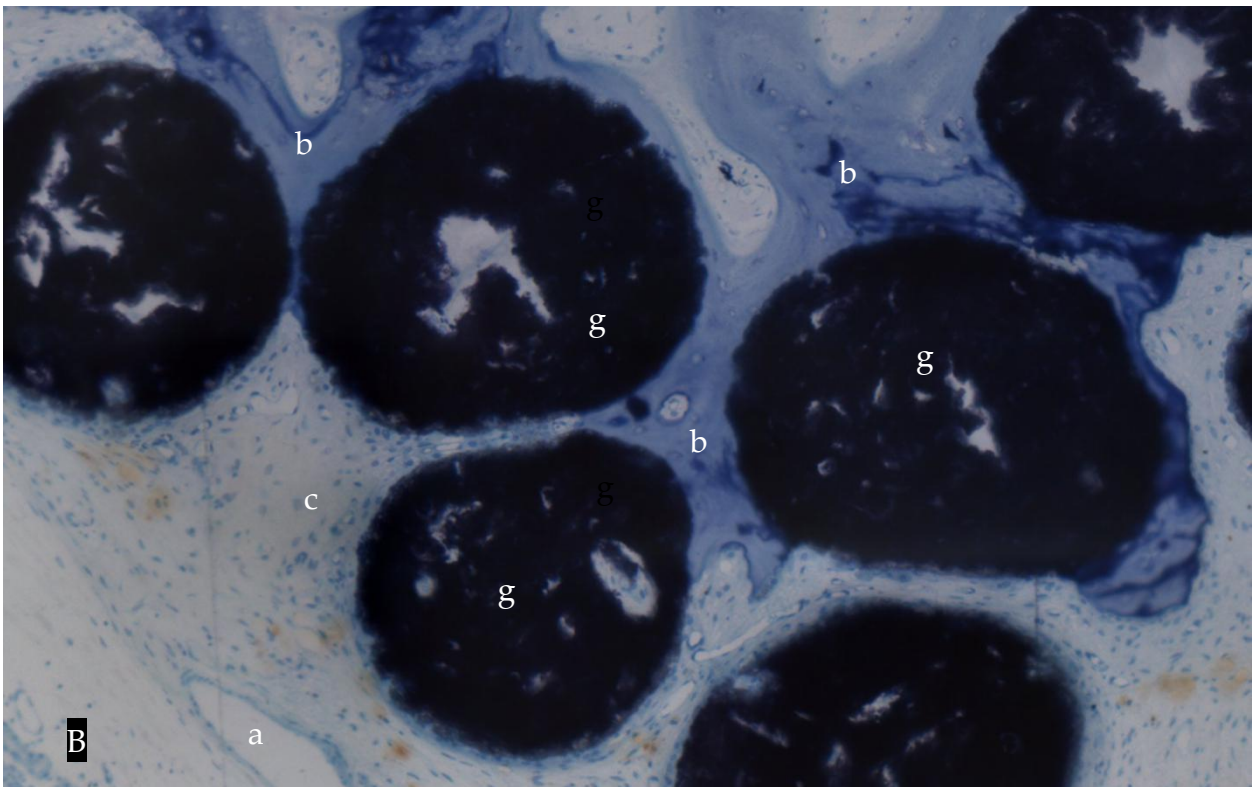
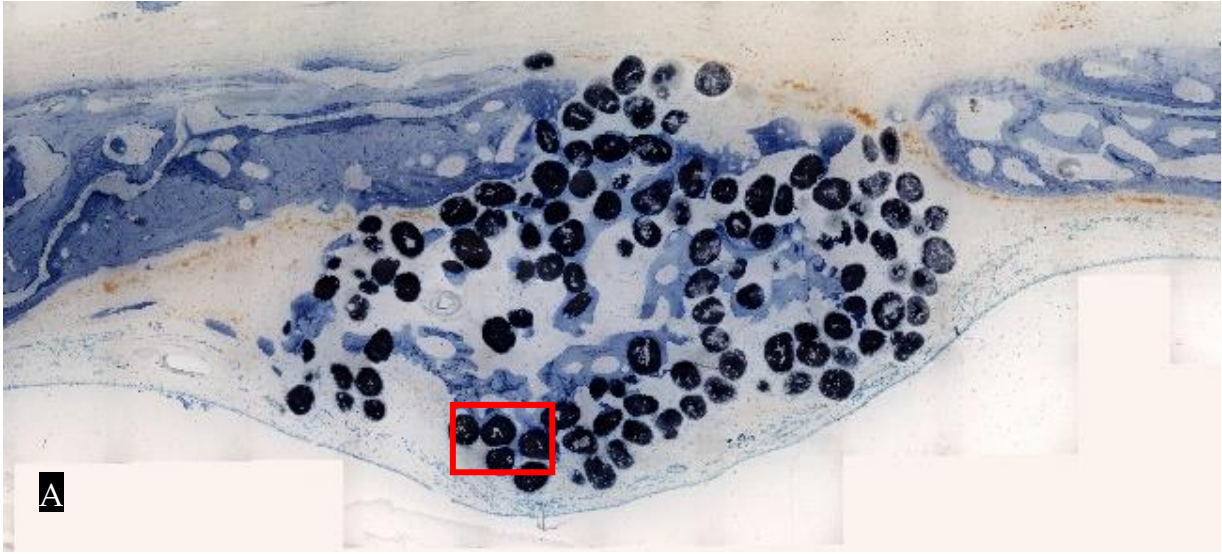


Figure 3-4 Cone Oss[®] augmented site (specimen 419)

C. Overview of the specimen. Red rectangle outlining the position of B

*D. Residual graft particles (x10 magnification, **b** – new bone; **c** – connective tissue; **g** – graft; **a** – capillary)*

3.3.3.3 SmartBone® sites

Seven out of ten SmartBone® sites presented with no augmentation (Figure 3-5) Non-resorbed grafting material was found in three out of ten sites grafted with SB. Two of those sites demonstrated no augmentation, i.e. no extra-skeletal bone was created by the grafting procedure. In one remaining specimen, the augmented area contained loose connective tissue with sparse islets of newly formed bone enveloping remaining particles of grafting material. The grafting material exhibited multiple resorption pits. These pits were in contact not only with the new bone but also with connective tissue, which suggests that the inflammatory process, rather than osteoclastic resorption, was responsible for the graft disappearance (Figure 3-6).

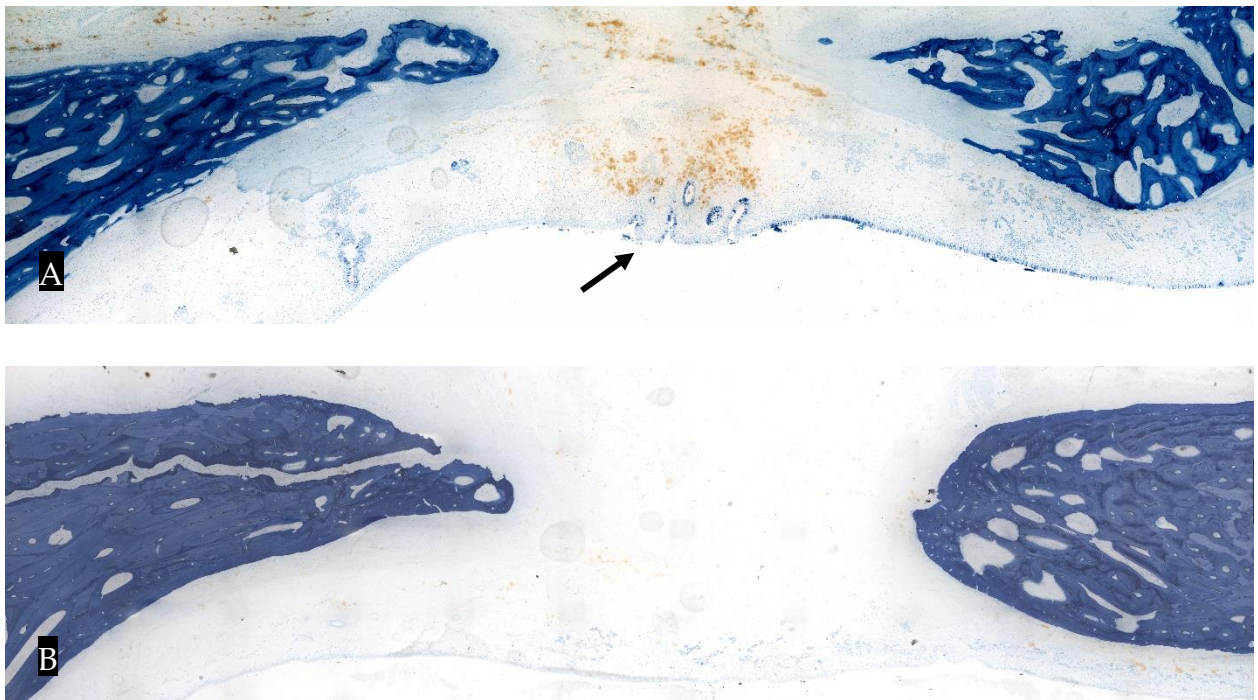


Figure 3-5 SmartBone® augmented sites

- A. *Specimen 416. Notice the irregular Schneiderian membrane (black arrow) with highly vascular sub-mucosa. No residual graft or newly formed bone is evident in ROI*
- B. *Specimen 420. No residual graft or newly formed bone is evident in ROI*

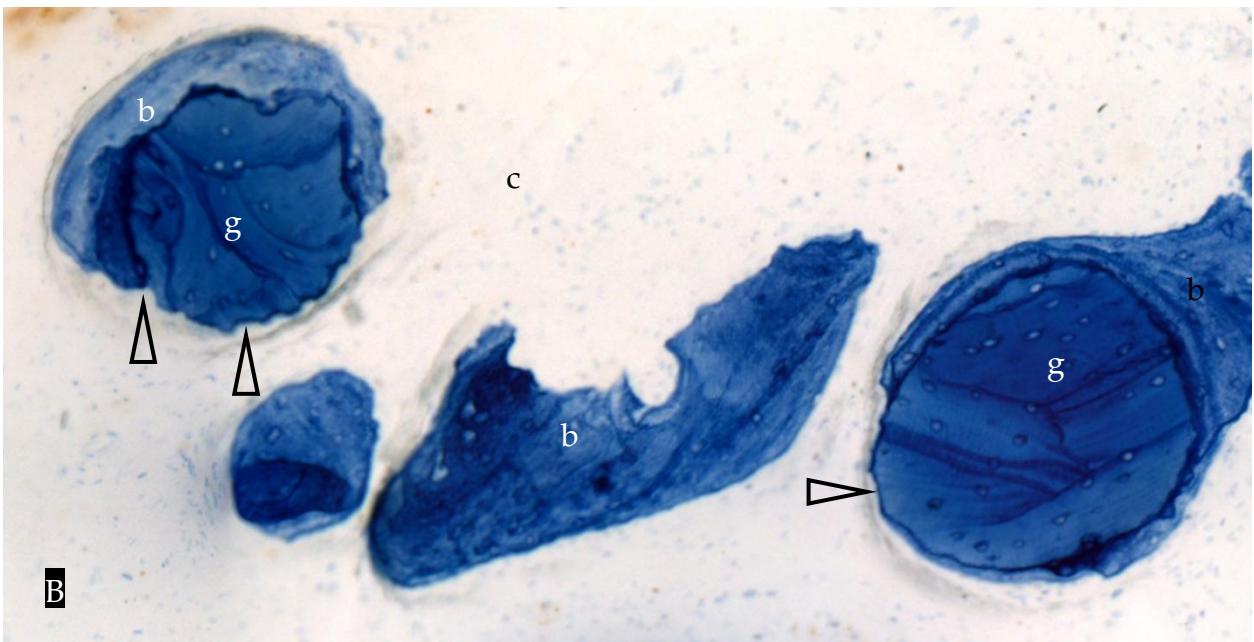
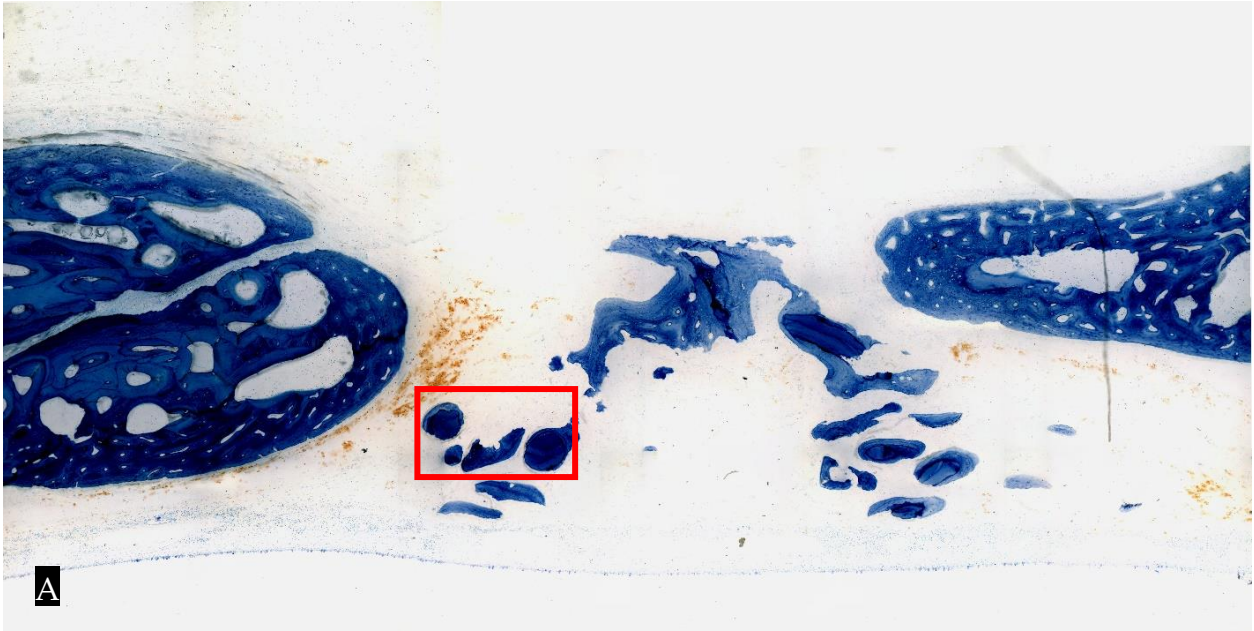


Figure 3-6 SmartBone[®] residual grafting material (specimen 418)

A. Overview. Red rectangle represents the positions of magnified B figure.

*B. Residual graft particles (x10 magnification **b** – new bone; **c** – connective tissue; **g** – graft; **empty arrowheads** – graft resorption pits in contact with connective tissue*

3.3.3.4 PARASORB Cone® sites

All sites presented with intact sinus epithelium and loose lamina propria, which was highly vascular near the epithelial basal membrane. In two out of ten sites, several isolated islets of woven bone were found within the submucosa. Three out of ten specimens demonstrated degenerate non-stained material in the region of interest (Figure 3-7). This material could be the residual non-resorbed grafting material, collagen. No CN site demonstrated successful augmentation.

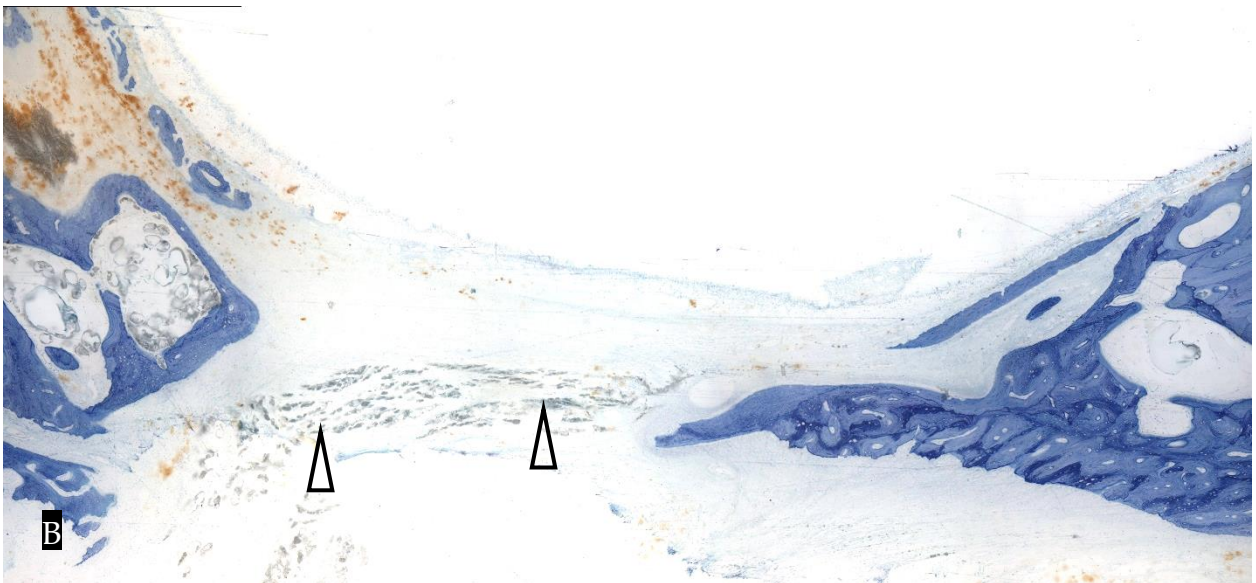
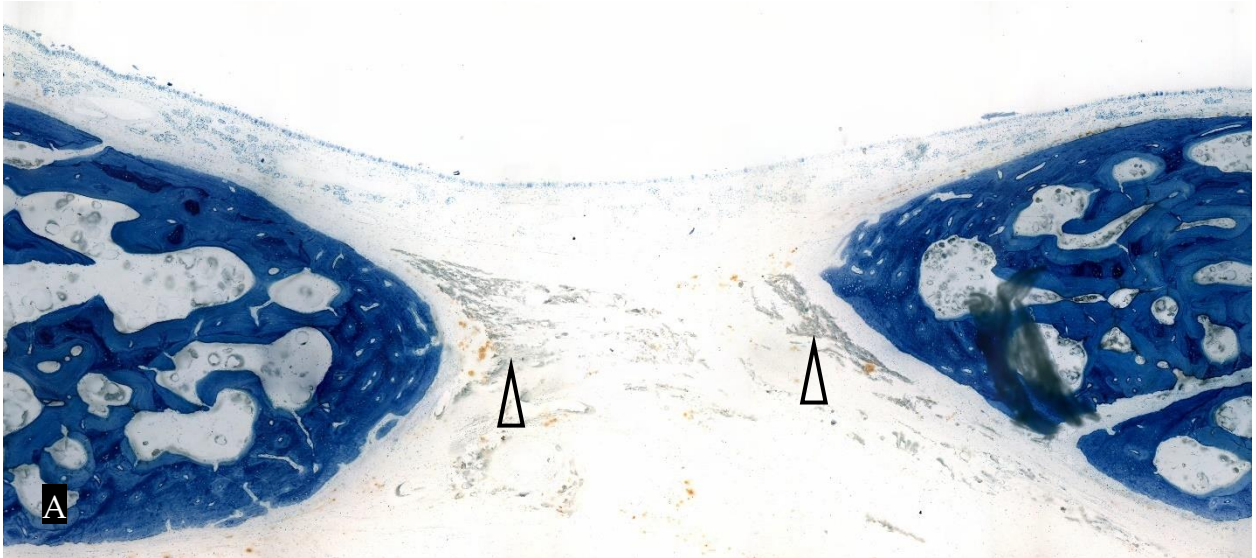


Figure 3-7 Cone® augmented sites

- A. Specimen 419. Collapsed Schneiderian membrane, failed augmentation. Degenerate residual grafted material is evident (empty arrowheads)*
- B. Specimen 414. Collapsed Schneiderian membrane, failed augmentation. Degenerate residual grafted material is evident (empty arrowheads)*

3.3.4 Histological artefacts

The methodology of slide preparation for histological staining involved grinding down the initially 650 μm thick slides to the thickness of 80-100 μm , and then polishing prior to staining. This process caused some debris to accumulate within the histological sections (Figure 3-8). Manual adjustments had to be made when sectioning the image, to exclude the debris particles from automatic thresholding.

The exothermic polymerization of MMA can produce gas bubbles, which were evident in some slides. When these bubbles presented inside the region of interest, they were included in the connective tissue area for histomorphometric calculations (Figure 3-9).

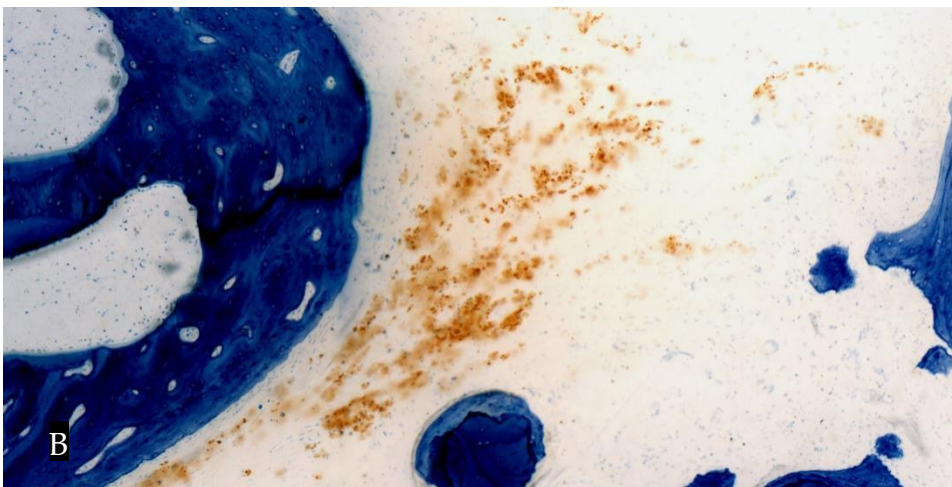
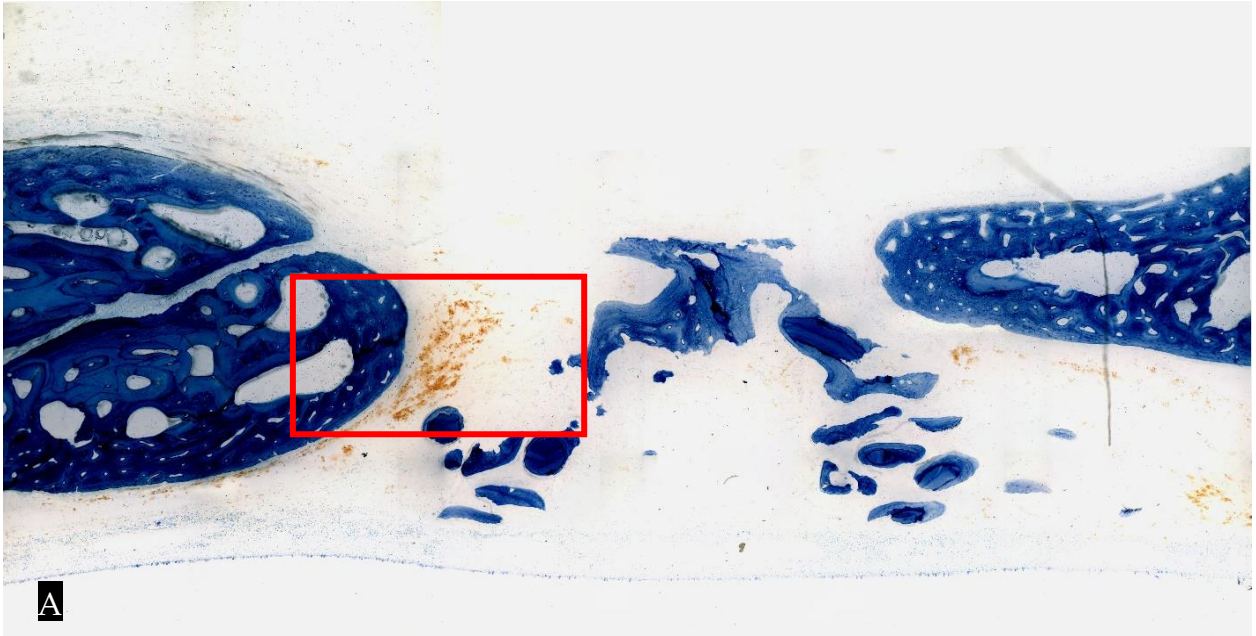


Figure 3-8 Histologic artefacts – stained debris. SB grafted site

- A. Overview. Red rectangle represents the positions of magnified B figure*
- B. Magnified image, stained debris*

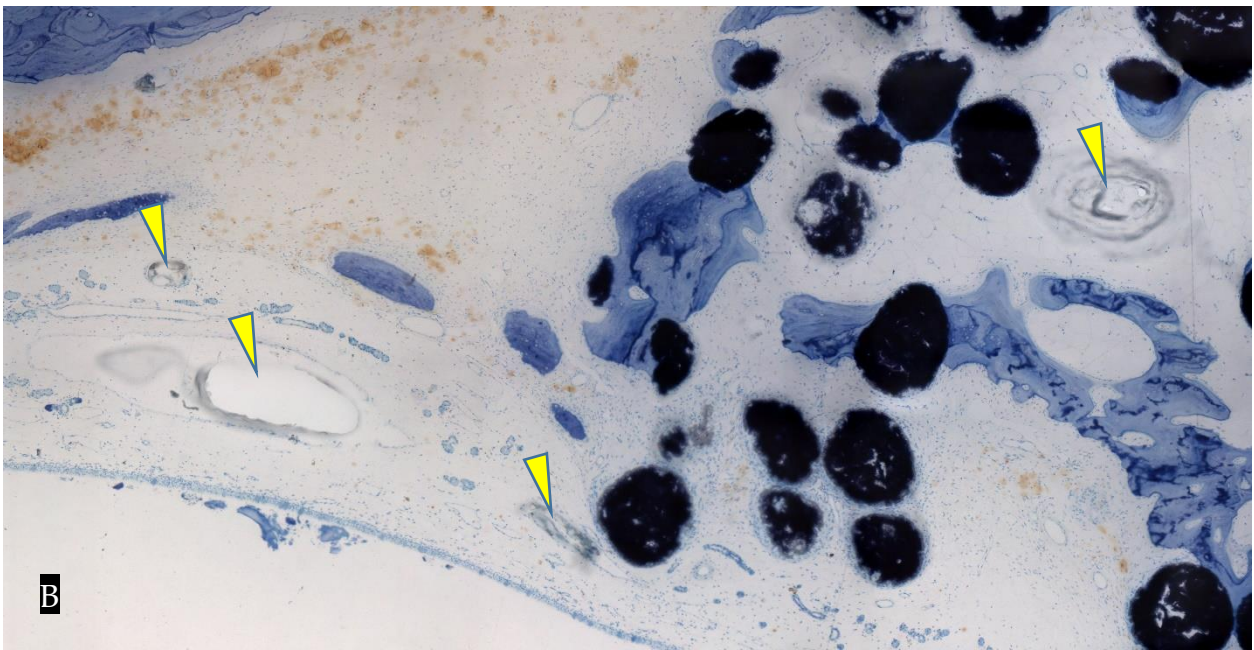
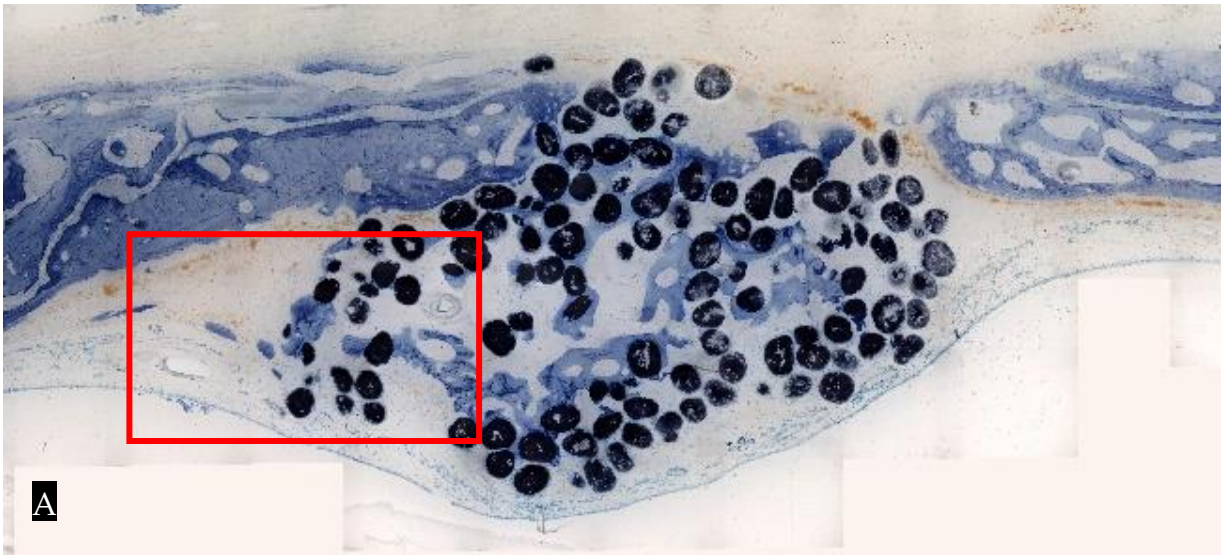


Figure 3-9 Gas bubbles artefacts.

- A. Overview. Red rectangle represents the positions of magnified B figure*
- B. Gas bubble artefacts (yellow arrows)*

3.3.5 Summary of findings in descriptive histology

The sinus mucosa presented as a characteristic, columnar, pseudostratified epithelium, and the mucosa was continuous in all but one specimen (grafted with Cone Oss®). The immediate submucosa was highly vascular.

The surgical access defect was partially repaired in all specimens and fully repaired in two of them. The repairing bone was laminar, with thin trabeculae and extensive marrow spaces. The new bone appeared on both the antral and the facial aspects of the original bone plates. In most cases, the edges of the original bone plates were completely resorbed, remodelled, and no longer identifiable.

Sites grafted with Bio-Oss® (BO) and Cone Oss® (CO) presented as augmented bell-shaped areas, containing the residual grafting material and the new bone. The new bone appeared to be in direct contact with BO and CO particles. Evidence of osteoclastic resorption was found for BO residual graft. The BO particles were irregularly distributed, and some were incorporated into repairing bone walls, while CO particles were tightly packed in the centre of the augmented site.

Most sites grafted with SmartBone® (SB), and all sites grafted with Cone® (CN), demonstrated no augmented area and no residual grafting material. In slides where some of the SB particles were retained, signs of resorption were evident, but osteoclasts were not present.

Histologic artefacts, in the form of residual debris from polishing and bubbles, were present in multiple specimens; however, they could be easily masked by software and had no impact on image analysis.

3.4 Histomorphometric analysis

Two coronal sections representing the centre of each experimental site were chosen to measure the fraction of hard tissues within the ROI. The mean between the two sections was used as the representative value for each experimental site.

The CN and SB grafted sites failed to demonstrate augmentation. Therefore no ROI was defined for them, and no statistical analysis was performed.

3.4.1 New bone, residual graft and connective tissue fractions

The connective tissue occupied the majority of the ROI for both BO (72%) and CO (82%). The residual grafting material occupied similar areas for BO (17%) and CO (18%). However, BO grafted sites on average demonstrated more than twice as much new bone in the ROI (10% for BO *versus* 4% for CO). Despite the absolute differences, the Wilcoxon signed rank test failed to demonstrate statistical significance between groups ($p = 0.11$). The standard deviation suggests a large variability of outcomes in both groups.

The areas of new bone, residual graft, and connective tissue are presented in Table 3-3 for each experimental site.

Table 3-3 Mean fractions of hard tissue in the ROI by treatment modality

Treatment modality	Residual graft, % (SD)	New bone, % (SD)	Connective tissue, % (SD)
Bio-Oss®, n=10	16% (10%)	9% (9%)	75% (14%)
Cone Oss®, n=10	17% (15%)	4% (5%)	79% (20%)
p-value	0.859	0.110	0.314

The data distribution is represented as a boxplot in Figure 3-10.

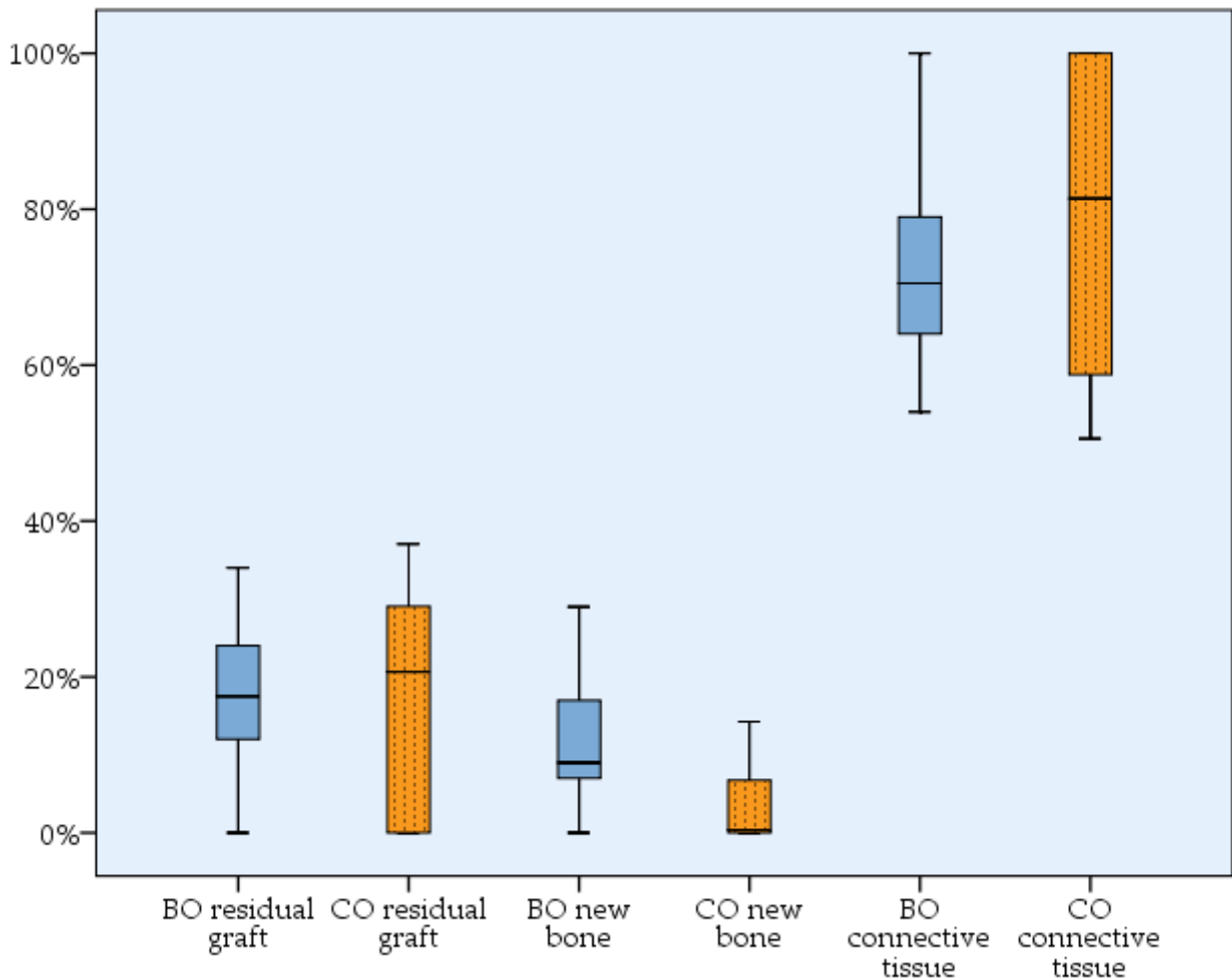


Figure 3-10 Hard and soft tissue fractions for Bio-Oss® (BO) and Cone Oss® (CO).

Note the overlap of the boxplots for the residual graft and connective tissue. The large standard deviation and small sample size obliterate the difference in NB between BO and CO groups.

In 3 BO sites and 5 CO sites the new bone failed to form in the augmented submucosa. If only the specimens with more than zero new bone formation are analyzed, the data variability will be reduced (Figure 3-11), which is demonstrated by lower standard deviations (Table 3-4). However, even in this case, the discrepancy for the new bone formation between CO and BO would remain ~2-fold (Table 3-4). The Wilcoxon signed

rank test fails to demonstrate statistically significant differences between groups. The statistical analysis, in this case, is based on 4 specimens only, due to the use of paired samples.

Table 3-4 Mean fractions of hard tissue in the ROIs with more than zero new bone

Treatment modality	Residual graft, % (SD)	New bone, % (SD)	Connective tissue, % (SD)
Bio-Oss®, n=7	21% (5%)	13% (8%)	66% (6%)
Cone Oss®, n=5	29% (10%)	8% (5%)	63% (18%)
p-value n=4 †	0.465	1.000	0.465

† - when 2 BO and 5 CO sites omitted, only 4 specimens could be used for the paired Wilcoxon signed rank test.

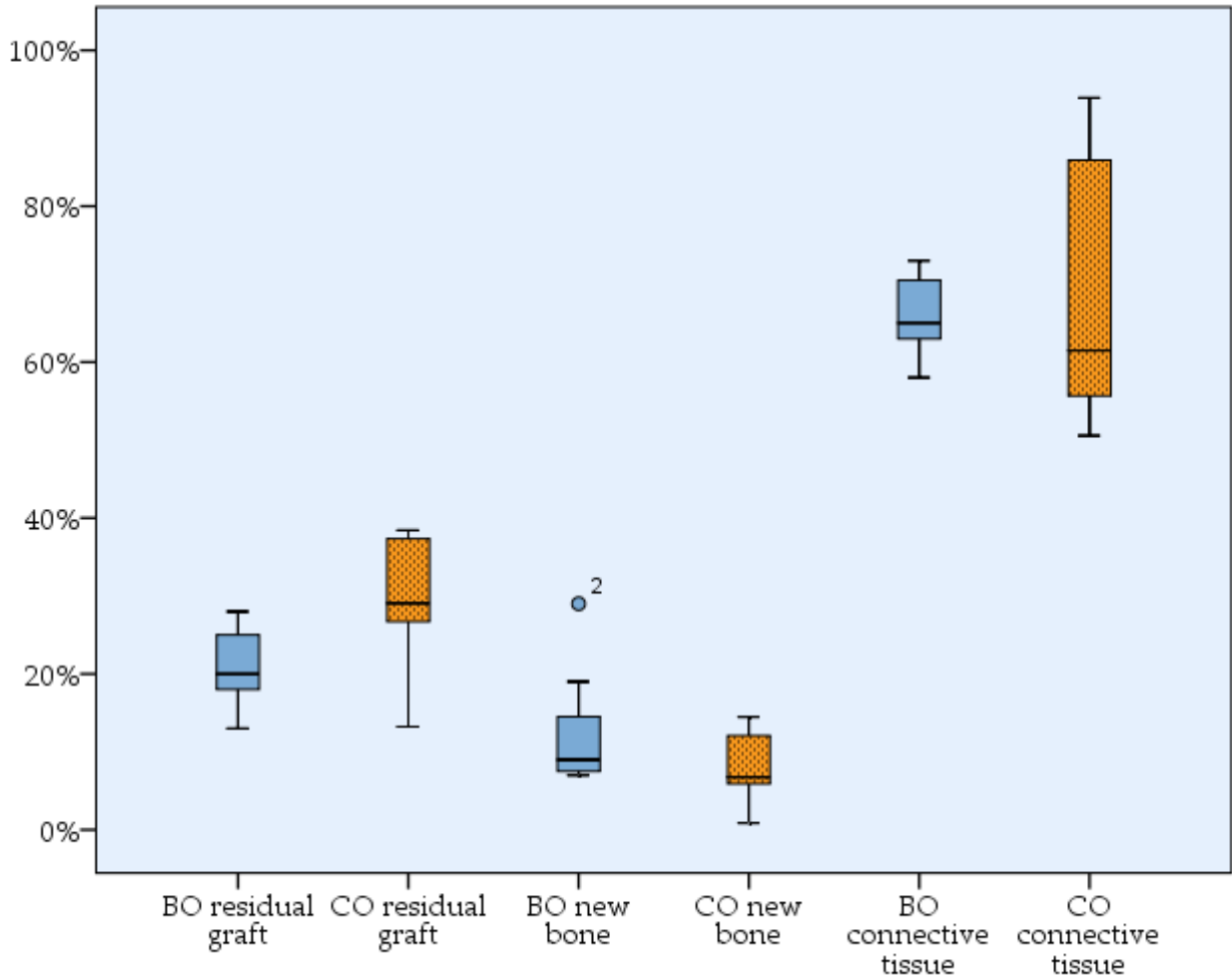


Figure 3-11 Tissue fractions for Bio-Oss® (BO) and Cone Oss® (CO) with more than zero new bone formation.

The intra-group variability is smaller than in Figure 3-10. The mean for the new bone areas is closer between CO and BO groups when the cases with no NB are excluded.

3.4.2 Augmentation height

The height of augmentation was measured for BO and CO (Table 3-5). The average height was almost identical for both BO and CO. Average height-to-width ratio for CO was twice as high as for BO sites, meaning that graft particles were held tighter together in the centre of the augmented site. These differences were not statistically significant

Table 3-5 Augmentation height

	Height, mm (SD)	Height/width ratio (SD)
	n=10	n=7 †
BO	2.74 mm (2.01 mm)	0.34 (0.20)
CO	2.75 mm (2.65 mm)	0.58 (0.34)
p	0.878	0.128

† - the sites with failed augmentations were excluded from analysis

3.4.3 Reliability and consistency

The consistency of measurements of histomorphometric analysis was assessed using the help from the examiner that did not otherwise participate in this study. Ten specimens of BO and CO were randomly selected, then the examiners assessed:

1. The total augmented area as specified in section 2.5.2.1
2. The fraction occupied by NB, RG and CT in the pre-defined area of interest.

Intraclass correlation coefficient (ICC) of assessments was calculated using two-way mixed model and absolute agreement type. Excellent correlation, as defined by Cicchetti (1994)³¹⁷, was demonstrated for all measurements, the results are presented in Table 3-6.

Table 3-6 Inter-examiner agreement

Measurement	Intraclass correlation coefficient
Total area of ROI	0.995
Residual graft	0.968
Connective tissue	0.985
New bone	0.994

Less than 0.40—poor agreement; between 0.40 and 0.59—fair; between 0.60 and 0.74—good; between 0.75 and 1.00—excellent.

The principal examiner assessed the same set of ten specimens two months prior to inter-examiner agreement test. The data from the earlier and later assessments were compared for intra-examiner consistency using ICC. Excellent correlation³¹⁷ was demonstrated for all measurements; the results are presented in Table 3-7

Table 3-7 Intra-examiner correlation

Measurement	Intraclass correlation coefficient
Total area of ROI	1.000
Residual graft	0.999
Connective tissue	1.000
New bone	0.990

Less than 0.40—poor agreement; between 0.40 and 0.59—fair; between 0.60 and 0.74—good; between 0.75 and 1.00—excellent.

ICC scores are influenced by data variability. Higher ICC scores can be achieved when assessing highly variable outcomes. Some of the specimens selected for inter-examiner agreement tests demonstrated failed augmentation with zero new bone and residual graft areas. Zeros in data-set sites may have increased the data variability and artificially increased the ICC scores. We calculated ICC for inter- and intra-examiner agreement omitting the failed augmentation sites (Table 3-8, Table 3-9). Both intra-examiner consistency and inter-examiner correlation remained high when using this analysis

Table 3-8 Inter-examiner agreement, successfully augmented sites only

Measurement	Intraclass correlation coefficient
Total area of ROI	0.989
Residual graft	0.951
Connective tissue	0.961
New bone	0.814

Less than 0.40—poor agreement; between 0.40 and 0.59—fair; between 0.60 and 0.74—good; between 0.75 and 1.00—excellent.

Table 3-9 Intra-examiner agreement, successfully augmented sites only

Measurement	Intraclass correlation coefficient
Total area of ROI	1.000
Residual graft	0.997
Connective tissue	0.998
New bone	0.989

Less than 0.40—poor agreement; between 0.40 and 0.59—fair; between 0.60 and 0.74—good; between 0.75 and 1.00—excellent.

3.4.4 Summary of findings in histomorphometric analysis

At 16 weeks of healing the sites grafted with SmartBone® (SB) and Cone® (CN) have failed to demonstrate augmentation and new bone formation, therefore no ROI was defined for them, and no histomorphometric analysis was performed.

Bio-Oss® (BO) and Cone Oss® (CO) grafted sites on average demonstrated similar fractions of the residual grafting material and the connective tissue. Despite demonstrating on average twice as large an area of the new bone, BO grafted sites did not differ statistically from CO grafted sites. The data was highly variable between specimens. In the present animal model, CO demonstrated equivalent new bone formation to BO for new bone formation.

Chapter 4. Discussion

4.1 Introduction

The present study aimed to test three novel bone substitutes for sinus grafting against a well-studied xenograft serving as a positive control. The study objective was to analyze the outcomes of sinus grafting, histologically and histomorphometrically, using a well-established sheep animal model. The sheep model for sinus grafting was developed by Haas et al.¹²¹. It was adopted and previously used by our institution²⁸¹.

4.2 Discussion of study outcomes

In this section, we will discuss the results of the current study, compare them to the evidence derived from previous studies in other animal and human models, and discuss their clinical relevance.

4.2.1 Summary of primary outcomes

After 16 weeks of healing, the sites grafted with Cone® (CN) and SmartBone® (SB) failed to demonstrate augmentation. The grafting material had completely disappeared from the majority of CN and SB grafted sites, leading to the collapse of the Schneiderian membrane (SM). No extra-skeletal bone was formed in the grafted area. The SB graft resorption was evident in three surgical sites where remnants of grafting material remained; however, no cells resembling osteoclasts, and no formations resembling Howship's lacunae, were found on the surface of the graft. We may hypothesize that SB particles were not lost to osteoclastic resorption, but rather underwent enzymatic dissolution in the extracellular matrix.

The BO and CO particles remained in the augmented space beneath the SM, and new extra-skeletal bone formed around these particles in the majority of surgical sites. The

newly formed bone was deposited directly onto the surface of BO and CO particles with the bone-graft complex formation. These histologic findings provide evidence for biocompatibility and osteoconductive properties of CO and BO.

No statistically significant difference was found for histomorphometric outcomes between CO and BO.

4.2.2 Histologic picture

After 16 weeks of healing, for all treatment modalities, the repair of bony walls of the sinus was still incomplete for most surgical sites. The surgical defect of 10 mm in the sheep maxilla is not a critical size defect³¹⁸. Therefore it is expected to heal completely given more healing time. The healing of the access window is seldom reported in the literature concerning sinus floor elevation. In a recent study using monkeys, one access window after 3 months and two after 6 months of healing appeared to be closed by newly formed bone, while the remainder were partially healed¹¹³.

In my study, CN collagen completely disappeared from all but three experimental sites, where the degenerate remnants of the material were still present within the sinus submucosa. CN consists of non-cross-linked equine collagen. It was developed to be used in alveolar ridge preservation (ARP) procedures. The rationale of placing a collagen cone into fresh extraction sockets is to stabilize the blood clot. Collagen resorbs in 4-8 weeks after implantation in rats, the resorption rate depends in part on cross-linking density of the collagen^{319, 320}. As the successful sinus floor augmentation requires that a space beneath the elevated Schneiderian membrane be maintained to permit new bone formation, we may conclude that the resorption of CN material occurred too rapidly, leading to the premature collapse of augmented space.

Sponges made of bovine collagen were used as controls in a goat SFE model²⁸⁶. The authors reported a continuous reduction of augmented volume in the sites grafted with

collagen while the test sites (grafted with collagen soaked with Bone Morphogenic Protein) remained stable. Ahn et al. (2011)³²¹ used collagen sponges (Zimmer™ Collaplug®) for sinus floor elevation through a lateral approach, in a clinical case series study on thirteen patients. In their study, the sites failed to demonstrate clinically relevant new bone formation. Although in my study the collagen cone was also ineffective for SFE, the information from CN sites was still useful as a contrast to CO grafted sites, as CO consists of the same equine non-cross-linked collagen, but is filled with alloplastic filler.

Similarly to CN, SB particles disappeared completely from most sites at 16 weeks post-implantation, with Schneiderian membrane collapse and no new extra-skeletal bone formation. It is not clear why the SB grafting material underwent such a quick resorption. It is manufactured from deproteinized bovine bone mineral (DBBM) and a composition of two polymers: polylactic acid (PLA) and poly-ε-caprolactone (PCL) as copolymer.

PLA has multiple biomedical applications including resorbable sutures, membranes and scaffolds. The degradation of PLA and copolymers is well documented for both in vitro and in vivo³²²⁻³²⁴. The addition of PCL to the composition is thought to slow down the rate of resorption of PLA and to improve its mechanical properties^{325, 326}. As humans and animals lack the enzyme to degrade PLA and PCL, the resorption proceeds via hydrolysis, rather than enzymatic degradation^{327, 328}. The hydrolysis of these materials is complex and is still not entirely understood. During degradation, they are thought to gradually lose fragments from the surface; these fragments break up into even smaller oligomers that are soluble in the extra-cellular matrix³²⁸. However, unpredictable bulk hydrolysis and quick resorption can sometimes be registered in vivo for certain PLA-PCL co-polymers³²⁹.

By changing the polymer composition, manufacturers can modify the resorption rate to suit the specific situation. In a clinical case series, Scarano et al. (2006) performed SFE in 94 patients with nine different grafting materials, including Bio-Oss®, autologous bone and poly-glycolic-poly-lactic acid copolymer (PLA-PGA). The biopsies were retrieved during implant placement in the grafted sites after 6 months. On histologic examination, this polymer appeared to be substituted by the newly formed bone (NB). NB constituted on average $33\% \pm 2.1\%$, marrow spaces $59\% \pm 2.3\%$, while residual PLA-PGA occupied $3\% \pm 2.1\%$ of augmented sites¹⁷⁶. Apparently, not all degradable polymers will be suited for SFE, although some may be efficient.

To date, only limited amount of empirical data has been gathered concerning the resorption of a specific formulation of DBBM combined with PLA-PCL complex. In a study by Petrici, the manufacturer of SB used a mathematical model for predicting the resorption rate of the material and stated it should be adequate for slow resorption and creeping substitution by the bone³³⁰. This was not confirmed by the empirical findings from my study.

Another series of in-vitro, in-vivo studies investigating biocompatibility and toxicity of SB was published by the same group³³¹. This series included two case reports of human patients. The authors used SB for vertical ridge augmentation and guided bone regeneration prior to implant placement. The biopsy was harvested from one of the patients at a 4-month time-point during the implant placement. The histologic investigation confirmed the presence of residual graft in direct contact with newly formed bone.

Another small-scale clinical case series study was recently published²⁹⁵: the authors performed lateral SFE in five patients with SB as grafting material. The implants were placed 4, 6, 7 and 9 months post-grafting and biopsies were retrieved. At 4 months SB was found to occupy 12% of the specimen; at 6 and 7 months, 0.5%; and at 9 months,

SB disappeared completely. Unlike in my study, the authors found that the new bone was replacing the graft, reaching 67% of the specimen area at 9 months. The small sample size of this study did not allow for statistical analysis of the results.

We may hypothesize that in our model, increased pH or temperature of the inflamed healing wound may have accelerated hydrolysis of the polymer coating, leading to inflammation-driven resorption of SB in the earlier stages of healing. A word should also be spoken about the bovine-derived deproteinized matrix of SB. It is treated via acid attack at a low temperature³⁰⁴. The non-sintered (low-temperature deproteinized) materials are thought to be resorbed at the higher rate¹⁹⁶. If this is true for the SB mineral content, it could have also contributed to its quick resorption and disappearance.

NB formation was documented around the particles of both BO and CO. The NB was deposited directly on the surface of the particles with no interposing tissues, confirming that BO and CO are both biocompatible and have osteoconductive properties.

The bone type was mostly lamellar, suggesting that the grafted site was relatively mature. In a previous study using the same model²⁸¹, the sinuses grafted with BO demonstrated a similar histologic picture after 12 weeks of healing. In a recent publication by Alayan et al. (2016)⁷, the researchers documented an increase in the lamellar bone fraction from 8 to 16 weeks of healing. In another study, after 12 and 26 weeks, sheep maxillary sites grafted with Straumann™ Bone Ceramic® and then restored with an implant showed mature trabecular bone enveloping the graft particles²⁸³. The observations from my study confirm the principle of the pattern for early bone development presented earlier³³², where the formation of highly organized bone tissue requires a mechanically stable surface, which is provided by the grafting material.

In my study, most of the BO particles seemed dispersed within the augmented site, without bone connecting between them. This is in line with the available histologic pictures from other studies^{7 272} using the same animal model. In a case series with human participants, the BO granules seemed to be more interconnected; however, this finding wasn't quantified¹⁸⁸. In a study by Haas, Donath et al. (1998)¹²¹, extensive bone formation around the particles of BO did not influence the bone contact with the implants that were placed in the grafted site. Phillip et al. (2014) found that the use of a graft filler enabled the bone to implant contact in the sheep sinus model after 26 weeks; however, the percentage of bone formed within the grafted site was not quantified²⁸³.

In my study, Howship's resorption lacunae were found on some BO particles, which is in line with previous reports^{333, 334}. It is known that osteoclastic resorption of BO happens at a slow pace, as the residual graft fraction was documented to decrease with time³³⁵. The extent of the osteoclastic resorption of BO is, however, unclear. BO particles have been shown histologically to persist in the grafted site for years after implantation^{162, 334}. The BO persistence in the grafted sites was shown to delay healing in a dog extraction sites model³³⁵. The authors commented that bone enveloping the xenograft might be considered a special type of foreign body reaction, which in the case of SFE may serve the purpose of maintaining the extra-skeletal space for the NB formation. Persistence of the BO was effective in supporting bone in-growth; however, we are unable to comment on the pace or the extent of BO resorption based on the single time-point in my study.

In the CO grafted sites, the granules of biphasic calcium phosphate (BCP) were tightly packed beneath the elevated Schneiderian membrane. New bone bridged between some of the granules in exactly half of the sites, the other half being devoid of new bone formation in the region of interest. The literature provides extensive evidence for

biocompatibility and osteoconductive properties of BCP in animals¹⁶¹ and humans^{204, 296, 336}. My study confirms the previous findings concerning biocompatibility and osteoconductivity, albeit overall performance of the material seemed to be inferior compared to the previous reports.

We found no evidence of osteoclastic resorption for CO particles at the 16-week time-point. Our findings contrast with the reports in the literature. Ohayon (2014)³³⁶ and Froum et al. (2008)³³⁷ found evidence for osteoclastic cells at the surface of the residual graft from human augmented sinus biopsies. While TCP alone is known for its quick and complete resorption in ECM, the biphasic, TCP-HA alloplast does not resorb as readily¹⁶¹. The study of Phillip et al. (2014)²⁸³ used TCP/HA biphasic granules in the sheep sinus. After 26 weeks, there was some evidence of surface resorption of the granules; however, the presence of osteoclasts was not specifically identified (personal communication).

It is possible that in my study the osteoclasts were present on the CO surface, but were not identified. Frenken et al. (2010)³³⁸ used osteoclast-specific TRAP staining to detect osteoclasts. TRAP-stained cells were found in small quantities on the surface of the biphasic TCP-HA alloplast (Straumann Bone Ceramic®).

We did not quantify inflammation in my study. The histologic method that we used does not allow for adequate immune cell recognition. Future studies may include paraffin-embedded sections stained with H&E, which are better suited for this type analysis.

4.2.3 Histomorphometric outcomes

In my study, the newly formed bone occupied 9% of the region of interest (ROI) in the sites grafted with BO. A previous study by our institution using Biomet 3i™ Endobon® (DBBM) in the sheep sinus also showed that 9.5% of the ROI was filled with new bone

after 16 weeks²⁸². However, these findings contrast sharply with the publications by other groups. In a recent study using a similar sheep model, the new bone area with BO was reported to be much higher after 16 weeks of healing - up to 50%⁷. In human trials, the amount of newly formed bone during the first year in cases treated with maxillary sinus augmentation using BO varies from 8% to 42%^{166, 289}.

The sites grafted with CO demonstrated 4% new bone formation in the ROI. No other animal or human trials have investigated formulations that match CO (an alloplast consisting of 40:60% TCP:HA in a collagen cone), however similar graft material composed of biphasic 40:60% TCP:HA without the collagen matrix has been documented in human^{206, 337, 338} and animal trials^{161, 339}. The NB area was reported to be between 20-30%, which contradicts our findings. We found that half of the CO sites did not develop new bone at all. If only the sites with some new bone formation were analyzed, the average NB fraction would have constituted 8%, which would have been lower than the figures reported in the literature.

Whilst the NB fraction is an important histologic outcome, its clinical significance is not well understood. The mineralised content of type IV bone in humans was demonstrated to be 28%⁴⁶. In the present study, the sites grafted with BO and CO corresponded with a very poor-quality bone. Pull-out tests correlate increased bone fraction with increased pull-out forces³⁴⁰. It is not known what percentage of vital bone must be formed in the grafted site to result in improved survival of the implants⁷⁴.

4.3 Discussion of the model and the method

In this section, we will outline the validity of the research method and the study limitations.

4.3.1 Animal model

4.3.1.1 Animal heterogeneity

For this study, eleven sheep were purchased from a commercially available flock. The experimental animals were not inbred and therefore were genetically heterogeneous study subjects.

The heterogeneity can impact graft-host interactions, the rate of bone healing, recovery from the surgery and reactions to medication, all of which leads to high variability of outcomes. Indeed, in this study, the standard deviation was substantial in all histomorphometric parameters. While the access window was only partially repaired in most sites, in one sheep (419), the antral wall of 3 out of 4 surgical sites (SB, CN, CO) was completely bridged, which may demonstrate faster bone healing rate in this animal.

On the other hand, the experimental results from heterogenous population could be applied to the human population (which is also heterogenic) with greater confidence.

In my study, we accounted for heterogeneity between the subjects by using the animal (rather than the experimental site) as a statistical unit.

4.3.1.2 Sinus anatomy in sheep

Ideally, a research model should exactly mimic the clinical situation in the human edentulous posterior maxilla, where a partially resorbed alveolus is overlying the thin cortical bony floor of the sinus. The maxillary sinus should be lined with a Schneiderian membrane, and there should be sufficient space in the sinus cavity to allow a clinically

relevant graft volume to be placed. Sheep sinus anatomy is considered sufficiently similar to that of humans in otolaryngology²⁸⁴ and surgical training³⁴¹. Estaca et al. (2008)²³⁰ performed a fresh sheep head dissection and stated that the lateral wall of the sheep sinus is relatively thin and easily trephined, resembling a situation in the human edentulous posterior maxilla.

The sinus wall in sheep can be reached by an extra-oral or intra-oral route. Intra-oral access requires a previous surgical vestibular dissection^{230, 342-344}. As this may complicate the recovery from surgery and cause unnecessary suffering for the animals, the extra-oral access was chosen. However, extra-oral access is not representative of the clinical situation in humans and extrapolation should be made cautiously.

4.3.1.3 Bone healing and graft incorporation in sheep

The consolidation of the graft is a normal bone repair modified by the presence of the graft. The bone microstructure in sheep is somewhat different from that in humans: young adult sheep mostly have primary bone: plexiform structures of woven and cortical bone combined together³⁴⁵. Also, the lamellar bone in 3-4-year-old ewes is organized in brick-like layers without a central artery, rather than in Haversian cylinder-like structures³⁴⁶. In my study, we saw the plexiform repair of the antral walls. The bone that formed around the BO and CO particles was also resembling a woven-lamellar complex with plexiform structure. It is difficult to assess how these differences in sheep bone morphology and repair impact the applicability of the model on the human population.

The animals were killed after 16 weeks of healing. It is possible that more of the NB would have formed in the grafted site given more time. The 16-week healing period was chosen to produce comparable outcomes with other groups that used sheep as SFE model^{7, 276, 297}. The healing rate in sheep is faster than in humans²⁷⁸. Using a critical size

defect ovine model, Duncan (2005)²⁹ has evaluated that 16 weeks of healing in sheep should correspond to 21 weeks of healing in humans, which was stated as an acceptable healing time for sinus floor elevation.

Normal body temperature in sheep is 38.3 – 39.9°C (www.merckvetmanual.com). The difference of 2 - 3°C can influence the rate of hydrolysis of degradable polymer materials^{347, 348}, leading to a faster resorption rate. This could have led to a faster resorption of PLA-PCL coated DBBM (SmartBone®) that we tested in my study.

4.3.2 Surgical procedure

The objective of sinus floor elevation (SFE) is to provide a recipient bed for implant placement. In many studies, the implants were placed concomitant with SFE to investigate implant-related outcomes, such as bone-to-implant contact^{126, 283, 340, 349}. Concomitant placement of implants may influence healing and graft consolidation. They can stabilize the grafting site by providing a rigid anchor. Boyne et al. (1993)²³⁸ placed implants in a primate sinus and found clear differences in healing around the different thread and apical configurations of identical TPS implants. Less bone formed at the apical end of open-ended and deep-threaded implants, while significantly more bone contacted the apex of otherwise identical round-ended implants. While the extent of the implant impact on the grafted site healing is unclear, my study was designed to reveal the process of graft consolidation and not the impact of bone substitutes on the osseointegration of dental implants.

Our first animal failed to recover from surgery. This complication was not related to the sinus surgery, but rather to prolonged operating time. Two research projects, our SFE study and the alveolar ridge preservation study by another group³⁰⁰ were using the same animals, which prolonged the procedure time. Measures were undertaken to shorten the operating time, and the operators experienced a steep learning curve with

the procedures. Subsequent animals were operated on more quickly and recovered with no complications.

Due to financial constraints and unavailability of dedicated facilities, we performed sinus grafting procedures without prior radiographic investigation of individual sinus anatomy of each animal. Doing so may increase the risk of intra-surgical complications, such as SM perforations, severing big vessels and unfavourable sinus anatomy. Indeed, we were forced to make one additional osteotomy due to constricted sinus space; we detected and repaired four SM perforations.

In our model, the surgical sites were covered with resorbable collagen membranes. Although frequently used in human lateral SFE procedures, the evidence for their use mostly comes from animal research. Barone et al. (2013)³⁵⁰ did not find significant histological differences between the membrane group and uncovered control. A recent systematic review failed to arrive at definitive recommendations ²⁵³. The documentation concerning the use of barrier membranes in ovine SFE model is scarce. Alayan et al. (2016)⁷ used a porcine collagen membrane, Bio-Gide® to cover the access windows, but his study did not include any control sites that were not covered by a membrane. A previous study by our group also used barrier membranes with no controls²⁸¹. The advantage of a barrier membrane in conjunction with a graft of BO in an ovine model was described by Adeyemo et al. (2008)³⁵¹, albeit in a mandibular site. Soft tissue encapsulation of BO particles was observed when the membrane was dislodged from the site.

In my study, there were three surgical sites with small (less than 5 mm) Schneiderian membrane perforations. In one animal, these were grafted with CO, CN and SB, and in another animal, the site was grafted with BO. The perforations were repaired using the Loma Linda pouch technique, as previously described³¹¹. The histological results for the BO site with a repaired membrane demonstrated irregularity in SM and limited

augmentation volume. The CO site histology demonstrated the complete failure of augmentation with no residual grafting particles. Hence, in my study, the Loma Linda pouch technique failed to protect the grafted site and prevent medial displacement of grafting material. Some authors have described the reduced bone formation and compromised implant survival rates with resorbable membrane repair of perforations^{352, 353}. No randomized studies in humans are available to substantiate the claim about the efficacy of sinus membrane perforations repair. In a recently published randomized animal study, the authors question the necessity for sinus membrane repair³⁵⁴.

In order to standardize the grafting procedures, we used the same measured amount of grafting materials for all experimental sites. This enabled us to compare the grafting sites with more confidence; however, this is not representative of the clinical situation, where the amount of grafting material is changed depending on the desired extent of augmentation, and the individual site anatomy. Also, when the inferior portion of the sinus is filled with grafting material, it creates a protected space for regeneration where the bone ingrowth may occur from three directions: medial, inferior and lateral. In our surgical model, only one direction was available for bone ingrowth, thereby creating “one wall defect” and possibly reducing the rate of graft consolidation.

The CN and CO grafting materials formulations that were used in this study are primarily intended for alveolar ridge preservation. Their conical shape is supposed to fit easily into the fresh extraction socket. The standardized quantity of pre-formed grafting material is also useful for research purposes. However, for SFE the handling of the conical-shaped grafting material is problematic. The operator has only limited control over the direction and the extent of graft placement. A gel-like or mouldable putty substrate which could adapt itself to the shape of the sinus, but still prevent the

dispersion of the particles of the grafting material, would have been more suited for SFE procedures.

4.3.3 Sources of bias

There were a number of possible sources of bias within the study that could have influenced the outcomes.

4.3.3.1 Randomization, allocation concealment, blinding

There was no allocation concealment and operator blinding implemented in the study. Instead, a predefined set of biomaterials was used for all the animals. This eliminated the allocation bias, but not the possible operator bias.

A single examiner trimmed the specimens, selected ground sections and analyzed all digitized microscopic images. It was impossible to blind the examiner for the type of biomaterial that was used in every specific site, due to obvious histologic differences between the biomaterials. To partially alleviate the possibility of examiner bias, inter-examiner comparisons were conducted with an independent examiner that was not part of the research group.

4.3.3.2 Specimen sectioning and histologic slide selection

In my study, we used embedded un-demineralised sections for histologic analysis. This technique is relatively simple and readily reproducible. The sections closest to the central part of the graft were selected based on radiographic imaging of the specimens. Between five to ten sections were cut from each specimen. Two of these sections were ground, stained and analyzed. It is possible that the selected sections were not representative of the entire experimental site, hereby introducing bias. Also, a learning curve existed for the operator: some sections were destroyed in the processing and could not be assessed. We analyzed not one, but two non-consecutive sections from each site in order to partially overcome the risk of bias from section selection.

4.3.3.3 ROI selection and analysis

The histomorphometric outcomes of the study depended on the selection of a region of interest (ROI) and its sectioning into the residual graft, new bone and connective tissue. We chose to include the entire augmented area into ROI but to exclude the new bone that repaired the antral walls. This was done to:

1. Analyze the area relevant to implant placement
2. Standardize the selection for all the specimens for reproducibility of results.

Ideally, to overcome the risk of examiner bias and achieve a reproducible result, automatic image sectioning (by software) should be implemented. In my study, no reliable software was identified for automatic sectioning of coloured histologic images, in part due to differences in staining between histologic slides. Therefore, the selection of ROI and its sectioning into new bone, residual graft and connective tissue was done manually. This might introduce an additional bias and influence the study outcomes.

4.3.4 Study limitations

Certain limitations were inherent in my study design. First, despite more than two-fold differences for new bone fraction between CO and BO, statistical significance was not achieved in my study. We speculated that my study had less than the adequate sample size. The previous study in an ovine model by our group²⁸¹ was not quantitative and did not provide information on the numbers required to achieve statistical significance. For my study, we selected a sample size of eleven, based on previous but slightly different studies which included simultaneous implant placement. The considerations for selecting the sample size were described in section 2.1.4.

No post-hoc power analysis was performed in this study. While questioning the sample size is legitimate, the post-hoc power analysis cannot provide further information as to desirable sample size. The results of post-hoc power calculations are

mathematically guaranteed to define any null-result study as underpowered. Based on the variability of my study data, we may speculate that larger sample size is required to achieve more clear-cut results.

The definition of ROI and the image sectioning were done manually by the primary investigator, which possibly introduced bias. Ideally, the image analysis should be done automatically. Despite the advances in machine learning systems, currently, no software solution exists for sectioning coloured histologic images. We performed intra- and inter-examiner reliability tests to reduce the possibility of bias from the manual image sectioning.

In this study, we could not analyze the extent of the repair of the surgical access windows. The original surgical defects became un-identifiable in multiple histological sections due to an exuberant bone repair. The surgical windows were not standardized due to our use of piezo-surgical instruments. In this study, the analysis of the repair of the surgical access window was not a primary objective. We believed that reducing the risk of SM perforations by using the piezo-surgical instruments would be more important than standardizing the surgical access size.

Another limitation comes from using a single time-point for all experimental animals. While providing more power to the study, this did not offer any insights as to the pace of graft consolidation and resorption. We are unable to comment on whether the BO or CO reached the limit of their potential or whether they would have retained the augmented volume when given a longer follow-up.

Finally, the extra-oral approach and the use of a standard amount of the grafting material are not representative of clinical practice of SFE.

Given the study limitations and the inherently limited applicability of animal research to humans, care should be exercised when assessing the outcomes of the present study.

4.4 Conclusions

The goal of my study was to evaluate three novel grafting materials for sinus floor elevation in a sheep model, using bovine xenograft (Geistlich Bio-Oss®) as a positive control. The tested products were: 1) equine collagen (PARASORB Cone®), 2) bovine non-sintered xenograft with polymer coating (IBI™ Smartbone®), 3) equine collagen cone filled with biphasic calcium phosphate (PARASORB Cone Oss®). After sacrificing all animals at the 16-week time-point, we evaluated histologic specimens for healing and graft consolidation patterns, carried out histomorphometric analysis and compared the tested materials with respect to the areas occupied by new bone, residual graft and connective tissue.

One animal failed to recover from general anaesthesia and was lost to analysis. All sites in the remaining animals healed uneventfully. The access windows in sheep antral walls demonstrated signs of bony repair with primary plexiform bone. As this bone replaced, in part, the original cortical plates, it was impossible to determine the extent of repair of the access windows.

At 16 weeks Cone® and Smartbone® disappeared from grafted sites, and the Schneiderian membrane collapsed. No extra-skeletal bone was formed in the augmented sites.

Both Bio-Oss® and Cone Oss® produced augmentation and new extra-skeletal bone formation. The new bone with both Bio-Oss® and Cone Oss® was comparatively low, which may be a result of the specific animal model used or insufficient time allocated for graft consolidation. There were no statistically significant differences in the new bone formation, connective tissue or residual graft areas between Bio-Oss® and Cone Oss®. We noted that on average twice as much new bone formed for Bio-Oss® than for Cone Oss®, although the results were highly variable.

My study used a previously developed animal model for sinus grafting in sheep with the extra-oral approach. This was the first time that the equine collagen-based grafting materials (Cone® and Cone Oss®) and polymer reinforced bovine xenograft (SmartBone®) had been tested in a large animal model.

The alloplastic filler of Cone Oss® is embedded in an equine collagen cone. While this makes handling of the alloplast easier, this formulation is less suitable for sinus floor elevation. The operator has only limited control over the direction and spread of the material. Gel- or putty-like mouldable matrix could be more suitable for sinus grafting while still providing better handling.

4.5 Recommendations for future research

Based on my study, we cannot recommend the use of the collagen Cone® or the particulate SmartBone® for sinus grafting. Studies could be conducted concerning different implementations of these materials, such as alveolar ridge preservation for Cone® or vertical ridge augmentation for SmartBone®. Also, an in-vitro investigation of the osteoclastic and hydrolytic resorption of SmartBone® could help to clarify the reasons for its disappearance from the grafted sinuses in my study.

The repair of the surgical access window after sinus floor elevation procedures is not adequately studied in the literature. The relationship between the window repair and the extent of the new bone formation in the grafted site could be further investigated. We discovered, that in the sheep model the margins of original surgical defects become un-identifiable histologically. A standardization of surgical access size could be considered to analyze the extent of the repair quantitatively:

1. By using standard-size trephine to create a surgical window. This approach bears more risk for Schneiderian membrane perforation by the trephine.
2. By using standard-size trephine after creating the initial non-standard access with piezo-tomes and elevating the Schneiderian membrane. This approach provides more control and less risk of perforating the membrane, which can be kept away from the trephine.
3. By using histologic markers such as staples or sutures through the residual sinus walls. This approach, however, introduces a foreign body which could alter the process of wound healing and graft incorporation.

This study assessed the outcomes at a single time-point to increase its power. This limited our ability to comment on healing trends, rates of new bone formation and

graft resorption. Future research could implement several time-points to investigate the extent and the rate of resorption of Cone Oss®.

Sinus floor elevation is performed to facilitate implant placement. Additional research is recommended to:

1. Quantify the impact of implant placement on the histologic outcomes of grafting. The sites grafted with Cone Oss® with and without concomitant implant placement could be histomorphometrically assessed.
2. Investigate the relationship between new bone formation in grafted sites, bone-to-implant contact and implant survival.

Finally, a biphasic composition of Cone Oss® could be further explored. An advantage of a completely synthetic material is its potential to be customized to a specific clinical demand. While the ideal ratio of hydroxyapatite and tricalcium phosphate was challenging to determine for general use¹⁶¹, it is possible that a ratio other than 60/40 will be especially suited for sinus floor elevation.

References

1. Jaffin RA, Berman CL. The excessive loss of Branemark fixtures in type IV bone: a 5-year analysis. *J Periodontol* 1991;62:2-4.
2. Kim YH, Choi NR, Kim YD. The factors that influence postoperative stability of the dental implants in posterior edentulous maxilla. *Maxillofac Plast Reconstr Surg* 2017;39:2.
3. Ekfeldt A, Christiansson U, Eriksson T, et al. A retrospective analysis of factors associated with multiple implant failures in maxillae. *Clin Oral Implants Res* 2001;12:462-467.
4. Telleman G, Raghoobar GM, Vissink A, den Hartog L, Huddleston Slater JJ, Meijer HJ. A systematic review of the prognosis of short (<10 mm) dental implants placed in the partially edentulous patient. *J Clin Periodontol* 2011;38:667-676.
5. Adell R, Lekholm U, Rockler B, Branemark PI. A 15-year study of osseointegrated implants in the treatment of the edentulous jaw. *Int J Oral Surg* 1981;10:387-416.
6. Scarano A, Degidi M, Iezzi G, Petrone G, Piattelli A. Correlation between implant stability quotient and bone-implant contact: a retrospective histological and histomorphometrical study of seven titanium implants retrieved from humans. *Clin Implant Dent Relat Res* 2006;8:218-222.
7. Alayan J, Vaquette C, Saifzadeh S, Hutmacher D, Ivanovski S. A histomorphometric assessment of collagen-stabilized anorganic bovine bone mineral in maxillary sinus augmentation - a randomized controlled trial in sheep. *Clin Oral Implants Res* 2016;27:734-743.
8. Barone A, Crespi R, Aldini NN, Fini M, Giardino R, Covani U. Maxillary sinus augmentation: histologic and histomorphometric analysis. *Int J Oral Maxillofac Implants* 2005;20:519-525.
9. Miloro M, Ghali G, Larsen P, Waite P. *Peterson's principles of oral and maxillofacial surgery*: PMPH-USA; 2004.
10. Lawson W, Patel ZM, Lin FY. The development and pathologic processes that influence maxillary sinus pneumatization. *Anat Rec (Hoboken)* 2008;291:1554-1563.
11. Wang RG, Jiang SC, Gu R. The cartilaginous nasal capsule and embryonic development of human paranasal sinuses. *J Otolaryngol* 1994;23:239-243.
12. Thomas A, Raman R. A comparative study of the pneumatization of the mastoid air cells and the frontal and maxillary sinuses. *AJNR Am J Neuroradiol* 1989;10:S88.
13. Shapiro R, Schorr S. A consideration of the systemic factors that influence frontal sinus pneumatization. *Invest Radiol* 1980;15:191-202.
14. Rosen MD, Sarnat BG. Change of volume of the maxillary sinus of the dog after extraction of adjacent teeth. *Oral Surg Oral Med Oral Pathol* 1955;8:420-429.
15. Sharan A, Madjar D. Maxillary sinus pneumatization following extractions: a radiographic study. *Int J Oral Maxillofac Implants* 2008;23:48-56.
16. Harorh A, Bocutoglu O. The comparison of vertical height and width of maxillary sinus by means of Waters' view radiograms taken from dentate and edentulous cases. *Ann Dent* 1995;54:47-49.
17. Ohba T, Langlais R, Morimoto Y, Tanaka T, Hashimoto K. Maxillary sinus floor in edentulous and dentate patients. *Indian J Dent Res* 2000;12:121-125.
18. Wolff J. The law of bone remodeling (Das gesetz der transformation der knochen). 1892.
19. Frost HM. Wolff's Law and bone's structural adaptations to mechanical usage: an overview for clinicians. *Angle Orthod* 1994;64:175-188.
20. Ulm CW, Solar P, Gsellmann B, Matejka M, Watzek G. The edentulous maxillary alveolar process in the region of the maxillary sinus--a study of physical dimension. *Int J Oral Maxillofac Surg* 1995;24:279-282.
21. Cawood JI, Howell RA. A classification of the edentulous jaws. *Int J Oral Maxillofac Surg* 1988;17:232-236.
22. Johnson K. A study of the dimensional changes occurring in the maxilla following tooth extraction. *Aust Dent J* 1969;14:241-244.

23. Lam RV. Contour changes of the alveolar processes following extractions. *The Journal of prosthetic dentistry* 1960;10:25-32.
24. Schropp L, Wenzel A, Kostopoulos L, Karring T. Bone healing and soft tissue contour changes following single-tooth extraction: a clinical and radiographic 12-month prospective study. *International Journal of Periodontics and Restorative Dentistry* 2003;23:313-324.
25. Misch CE. Maxillary sinus augmentation for endosteal implants: organized alternative treatment plans. *Int J Oral Implantol* 1987;4:49-58.
26. van den Bergh JP, ten Bruggenkate CM, Disch FJ, Tuinzing DB. Anatomical aspects of sinus floor elevations. *Clin Oral Implants Res* 2000;11:256-265.
27. Fugazzotto PA. Augmentation of the posterior maxilla: a proposed hierarchy of treatment selection. *J Periodontol* 2003;74:1682-1691.
28. Peleg M, Garg AK, Mazor Z. Predictability of simultaneous implant placement in the severely atrophic posterior maxilla: a 9-year longitudinal experience study of 2,132 implants placed into 731 human sinus grafts. *Int J Oral Maxillofac Implants* 2006;21:94.
29. Jensen OT. *The Sinus Bone Graft, Second Edition*. Chicago Ill. : Quintessence Pub. Co.; 2006.
30. Chrcanovic BR, Albrektsson T, Wennerberg A. Bone Quality and Quantity and Dental Implant Failure: A Systematic Review and Meta-analysis. *Int J Prosthodont* 2017;30:219-237.
31. Juodzbalys G, Kubilius M. Clinical and radiological classification of the jawbone anatomy in endosseous dental implant treatment. *J Oral Maxillofac Res* 2013;4:e2.
32. Zarb GA, Albrektsson T. *Tissue-integrated prostheses: osseointegration in clinical dentistry*: Quintessence Pub Co; 1985.
33. Turkyilmaz I, McGlumphy EA. Influence of bone density on implant stability parameters and implant success: a retrospective clinical study. *BMC Oral Health* 2008;8:32.
34. Shahlaie M, Gantes B, Schulz E, Riggs M, Crigger M. Bone density assessments of dental implant sites: 1. Quantitative computed tomography. *Int J Oral Maxillofac Implants* 2003;18:224-231.
35. Aranyarachkul P, Caruso J, Gantes B, et al. Bone density assessments of dental implant sites: 2. Quantitative cone-beam computerized tomography. *Int J Oral Maxillofac Implants* 2005;20:416-424.
36. Traini T, Piattelli A, Caputi S, et al. Regeneration of human bone using different bone substitute biomaterials. *Clin Implant Dent Relat Res* 2015;17:150-162.
37. Bergkvist G, Sahlholm S, Klintström E, Lindh C, Koh K-J. Bone Density at Implant Sites and Its Relationship to Assessment of Bone Quality and Treatment Outcome. *Int J Oral Maxillofac Implants* 2010;25:321-328.
38. Friberg B, Jemt T, Lekholm U. Early failures in 4,641 consecutively placed Branemark dental implants: a study from stage 1 surgery to the connection of completed prostheses. *Int J Oral Maxillofac Implants* 1991;6:142-146.
39. van Steenberghe D, Jacobs R, Desnyder M, Maffei G, Quirynen M. The relative impact of local and endogenous patient-related factors on implant failure up to the abutment stage. *Clin Oral Implants Res* 2002;13:617-622.
40. Ulm C, Tepper G, Blahout R, Rausch-Fan X, Hienz S, Matejka M. Characteristic features of trabecular bone in edentulous mandibles. *Clin Oral Implants Res* 2009;20:594-600.
41. Fuh LJ, Huang HL, Chen CS, et al. Variations in bone density at dental implant sites in different regions of the jawbone. *J Oral Rehabil* 2010;37:346-351.
42. Turkyilmaz I, Tozum TF, Tumer C. Bone density assessments of oral implant sites using computerized tomography. *J Oral Rehabil* 2007;34:267-272.
43. de Oliveira RC, Leles CR, Normanha LM, Lindh C, Ribeiro-Rotta RF. Assessments of trabecular bone density at implant sites on CT images. *Oral Surg Oral Med Oral Pathol Oral Radiol Endod* 2008;105:231-238.
44. Drago CJ. Rates of osseointegration of dental implants with regard to anatomical location. *J Prosthodont* 1992;1:29-31.
45. Glauser R, Ree A, Lundgren A, Gottlow J, Hammerle CHR, Scharer P. Immediate Occlusal Loading of Brånemark Implants Applied in Various Jawbone Regions: A Prospective, 1-Year Clinical Study. *Clin Implant Dent Relat Res* 2001;3:204-213.
46. Rao T, Rao W. Bone classification: clinical-histomorphometric comparison. *Clin Oral Implants Res* 1999;10:1-7.

47. Chappard D, Aguado E, Hure G, Grizon F, Basle MF. The early remodeling phases around titanium implants: a histomorphometric assessment of bone quality in a 3- and 6-month study in sheep. *Int J Oral Maxillofac Implants* 1999;14:189-196.
48. Kim Y-H, Koak J-Y, Chang I-T, Wennerberg A, Heo S-J. A histomorphometric analysis of the effects of various surface treatment methods on osseointegration. *Int J Oral Maxillofac Implants* 2003;18.
49. Berglundh T, Lindhe J. Healing around implants placed in bone defects treated with Bio-OssR. An experimental study in the dog. *Clin Oral Implants Res* 1997;8:117-124.
50. Wetzel AC, Stich H, Caffesse RG. Bone apposition onto oral implants in the sinus area filled with different grafting materials. A histological study in beagle dogs. *Clin Oral Implants Res* 1995;6:155-163.
51. Valentini P, Abensur D, Densari D, Graziani JN, Hammerle C. Histological evaluation of Bio-Oss in a 2-stage sinus floor elevation and implantation procedure. A human case report. *Clin Oral Implants Res* 1998;9:59-64.
52. Araujo MG, Linder E, Lindhe J. Bio-Oss collagen in the buccal gap at immediate implants: a 6-month study in the dog. *Clin Oral Implants Res* 2011;22:1-8.
53. Hallman M, Sennerby L, Lundgren S. A clinical and histologic evaluation of implant integration in the posterior maxilla after sinus floor augmentation with autogenous bone, bovine hydroxyapatite, or a 20:80 mixture. *Int J Oral Maxillofac Implants* 2002;17:635-643.
54. Polyzois I, Renvert S, Bosshardt DD, Lang NP, Claffey N. Effect of Bio-Oss on osseointegration of dental implants surrounded by circumferential bone defects of different dimensions: an experimental study in the dog. *Clin Oral Implants Res* 2007;18:304-310.
55. Cameron HU, Pilliar RM, MacNab I. The effect of movement on the bonding of porous metal to bone. *J Biomed Mater Res* 1973;7:301-311.
56. Hoshaw SJ, Brunski JB, Cochran GV. Mechanical Loading of Brånemark Implants Affects Interfacial Bone Modeling and Remodeling. *Int J Oral Maxillofac Implants* 1994;9.
57. del Valle V, Faulkner G, Wolfaardt J. Craniofacial osseointegrated implant-induced strain distribution: a numerical study. *Int J Oral Maxillofac Implants* 1997;12:200-210.
58. Quirynen M, Naert I, van Steenberghe D. Fixture design and overload influence marginal bone loss and future success in the BranemarkR system. *Clin Oral Implants Res* 1992;3:104-111.
59. Stanford CM, Brand RA. Toward an understanding of implant occlusion and strain adaptive bone modeling and remodeling. *J Prosthet Dent* 1999;81:553-561.
60. Jemt T, Lekholm U, Adell R. Osseointegrated Implants in the Treatment of Partially Edentulous Patients: A Preliminary Study on 876 Consecutively Placed Fixtures. *Int J Oral Maxillofac Implants* 1989;4.
61. Zitzmann NU, Berglundh T. Definition and prevalence of peri-implant diseases. *J Clin Periodontol* 2008;35:286-291.
62. Heitz-Mayfield LJ. Peri-implant diseases: diagnosis and risk indicators. *J Clin Periodontol* 2008;35:292-304.
63. Albrektsson T, Isidor F. Criteria for success and failure of an implant system. Consensus report. In: *Proceedings of the 1st European workshop on Periodontology Chicago, IL: Quintessence*, 1994:243-244.
64. Lang NP, Berglundh T, Working Group 4 of Seventh European Workshop on P. Periimplant diseases: where are we now?--Consensus of the Seventh European Workshop on Periodontology. *J Clin Periodontol* 2011;38 Suppl 11:178-181.
65. Becker ST, Beck-Broichsitter BE, Graetz C, Dorfer CE, Wiltfang J, Hasler R. Peri-implantitis versus periodontitis: functional differences indicated by transcriptome profiling. *Clin Implant Dent Relat Res* 2014;16:401-411.
66. Calvo-Guirado JL, Gomez-Moreno G, Delgado-Ruiz RA, Mate Sanchez de Val JE, Negri B, Ramirez Fernandez MP. Clinical and radiographic evaluation of osseotite-expanded platform implants related to crestal bone loss: a 10-year study. *Clin Oral Implants Res* 2014;25:352-358.
67. Esposito M, Hirsch JM, Lekholm U, Thomsen P. Biological factors contributing to failures of osseointegrated oral implants. (II). Etiopathogenesis. *Eur J Oral Sci* 1998;106:721-764.
68. Sanz M, Chapple IL, Working Group 4 of the VEWoP. Clinical research on peri-implant diseases: consensus report of Working Group 4. *J Clin Periodontol* 2012;39 Suppl 12:202-206.
69. Albrektsson T, Chrcanovic B, Ostman PO, Sennerby L. Initial and long-term crestal bone responses to modern dental implants. *Periodontol 2000* 2017;73:41-50.

70. Stegaroiu R, Sato T, Kusakari H, Miyakawa O. Influence of restoration type on stress distribution in bone around implants: a three-dimensional finite element analysis. *Int J Oral Maxillofac Implants* 1998;13:82-90.
71. Bidez M, Misch C. Force transfer in implant dentistry: basic concepts and principles. *J Oral Implantol* 1991;18:264-274.
72. Misch CE. Density of bone: effect on treatment plans, surgical approach, healing, and progressive bone loading. *Int J Oral Implantol* 1990;6:23-31.
73. Tepper G, Haas R, Zechner W, Krach W, Watzek G. Three-dimensional finite element analysis of implant stability in the atrophic posterior maxilla: a mathematical study of the sinus floor augmentation. *Clin Oral Implants Res* 2002;13:657-665.
74. Wallace SS, Froum SJ. Effect of maxillary sinus augmentation on the survival of endosseous dental implants. A systematic review. *Ann Periodontol* 2003;8:328-343.
75. Del Fabbro M, Wallace SS, Testori T. Long-term implant survival in the grafted maxillary sinus: a systematic review. *Int J Periodontics Restorative Dent* 2013;33:773-783.
76. Nkenke E, Stelzle F. Clinical outcomes of sinus floor augmentation for implant placement using autogenous bone or bone substitutes: a systematic review. *Clin Oral Implants Res* 2009;20 Suppl 4:124-133.
77. Pjetursson BE, Tan WC, Zwahlen M, Lang NP. A systematic review of the success of sinus floor elevation and survival of implants inserted in combination with sinus floor elevation. *J Clin Periodontol* 2008;35:216-240.
78. Albrektsson T, Johansson C. Osteoinduction, osteoconduction and osseointegration. *Eur Spine J* 2001;10 Suppl 2:S96-101.
79. Reddi AH, Huggins C. Biochemical sequences in the transformation of normal fibroblasts in adolescent rats. *Proc Natl Acad Sci U S A* 1972;69:1601-1605.
80. Scott CK, Hightower JA. The matrix of endochondral bone differs from the matrix of intramembranous bone. *Calcif Tissue Int* 1991;49:349-354.
81. Shapiro F. Bone development and its relation to fracture repair. The role of mesenchymal osteoblasts and surface osteoblasts. *Eur Cell Mater* 2008;15:53-76.
82. Johansson CB, Han CH, Wennerberg A, Albrektsson T. A quantitative comparison of machined commercially pure titanium and titanium-aluminum-vanadium implants in rabbit bone. *Int J Oral Maxillofac Implants* 1998;13:315-321.
83. Hammerle CHF, Schmid J, Olah AJ, Lang NP. Influence of initial implant mobility on the integration of titanium implants. An experimental study in rabbits. *Clin Oral Implants Res* 1996;7:120-127.
84. Dahlin C, Sennerby L, Lekholm U, Linde A, Nyman S. Generation of new bone around titanium implants using a membrane technique: an experimental study in rabbits. *The International Journal of Oral & maxillofacial Implants* 1989;4:19.
85. Duncan WJ. Sheep Mandibular Animal Models for Dental Implantology Research: A Thesis Submitted for the Degree of Doctor of Philosophy at the University of Otago, Dunedin, New Zealand: University of Otago; 2005.
86. Smith JD, Abramson M. Membranous vs Endochondral Bone Autografts. *Arch Otolaryngol Head Neck Surg* 1974;99:203-205.
87. Zins JE, Whitaker LA. Membranous versus endochondral bone: implications for craniofacial reconstruction. *Plast Reconstr Surg* 1983;72:778-785.
88. Lieberman JR, Daluiski A, Einhorn TA. The role of growth factors in the repair of bone. Biology and clinical applications. *J Bone Joint Surg Am* 2002;84-A:1032-1044.
89. Dimitriou R, Tsiridis E, Giannoudis PV. Current concepts of molecular aspects of bone healing. *Injury* 2005;36:1392-1404.
90. Muschler GF, Nakamoto C, Griffith LG. Engineering principles of clinical cell-based tissue engineering. *J Bone Joint Surg Am* 2004;86-A:1541-1558.
91. Rodriguez PG, Felix FN, Woodley DT, Shim EK. The role of oxygen in wound healing: a review of the literature. *Dermatol Surg* 2008;34:1159-1169.
92. Santos MI, Reis RL. Vascularization in bone tissue engineering: physiology, current strategies, major hurdles and future challenges. *Macromol Biosci* 2010;10:12-27.

93. Pittenger MF, Mackay AM, Beck SC, et al. Multilineage potential of adult human mesenchymal stem cells. *Science* 1999;284:143-147.
94. Eghbali-Fatourehchi GZ, Lamsam J, Fraser D, Nagel D, Riggs BL, Khosla S. Circulating osteoblast-lineage cells in humans. *N Engl J Med* 2005;352:1959-1966.
95. Doherty MJ, Ashton BA, Walsh S, Beresford JN, Grant ME, Canfield AE. Vascular pericytes express osteogenic potential in vitro and in vivo. *J Bone Miner Res* 1998;13:828-838.
96. Spradling A, Drummond-Barbosa D, Kai T. Stem cells find their niche. *Nature* 2001;414:98-104.
97. Srouji S, Kizhner T, Ben David D, Riminucci M, Bianco P, Livne E. The Schneiderian membrane contains osteoprogenitor cells: in vivo and in vitro study. *Calcif Tissue Int* 2009;84:138-145.
98. Srouji S, Ben-David D, Lotan R, Riminucci M, Livne E, Bianco P. The innate osteogenic potential of the maxillary sinus (Schneiderian) membrane: an ectopic tissue transplant model simulating sinus lifting. *Int J Oral Maxillofac Surg* 2010;39:793-801.
99. Scala A, Botticelli D, Faeda RS, Garcia Rangel I, Jr., Americo de Oliveira J, Lang NP. Lack of influence of the Schneiderian membrane in forming new bone apical to implants simultaneously installed with sinus floor elevation: an experimental study in monkeys. *Clin Oral Implants Res* 2012;23:175-181.
100. Schenk RK, Buser D. Osseointegration: a reality. *Periodontol* 2000 1998;17:22-35.
101. Frost HMMD. *Bone remodelling dynamics: The Henry Ford Hospital surgical monographs*; 1963.
102. Kalfas IH. Principles of bone healing. *Neurosurg Focus* 2001;10:E1.
103. Frost HM. A 2003 update of bone physiology and Wolff's Law for clinicians. *Angle Orthod* 2004;74:3-15.
104. Frost HM. Changing concepts in skeletal physiology: Wolff's Law, the Mechanostat, and the "Utah Paradigm". *Am J Hum Biol* 1998;10:599-605.
105. Burr DB. Targeted and nontargeted remodeling. *Bone* 2002;30:2-4.
106. Martin RB. Toward a unifying theory of bone remodeling. *Bone* 2000;26:1-6.
107. Frost HMMD. The Biology of Fracture Healing: An Overview for Clinicians. Part I. *Clinical Orthopaedics & Related Research November* 1989;248:283-293.
108. Frost HM. The biology of fracture healing. An overview for clinicians. Part II. *Clin Orthop Relat Res* 1989;248:294-309.
109. Thomsen JS, Ebbesen EN, Mosekilde L. Relationships Between Static Histomorphometry and Bone Strength Measurements in Human Iliac Crest Bone Biopsies. *Bone* 1998;22:153-163.
110. Schmitz JP, Hollinger JO. The critical size defect as an experimental model for craniomaxillofacial nonunions. In: WALTER REED ARMY MEDICAL CENTER WASHINGTON DC, 1985.
111. Viljanen VV, Gao TJ, Lindholm TC, Lindholm TS, Kommonen B. Xenogeneic moose (*Alces alces*) bone morphogenetic protein (mBMP)-induced repair of critical-size skull defects in sheep. *Int J Oral Maxillofac Surg* 1996;25:217-222.
112. Bosch C, Melsen B, Vargervik K. Importance of the critical-size bone defect in testing bone-regenerating materials. *J Craniofac Surg* 1998;9:310-316.
113. Schweikert M, Botticelli D, de Oliveira JA, Scala A, Salata LA, Lang NP. Use of a titanium device in lateral sinus floor elevation: an experimental study in monkeys. *Clin Oral Implants Res* 2012;23:100-105.
114. Palma VC, Magro-Filho O, de Oliveria JA, Lundgren S, Salata LA, Sennerby L. Bone reformation and implant integration following maxillary sinus membrane elevation: an experimental study in primates. *Clin Implant Dent Relat Res* 2006;8:11-24.
115. Cricchio G, Palma VC, Faria PE, et al. Histological outcomes on the development of new space-making devices for maxillary sinus floor augmentation. *Clin Implant Dent Relat Res* 2011;13:224-230.
116. Scala A, Botticelli D, Rangel IG, Jr., de Oliveira JA, Okamoto R, Lang NP. Early healing after elevation of the maxillary sinus floor applying a lateral access: a histological study in monkeys. *Clin Oral Implants Res* 2010;21:1320-1326.
117. Lundgren S, Andersson S, Gualini F, Sennerby L. Bone reformation with sinus membrane elevation: a new surgical technique for maxillary sinus floor augmentation. *Clin Implant Dent Relat Res* 2004;6:165-173.
118. Johansson LA, Isaksson S, Adolffsson E, Lindh C, Sennerby L. Bone regeneration using a hollow hydroxyapatite space-maintaining device for maxillary sinus floor augmentation--a clinical pilot study. *Clin Implant Dent Relat Res* 2012;14:575-584.

119. Xu H, Shimizu Y, Asai S, Ooya K. Grafting of deproteinized bone particles inhibits bone resorption after maxillary sinus floor elevation. *Clin Oral Implants Res* 2004;15:126-133.
120. Kim HR, Choi BH, Xuan F, Jeong SM. The use of autologous venous blood for maxillary sinus floor augmentation in conjunction with sinus membrane elevation: an experimental study. *Clin Oral Implants Res* 2010;21:346-349.
121. Haas R, Donath K, Fodinger M, Watzek G. Bovine hydroxyapatite for maxillary sinus grafting: comparative histomorphometric findings in sheep. *Clin Oral Implants Res* 1998;9:107-116.
122. Albrektsson T. Principles of osseointegration. *Dental and Maxillofacial Implantology, Mosby-Wolfe, London* 1995:9-19.
123. Kilpadi KL, Chang PL, Bellis SL. Hydroxylapatite binds more serum proteins, purified integrins, and osteoblast precursor cells than titanium or steel. *J Biomed Mater Res* 2001;57:258-267.
124. Matsui N, Nozaki K, Ishihara K, Yamashita K, Nagai A. Concentration-dependent effects of fibronectin adsorbed on hydroxyapatite surfaces on osteoblast adhesion. *Mater Sci Eng C Mater Biol Appl* 2015;48:378-383.
125. Wilson CJ, Clegg RE, Leavesley DI, Percy MJ. Mediation of biomaterial-cell interactions by adsorbed proteins: a review. *Tissue Eng* 2005;11:1-18.
126. Gutwald R, Haberstroh J, Stricker A, et al. Influence of rhBMP-2 on bone formation and osseointegration in different implant systems after sinus-floor elevation. An in vivo study on sheep. *J Craniomaxillofac Surg* 2010;38:571-579.
127. Boyne PJ, Marx RE, Nevins M, et al. A feasibility study evaluating rhBMP-2/absorbable collagen sponge for maxillary sinus floor augmentation. *Int J Periodontics Restorative Dent* 1997;17:11-25.
128. Jakse N, Tangl S, Gilli R, et al. Influence of PRP on autogenous sinus grafts. An experimental study on sheep. *Clin Oral Implants Res* 2003;14:578-583.
129. Schliephake H. Bone growth factors in maxillofacial skeletal reconstruction. *Int J Oral Maxillofac Surg* 2002;31:469-484.
130. Baylink DJ, Finkelman RD, Mohan S. Growth factors to stimulate bone formation. *J Bone Miner Res* 1993;8 Suppl 2:S565-572.
131. Del Fabbro M, Bortolin M, Taschieri S, Weinstein RL. Effect of autologous growth factors in maxillary sinus augmentation: a systematic review. *Clin Implant Dent Relat Res* 2013;15:205-216.
132. Abdallah MN, Tran SD, Abughanam G, et al. Biomaterial surface proteomic signature determines interaction with epithelial cells. *Acta Biomater* 2017;54:150-163.
133. Nashimoto M, Matsuzaka K, Yoshinari M, Shimono M, Inoue T. The effect of surface pore size on the differentiation of rat bone marrow cells: morphological observations and expression of bone related protein mRNA. *Bull Tokyo Dent Coll* 2004;45:201-211.
134. Gruber R, Baron M, Busenlechner D, Kandler B, Fuerst G, Watzek G. Proliferation and osteogenic differentiation of cells from cortical bone cylinders, bone particles from mill, and drilling dust. *J Oral Maxillofac Surg* 2005;63:238-243.
135. Ray RD. Vascularization of bone grafts and implants. *Clin Orthop Relat Res* 1972;87:43-48.
136. Ray RD, Sabet TY. Bone Grafts: Cellular Survival Versus Induction: AN EXPERIMENTAL STUDY IN MICE. *JBS* 1963;45:337-344.
137. Khan SN, Cammisa FP, Jr., Sandhu HS, Diwan AD, Girardi FP, Lane JM. The biology of bone grafting. *J Am Acad Orthop Surg* 2005;13:77-86.
138. Lee DY, Cho TJ, Kim JA, et al. Mobilization of endothelial progenitor cells in fracture healing and distraction osteogenesis. *Bone* 2008;42:932-941.
139. Gotz W, Reichert C, Canullo L, Jager A, Heinemann F. Coupling of osteogenesis and angiogenesis in bone substitute healing - a brief overview. *Ann Anat* 2012;194:171-173.
140. Chow DC, Wenning LA, Miller WM, Papoutsakis ET. Modeling pO₂ distributions in the bone marrow hematopoietic compartment. II. Modified Kroghian models. *Biophys J* 2001;81:685-696.
141. Chow DC, Wenning LA, Miller WM, Papoutsakis ET. Modeling pO₂ distributions in the bone marrow hematopoietic compartment. I. Krogh's model. *Biophys J* 2001;81:675-684.
142. Lieberman JR, Friedlaender GE. *Bone Regeneration and Repair*. New Jersey: Humana press; 2005: 398.
143. Buser D. 20 years of guided bone regeneration. In: Quintessence publishing, 2009.

144. Hing KA, Best SM, Tanner KE, Bonfield W, Revell PA. Mediation of bone ingrowth in porous hydroxyapatite bone graft substitutes. *J Biomed Mater Res A* 2004;68:187-200.
145. Karageorgiou V, Kaplan D. Porosity of 3D biomaterial scaffolds and osteogenesis. *Biomaterials* 2005;26:5474-5491.
146. Klawitter J, Bagwell J, Weinstein A, Sauer B, Pruitt J. An evaluation of bone growth into porous high density polyethylene. *Journal of Biomedical Materials Research Part A* 1976;10:311-323.
147. Vandeweghe S, Leconte C, Ono D, Coelho PG, Jimbo R. Comparison of histological and three-dimensional characteristics of porous titanium granules and deproteinized bovine particulate grafts used for sinus floor augmentation in humans: a pilot study. *Implant Dent* 2013;22:339-343.
148. Daculsi G, Passuti N. Effect of the macroporosity for osseous substitution of calcium phosphate ceramics. *Biomaterials* 1990;11:86-87.
149. Uchida A, Nade S, McCartney E, Ching W. The use of ceramics for bone replacement. A comparative study of three different porous ceramics. *Bone & Joint Journal* 1984;66:269-275.
150. Eggli PS, Muller W, Schenk RK. Porous hydroxyapatite and tricalcium phosphate cylinders with two different pore size ranges implanted in the cancellous bone of rabbits. A comparative histomorphometric and histologic study of bony ingrowth and implant substitution. *Clin Orthop Relat Res* 1988;232:127-138.
151. Lu JX, Flauter B, Anselme K, et al. Role of interconnections in porous bioceramics on bone recolonization in vitro and in vivo. *J Mater Sci Mater Med* 1999;10:111-120.
152. Busenlechner D, Tangl S, Mair B, et al. Simultaneous in vivo comparison of bone substitutes in a guided bone regeneration model. *Biomaterials* 2008;29:3195-3200.
153. Clokie CM, Moghadam H, Jackson MT, Sandor GK. Closure of critical sized defects with allogenic and alloplastic bone substitutes. *J Craniofac Surg* 2002;13:111-121; discussion 122-113.
154. Reynolds MA, Aichelmann-Reidy ME, Kassolis JD, Prasad HS, Rohrer MD. Calcium sulfate-carboxymethylcellulose bone graft binder: Histologic and morphometric evaluation in a critical size defect. *J Biomed Mater Res B Appl Biomater* 2007;83:451-458.
155. Busenlechner D, Huber CD, Vasak C, Dobsak A, Gruber R, Watzek G. Sinus augmentation analysis revised: the gradient of graft consolidation. *Clin Oral Implants Res* 2009;20:1078-1083.
156. Fuerst G, Tangl S, Gruber R, Gahleitner A, Sanroman F, Watzek G. Bone formation following sinus grafting with autogenous bone-derived cells and bovine bone mineral in minipigs: preliminary findings. *Clin Oral Implants Res* 2004;15:733-740.
157. Artzi Z, Kozlovsky A, Nemcovsky CE, Weinreb M. The amount of newly formed bone in sinus grafting procedures depends on tissue depth as well as the type and residual amount of the grafted material. *J Clin Periodontol* 2005;32:193-199.
158. Orsini G, Traini T, Scarano A, et al. Maxillary sinus augmentation with Bio-Oss particles: a light, scanning, and transmission electron microscopy study in man. *J Biomed Mater Res B Appl Biomater* 2005;74:448-457.
159. Busenlechner D, Tangl S, Arnhart C, et al. Resorption of deproteinized bovine bone mineral in a porcine calvaria augmentation model. *Clin Oral Implants Res* 2012;23:95-99.
160. LeGeros RZ. Calcium phosphate-based osteoinductive materials. *Chem Rev* 2008;108:4742-4753.
161. Jensen SS, Bornstein MM, Dard M, Bosshardt DD, Buser D. Comparative study of biphasic calcium phosphates with different HA/TCP ratios in mandibular bone defects. A long-term histomorphometric study in minipigs. *J Biomed Mater Res B Appl Biomater* 2009;90:171-181.
162. Sartori S, Silvestri M, Forni F, Icaro Cornaglia A, Tesei P, Cattaneo V. Ten-year follow-up in a maxillary sinus augmentation using anorganic bovine bone (Bio-Oss). A case report with histomorphometric evaluation. *Clin Oral Implants Res* 2003;14:369-372.
163. Frost HM. The regional acceleratory phenomenon: a review. *Henry Ford Hosp Med J* 1983;31:3-9.
164. Abrahamsson I, Berglundh T, Linder E, Lang NP, Lindhe J. Early bone formation adjacent to rough and turned endosseous implant surfaces. An experimental study in the dog. *Clin Oral Implants Res* 2004;15:381-392.
165. Smiler DG, Johnson P, Lozada JLe, et al. Sinus lift grafts and endosseous implants. Treatment of the atrophic posterior maxilla. *Dental Clinics of North America* 1992;36:151-186; discussion 187-158.

166. Merckx MA, Maltha JC, Stoeltinga PJ. Assessment of the value of anorganic bone additives in sinus floor augmentation: a review of clinical reports. *Int J Oral Maxillofac Surg* 2003;32:1-6.
167. Kohal RJ, Gubik S, Strohl C, et al. Effect of two different healing times on the mineralization of newly formed bone using a bovine bone substitute in sinus floor augmentation: a randomized, controlled, clinical and histological investigation. *J Clin Periodontol* 2015;42:1052-1059.
168. Schlegel KA, Schultze-Mosgau S, Wiltfang J, Neukam FW, Rupprecht S, Thorwarth M. Changes of mineralization of free autogenous bone grafts used for sinus floor elevation. *Clin Oral Implants Res* 2006;17:673-678.
169. Kalk WW, Raghoobar GM, Jansma J, Boering G. Morbidity from iliac crest bone harvesting. *J Oral Maxillofac Surg* 1996;54:1424-1429; discussion 1430.
170. Raghoobar GM, Batenburg RH, Timmenga NM, Vissink A, Reintsema H. Morbidity and complications of bone grafting of the floor of the maxillary sinus for the placement of endosseous implants. *Mund Kiefer Gesichtschir* 1999;3 Suppl 1:S65-69.
171. Hall MB. Morbidity from iliac crest bone harvesting. *J Oral Maxillofac Surg* 1996;54:1430.
172. Browaeys H, Bouvry P, De Bruyn H. A literature review on biomaterials in sinus augmentation procedures. *Clin Implant Dent Relat Res* 2007;9:166-177.
173. Shanbhag S, Shanbhag V, Stavropoulos A. Volume changes of maxillary sinus augmentations over time: a systematic review. *Int J Oral Maxillofac Implants* 2014;29:881-892.
174. Gerressen M, Riediger D, Hilgers RD, Holzle F, Noroozi N, Ghassemi A. The Volume Behavior of Autogenous Iliac Bone Grafts After Sinus Floor Elevation: A Clinical Pilot Study. *J Oral Implantol* 2015;41:276-283.
175. Lavernia CJ, Malinin TI, Temple HT, Moreyra CE. Bone and tissue allograft use by orthopaedic surgeons. *J Arthroplasty* 2004;19:430-435.
176. Scarano A, Degidi M, Iezzi G, et al. Maxillary sinus augmentation with different biomaterials: a comparative histologic and histomorphometric study in man. *Implant Dent* 2006;15:197-207.
177. Lyford RH, Mills MP, Knapp CI, Scheyer ET, Mellonig JT. Clinical evaluation of freeze-dried block allografts for alveolar ridge augmentation: a case series. *Int J Periodontics Restorative Dent* 2003;23:417-425.
178. Jensen OT, Shulman LB, Block MS, Iacono VJ. Report of the sinus consensus conference of 1996. *The International Journal of Oral & maxillofacial Implants* 1997;13:11-45.
179. Jensen SS, Aaboe M, Pinholt EM, Hjorting-Hansen E, Melsen F, Ruyter IE. Tissue reaction and material characteristics of four bone substitutes. *Int J Oral Maxillofac Implants* 1996;11:55-66.
180. Kim Y, Nowzari H, Rich SK. Risk of Prion Disease Transmission through Bovine-Derived Bone Substitutes: A Systematic Review. *Clin Implant Dent Relat Res* 2013;15:645-653.
181. Mokbel N, Bou Serhal C, Matni G, Naaman N. Healing patterns of critical size bony defects in rat following bone graft. *Oral Maxillofac Surg* 2008;12:73-78.
182. Di Stefano DA, Gastaldi G, Vinci R, et al. Bone Formation Following Sinus Augmentation with an Equine-Derived Bone Graft: A Retrospective Histologic and Histomorphometric Study with 36-Month Follow-up. *Int J Oral Maxillofac Implants* 2016;31:406-412.
183. McAllister BS, Margolin MD, Cogan AG, Buck D, Hollinger JO, Lynch SE. Eighteen-month radiographic and histologic evaluation of sinus grafting with anorganic bovine bone in the chimpanzee. *Int J Oral Maxillofac Implants* 1999;14:361-368.
184. Artzi Z, Weinreb M, Givol N, et al. Biomaterial resorption rate and healing site morphology of inorganic bovine bone and beta-tricalcium phosphate in the canine: a 24-month longitudinal histologic study and morphometric analysis. *Int J Oral Maxillofac Implants* 2004;19:357-368.
185. Galindo-Moreno P, Hernandez-Cortes P, Mesa F, et al. Slow resorption of anorganic bovine bone by osteoclasts in maxillary sinus augmentation. *Clin Implant Dent Relat Res* 2013;15:858-866.
186. Klein MO, Kammerer PW, Gotz H, Duschner H, Wagner W. Long-term bony integration and resorption kinetics of a xenogeneic bone substitute after sinus floor augmentation: histomorphometric analyses of human biopsy specimens. *Int J Periodontics Restorative Dent* 2013;33:e101-110.
187. Mordenfeld A, Hallman M, Johansson CB, Albrektsson T. Histological and histomorphometrical analyses of biopsies harvested 11 years after maxillary sinus floor augmentation with deproteinized bovine and autogenous bone. *Clin Oral Implants Res* 2010;21:961-970.

188. Wang F, Zhou W, Monje A, Huang W, Wang Y, Wu Y. Influence of Healing Period Upon Bone Turn Over on Maxillary Sinus Floor Augmentation Grafted Solely with Deproteinized Bovine Bone Mineral: A Prospective Human Histological and Clinical Trial. *Clin Implant Dent Relat Res* 2017;19:341-350.
189. Wallace SS, Tarnow DP, Froum SJ, et al. Maxillary sinus elevation by lateral window approach: evolution of technology and technique. *J Evid Based Dent Pract* 2012;12:161-171.
190. Jensen T, Schou S, Stavropoulos A, Terheyden H, Holmstrup P. Maxillary sinus floor augmentation with Bio-Oss or Bio-Oss mixed with autogenous bone as graft: a systematic review. *Clin Oral Implants Res* 2012;23:263-273.
191. Mardinger O, Chaushu G, Sigalov S, Herzberg R, Shlomi B, Schwartz-Arad D. Factors affecting changes in sinus graft height between and above the placed implants. *Oral Surgery, Oral Medicine, Oral Pathology, Oral Radiology, and Endodontology* 2011;111:e6-e11.
192. Yildirim M, Spiekermann H, Handt S, Edelhoff D. Maxillary sinus augmentation with the xenograft Bio-Oss and autogenous intraoral bone for qualitative improvement of the implant site: a histologic and histomorphometric clinical study in humans. *Int J Oral Maxillofac Implants* 2001;16:23-33.
193. Hatano N, Shimizu Y, Ooya K. A clinical long-term radiographic evaluation of graft height changes after maxillary sinus floor augmentation with a 2:1 autogenous bone/xenograft mixture and simultaneous placement of dental implants. *Clin Oral Implants Res* 2004;15:339-345.
194. Umanjec-Korac S, Wu G, Hassan B, Liu Y, Wismeijer D. A retrospective analysis of the resorption rate of deproteinized bovine bone as maxillary sinus graft material on cone beam computed tomography. *Clin Oral Implants Res* 2014;25:781-785.
195. Goller G, Oktar F, Agathopoulos S, et al. Effect of sintering temperature on mechanical and microstructural properties of bovine hydroxyapatite (BHA). *Journal of sol-gel science and technology* 2006;37:111-115.
196. Gomi K, Lowenberg B, Shapiro G, Davies JE. Resorption of sintered synthetic hydroxyapatite by osteoclasts in vitro. *Biomaterials* 1993;14:91-96.
197. Panagiotou D, Ozkan Karaca E, Dirikan Ipci S, Cakar G, Olgac V, Yilmaz S. Comparison of two different xenografts in bilateral sinus augmentation: radiographic and histologic findings. *Quintessence Int* 2015;46:611-619.
198. Fienitz T, Moses O, Klemm C, et al. Histological and radiological evaluation of sintered and non-sintered deproteinized bovine bone substitute materials in sinus augmentation procedures. A prospective, randomized-controlled, clinical multicenter study. *Clin Oral Investig* 2017;21:787-794.
199. Karageorgiou V, Kaplan D. Porosity of 3D biomaterial scaffolds and osteogenesis. *Biomaterials* 2005;26:5474-5491.
200. Figueiredo M, Henriques J, Martins G, Guerra F, Judas F, Figueiredo H. Physicochemical characterization of biomaterials commonly used in dentistry as bone substitutes--comparison with human bone. *J Biomed Mater Res B Appl Biomater* 2010;92:409-419.
201. Ozyuvaci H, Bilgic B, Firatli E. Radiologic and histomorphometric evaluation of maxillary sinus grafting with alloplastic graft materials. *J Periodontol* 2003;74:909-915.
202. Tadjedin ES, Lange GL, Holzmann PJ, Kuiper L, Burger EH. Histological observations on biopsies harvested following sinus floor elevation using a bioactive glass material of narrow size range. *Clin Oral Implants Res* 2000;11:334-344.
203. Malorana C, Sigurtà D, Mirandola A, Garlini G, Santoro F. Sinus elevation with alloplasts or xenogenic materials and implants: an up-to-4-year clinical and radiologic follow-up. *Int J Oral Maxillofac Implants* 2006;21:426-432.
204. de Lange GL, Overman JR, Farre-Guasch E, et al. A histomorphometric and micro-computed tomography study of bone regeneration in the maxillary sinus comparing biphasic calcium phosphate and deproteinized cancellous bovine bone in a human split-mouth model. *Oral Surg Oral Med Oral Pathol Oral Radiol* 2014;117:8-22.
205. Kuhl S, Payer M, Kirmeier R, Wildburger A, Acham S, Jakse N. The influence of particulated autogenous bone on the early volume stability of maxillary sinus grafts with biphasic calcium phosphate: a randomized clinical trial. *Clin Implant Dent Relat Res* 2015;17:173-178.

206. Cordaro L, Bosshardt DD, Palattella P, Rao W, Serino G, Chiapasco M. Maxillary sinus grafting with Bio-Oss or Straumann Bone Ceramic: histomorphometric results from a randomized controlled multicenter clinical trial. *Clin Oral Implants Res* 2008;19:796-803.
207. Szabo G, Huys L, Coulthard P, et al. A prospective multicenter randomized clinical trial of autogenous bone versus beta-tricalcium phosphate graft alone for bilateral sinus elevation: histologic and histomorphometric evaluation. *Int J Oral Maxillofac Implants* 2005;20:371-381.
208. Chiapasco M, Zaniboni M, Boisco M. Augmentation procedures for the rehabilitation of deficient edentulous ridges with oral implants. *Clin Oral Implants Res* 2006;17 Suppl 2:136-159.
209. Del Fabbro M, Testori T, Francetti L, Weinstein R. Systematic review of survival rates for implants placed in the grafted maxillary sinus. *Int J Periodontics Restorative Dent* 2004;24:565-577.
210. Klijn RJ, Meijer GJ, Bronkhorst EM, Jansen JA. A meta-analysis of histomorphometric results and graft healing time of various biomaterials compared to autologous bone used as sinus floor augmentation material in humans. *Tissue Eng Part B Rev* 2010;16:493-507.
211. Munakata M, Tachikawa N, Yamaguchi Y, Sanda M, Kasugai S. The Maxillary Sinus Floor Elevation Using a Poly-L-Lactic Acid Device to Create Space Without Bone Graft: Case Series Study of Five Patients. *J Oral Implantol* 2016;42:278-284.
212. Larsson L, Decker AM, Nibali L, Pilipchuk SP, Berglundh T, Giannobile WV. Regenerative Medicine for Periodontal and Peri-implant Diseases. *J Dent Res* 2016;95:255-266.
213. Ramseier CA, Rasperini G, Batia S, Giannobile WV. Advanced reconstructive technologies for periodontal tissue repair. *Periodontol 2000* 2012;59:185-202.
214. Tarnow DP, Wallace SS, Froum SJ, Rohrer MD, Cho S-C. Histologic and clinical comparison of bilateral sinus floor elevations with and without barrier membrane placement in 12 patients: part 3 of an ongoing prospective study. *Int J Periodontics Restorative Dent* 2000;20:116-125.
215. Lederman PD, Schenk RK, Buser D. Long-lasting osseointegration of immediately loaded, bar-connected TPS screws after 12 years of function: a histologic case report of a 95-year-old patient. *Int J Periodontics Restorative Dent* 1998;18:552-563.
216. Felice P, Scarano A, Pistilli R, et al. A comparison of two techniques to augment maxillary sinuses using the lateral window approach: rigid synthetic resorbable barriers versus anorganic bovine bone. Five-month post-loading clinical and histological results of a pilot randomised controlled clinical trial. *Eur J Oral Implantol* 2009;2:293-306.
217. Cochran DL, Schenk RK, Lussi A, Higginbottom FL, Buser D. Bone response to unloaded and loaded titanium implants with a sandblasted and acid-etched surface: a histometric study in the canine mandible. *J Biomed Mater Res* 1998;40:1-11.
218. Ramp LC, Jeffcoat RL. Dynamic behavior of implants as a measure of osseointegration. *Int J Oral Maxillofac Implants* 2001;16:637-645.
219. Esposito M, Grusovin MG, Rees J, et al. Effectiveness of sinus lift procedures for dental implant rehabilitation: a Cochrane systematic review. *Eur J Oral Implantol* 2010;3:7-26.
220. Boyne PJ, James RA. Grafting of the maxillary sinus floor with autogenous marrow and bone. *J Oral Surg* 1980;38:613-616.
221. Tatum H, Jr. Maxillary and sinus implant reconstructions. *Dent Clin North Am* 1986;30:207-229.
222. Drettner B. Pathophysiology of paranasal sinuses with clinical implications. *Clin Otolaryngol Allied Sci* 1980;5:277-284.
223. Kim MJ, Jung UW, Kim CS, et al. Maxillary sinus septa: prevalence, height, location, and morphology. A reformatted computed tomography scan analysis. *J Periodontol* 2006;77:903-908.
224. Underwood AS. An inquiry into the anatomy and pathology of the maxillary sinus. *J Anat Physiol* 1910;44:354-369.
225. Krennmair G, Ulm CW, Lugmayr H, Solar P. The incidence, location, and height of maxillary sinus septa in the edentulous and dentate maxilla. *J Oral Maxillofac Surg* 1999;57:667-671; discussion 671-662.
226. Betts NJ, Miloro M. Modification of the sinus lift procedure for septa in the maxillary antrum. *Journal of Oral and Maxillofacial Surgery* 1994;52:332-333.
227. Stiernia P, Carlsoo B. Histopathological observations in chronic maxillary sinusitis. *Acta Otolaryngol* 1990;110:450-458.

228. Quirynen M, Lefever D, Hellings P, Jacobs R. Transient swelling of the Schneiderian membrane after transversal sinus augmentation: a pilot study. *Clin Oral Implants Res* 2014;25:36-41.
229. Makary C, Rebaudi A, Menhall A, Naaman N. Changes in Sinus Membrane Thickness After Lateral Sinus Floor Elevation: A Radiographic Study. *Int J Oral Maxillofac Implants* 2016;31:331-337.
230. Estaca E, Cabezas J, Uson J, Sanchez-Margallo F, Morell E, Latorre R. Maxillary sinus-floor elevation: an animal model. *Clin Oral Implants Res* 2008;19:1044-1048.
231. Rosano G, Taschieri S, Gaudy JF, Del Fabbro M. Maxillary sinus vascularization: a cadaveric study. *J Craniofac Surg* 2009;20:940-943.
232. Gauthier A, Lezy JP, Vacher C. Vascularization of the palate in maxillary osteotomies: anatomical study. *Surg Radiol Anat* 2002;24:13-17.
233. Rosano G, Taschieri S, Gaudy JF, Weinstein T, Del Fabbro M. Maxillary sinus vascular anatomy and its relation to sinus lift surgery. *Clin Oral Implants Res* 2011;22:711-715.
234. Chanavaz M. Anatomy and histophysiology of the periosteum: quantification of the periosteal blood supply to the adjacent bone with 85Sr and gamma spectrometry. *J Oral Implantol* 1995;21:214-219.
235. Danesh-Sani SA, Loomer PM, Wallace SS. A comprehensive clinical review of maxillary sinus floor elevation: anatomy, techniques, biomaterials and complications. *Br J Oral Maxillofac Surg* 2016;54:724-730.
236. Monje A, Catena A, Monje F, et al. Maxillary sinus lateral wall thickness and morphologic patterns in the atrophic posterior maxilla. *J Periodontol* 2014;85:676-682.
237. Fenner M, Vairaktaris E, Fischer K, Schlegel KA, Neukam FW, Nkenke E. Influence of residual alveolar bone height on osseointegration of implants in the maxilla: a pilot study. *Clin Oral Implants Res* 2009;20:555-559.
238. Boyne PJ. Analysis of performance of root-form endosseous implants placed in the maxillary sinus. *J Long Term Eff Med Implants* 1993;3:143-159.
239. Pinchasov G, Juodzbaly G. Graft-free sinus augmentation procedure: a literature review. *J Oral Maxillofac Res* 2014;5:e1.
240. Cricchio G, Palma VC, Faria PE, et al. Histological findings following the use of a space-making device for bone reformation and implant integration in the maxillary sinus of primates. *Clin Implant Dent Relat Res* 2009;11 Suppl 1:e14-22.
241. Nasr S, Slot DE, Bahaa S, Dorfer CE, Fawzy El-Sayed KM. Dental implants combined with sinus augmentation: What is the merit of bone grafting? A systematic review. *J Craniomaxillofac Surg* 2016;44:1607-1617.
242. Pandey RK, Panda SS. Drilling of bone: A comprehensive review. *J Clin Orthop Trauma* 2013;4:15-30.
243. Eriksson AR, Albrektsson T, Albrektsson B. Heat caused by drilling cortical bone. Temperature measured in vivo in patients and animals. *Acta Orthop Scand* 1984;55:629-631.
244. Vercellotti T, De Paoli S, Nevins M. The piezoelectric bony window osteotomy and sinus membrane elevation: introduction of a new technique for simplification of the sinus augmentation procedure. *Int J Periodontics Restorative Dent* 2001;21:561-567.
245. Leclercq P, Zenati C, Amr S, Dohan DM. Ultrasonic bone cut part 1: State-of-the-art technologies and common applications. *J Oral Maxillofac Surg* 2008;66:177-182.
246. Hoigne DJ, Stubinger S, Von Kaenel O, Shamdasani S, Hasenboehler P. Piezoelectric osteotomy in hand surgery: first experiences with a new technique. *BMC Musculoskelet Disord* 2006;7:36.
247. Paolo Trisi D, Marco Colagiovanni D. Ultrasonic vs. drill osteotomy. A clinical and histologic study in the sheep mandible. *Journal of Osteology and Biomaterials* 2011;2:21-31.
248. Preti G, Martinasso G, Peirone B, et al. Cytokines and growth factors involved in the osseointegration of oral titanium implants positioned using piezoelectric bone surgery versus a drill technique: a pilot study in minipigs. *J Periodontol* 2007;78:716-722.
249. Atieh MA, Alsabeeha NH, Tawse-Smith A, Faggion CM, Jr., Duncan WJ. Piezoelectric surgery vs rotary instruments for lateral maxillary sinus floor elevation: a systematic review and meta-analysis of intra- and postoperative complications. *Int J Oral Maxillofac Implants* 2015;30:1262-1271.
250. Dahlin C, Linde A, Gottlow J, Nyman S. Healing of bone defects by guided tissue regeneration. *Plast Reconstr Surg* 1988;81:672-676.

251. Yu DH. Sinus Floor Elevation Using Anorganic Bovine Bone Matrix (OsteoGraf/N) With and Without Autogenous Bone: A Clinical, Histologic, Radiographic, and Histomorphometric Analysis—Part 2 of an Ongoing Prospective Study. *Implant Dent* 2002;11:185-188.
252. Suarez-Lopez Del Amo F, Ortega-Oller I, Catena A, et al. Effect of barrier membranes on the outcomes of maxillary sinus floor augmentation: a meta-analysis of histomorphometric outcomes. *Int J Oral Maxillofac Implants* 2015;30:607-618.
253. Esposito M, Felice P, Worthington Helen V. Interventions for replacing missing teeth: augmentation procedures of the maxillary sinus. *Cochrane Database Syst Rev* [serial online]. 2014(5).
254. Winkler S, Morris HF, Ochi S. Implant survival to 36 months as related to length and diameter. *Ann Periodontol* 2000;5:22-31.
255. Atieh MA, Zadeh H, Stanford CM, Cooper LF. Survival of short dental implants for treatment of posterior partial edentulism: a systematic review. *Int J Oral Maxillofac Implants* 2012;27:1323-1331.
256. Monje A, Chan HL, Fu JH, Suarez F, Galindo-Moreno P, Wang HL. Are short dental implants (<10 mm) effective? a meta-analysis on prospective clinical trials. *J Periodontol* 2013;84:895-904.
257. Srinivasan M, Vazquez L, Rieder P, Moraguez O, Bernard JP, Belser UC. Survival rates of short (6 mm) micro- rough surface implants: a review of literature and meta- analysis. In. vol. 25, 2014:539-545.
258. Nedir R, Bischof M, Szmukler-Moncler S, Bernard JP, Samson J. Predicting osseointegration by means of implant primary stability. *Clin Oral Implants Res* 2004;15:520-528.
259. Tawil G, Aboujaoude N, Younan R. Influence of prosthetic parameters on the survival and complication rates of short implants. *Int J Oral Maxillofac Implants* 2006;21:275-282.
260. Ferrigno N, Laureti M, Fanali S. Dental implants placement in conjunction with osteotome sinus floor elevation: a 12-year life-table analysis from a prospective study on 588 ITI® implants. *Clin Oral Implants Res* 2006;17:194-205.
261. Widmark G, Andersson B, Carlsson GE, Lindvall A-M, Ivanoff C-J. Rehabilitation of patients with severely resorbed maxillae by means of implants with or without bone grafts: a 3-to 5-year follow-up clinical report. *Int J Oral Maxillofac Implants* 2001;16:73-79.
262. Malevez C, Abarca M, Durdu F, Daelemans P. Clinical outcome of 103 consecutive zygomatic implants: a 6-48 months follow-up study. *Clin Oral Implants Res* 2004;15:18-22.
263. Malo P, Rangert B, Nobre M. All-on-4 Immediate-Function Concept with Brånemark System® Implants for Completely Edentulous Maxillae: A 1-Year Retrospective Clinical Study. *Clin Implant Dent Relat Res* 2005;7:s88-s94.
264. Aparicio C, Perales P, Rangert B. Tilted implants as an alternative to maxillary sinus grafting: a clinical, radiologic, and periotest study. *Clin Implant Dent Relat Res* 2001;3:39-49.
265. Pearce AI, Richards RG, Milz S, Schneider E, Pearce SG. Animal models for implant biomaterial research in bone: a review. *Eur Cell Mater* 2007;13:1-10.
266. Li Y, Chen S-K, Li L, Qin L, Wang X-L, Lai Y-X. Bone defect animal models for testing efficacy of bone substitute biomaterials. *Journal of Orthopaedic Translation* 2015;3:95-104.
267. Lambert F, Leonard A, Drion P, Sourice S, Pilet P, Rompen E. The effect of collagenated space filling materials in sinus bone augmentation: a study in rabbits. *Clin Oral Implants Res* 2013;24:505-511.
268. Jiang XQ, Sun XJ, Lai HC, Zhao J, Wang SY, Zhang ZY. Maxillary sinus floor elevation using a tissue-engineered bone complex with beta-TCP and BMP-2 gene-modified bMSCs in rabbits. *Clin Oral Implants Res* 2009;20:1333-1340.
269. Kumlien J, Schiratzki H. The vascular arrangement of the sinus mucosa. A study in rabbits. *Acta Otolaryngol* 1985;99:122-132.
270. Asai S, Shimizu Y, Ooya K. Maxillary sinus augmentation model in rabbits: effect of occluded nasal ostium on new bone formation. *Clin Oral Implants Res* 2002;13:405-409.
271. Aerssens J, Boonen S, Lowet G, Dequeker J. Interspecies differences in bone composition, density, and quality: potential implications for in vivo bone research. *Endocrinology* 1998;139:663-670.
272. Haas R, Mailath G, Dörtbudak O, Watzek G. Bovine hydroxyapatite for maxillary sinus augmentation: analysis of interfacial bond strength of dental implants using pull-out tests. *Clin Oral Implants Res* 1998;9:117-122.

273. Stelzle F, Benner KU. An animal model for sinus floor elevation with great elevation heights. Macroscopic, microscopic, radiological and micro-CT analysis: ex vivo. *Clin Oral Implants Res* 2010;21:1370-1378.
274. Terheyden H, Jepsen S, Möller B, Tucker MM, Rueger DC. Sinus floor augmentation with simultaneous placement of dental implants using a combination of deproteinized bone xenografts and recombinant human osteogenic protein-1. A histometric study in miniature pigs. *Clin Oral Implants Res* 1999;10:510-521.
275. Holy C, Fialkov J, Shoichet M, Davies J. In vivo models for bone tissue-engineering constructs. *Bone engineering Toronto: em squared Inc* 2000:496-504.
276. Grageda E, Lozada JL, Boyne PJ, Caplanis N, McMillan PJ. Bone formation in the maxillary sinus by using platelet-rich plasma: an experimental study in sheep. *J Oral Implantol* 2005;31:2-17.
277. Nevins M, Kirker-Head C, Nevins M, Wozney JA, Palmer R, Graham D. Bone formation in the goat maxillary sinus induced by absorbable collagen sponge implants impregnated with recombinant human bone morphogenetic protein-2. *Int J Periodontics Restorative Dent* 1996;16:8-19.
278. Duncan WJ. Sheep mandibular models for dental implantology research: Otago University; 2005.
279. Duncan W. Modelling bone regeneration in ovis aries. In: *The Past, Present and Future of Periodontology Proceedings of the 10th Asian Pacific Society of Periodontology Meeting*, 2014:68-77.
280. Godoy Zanicotti D, Coates DE, Duncan WJ. In vivo bone regeneration on titanium devices using serum-free grown adipose-derived stem cells, in a sheep femur model. *Clin Oral Implants Res* 2017;28:64-75.
281. Smith MMD, W.J.; Coates, D.E. Attributes of Bio-Oss® and Moa-Bone® graft materials in a pilot study using the sheep maxillary sinus model. *J Periodontal Res* 2017;in press.
282. Ko D. The accuracy of cone beam computed tomography (CBCT) to determine newly formed bone within grafted maxillary sinus in sheep: University of Otago; 2015.
283. Philipp A, Duncan W, Roos M, Hammerle CH, Attin T, Schmidlin PR. Comparison of SLA(R) or SLActive(R) implants placed in the maxillary sinus with or without synthetic bone graft materials--an animal study in sheep. *Clin Oral Implants Res* 2014;25:1142-1148.
284. Brumund KT, Graham SM, Beck KC, Hoffman EA, McLennan G. The effect of maxillary sinus antrostomy size on xenon ventilation in the sheep model. *Otolaryngol Head Neck Surg* 2004;131:528-533.
285. Nafei A, Danielsen C, Linde F, Hvid I. Properties of growing trabecular ovine bone. *Bone & Joint Journal* 2000;82:910-920.
286. Kirker-Head CA, Nevins M, Palmer R, Nevins ML, Schelling SH. A new animal model for maxillary sinus floor augmentation: evaluation parameters. *Int J Oral Maxillofac Implants* 1997;12:403-411.
287. Margolin MD, Cogan AG, Taylor M, et al. Maxillary sinus augmentation in the non-human primate: a comparative radiographic and histologic study between recombinant human osteogenic protein-1 and natural bone mineral. *J Periodontol* 1998;69:911-919.
288. Piccinini M, Rebaudi A, Sglavo VM, Buccioti F, Pierfrancesco R. A new HA/TTCP material for bone augmentation: an in vivo histological pilot study in primates sinus grafting. *Implant Dent* 2013;22:83-90.
289. Corbella S, Taschieri S, Weinstein R, Del Fabbro M. Histomorphometric outcomes after lateral sinus floor elevation procedure: a systematic review of the literature and meta-analysis. *Clin Oral Implants Res* 2016;27:1106-1122.
290. Maria Soardi C, Spinato S, Zaffe D, Wang HL. Atrophic maxillary floor augmentation by mineralized human bone allograft in sinuses of different size: an histologic and histomorphometric analysis. *Clin Oral Implants Res* 2011;22:560-566.
291. Bancroft JD, Gamble M. *Theory and practice of histological techniques*: Elsevier Health Sciences; 2008.
292. Zerbo IR, Bronckers AL, De Lange G, Burger EH. Localisation of osteogenic and osteoclastic cells in porous β -tricalcium phosphate particles used for human maxillary sinus floor elevation. *Biomaterials* 2005;26:1445-1451.
293. Skoglund A, Hising P, Young C. A clinical and histologic examination in humans of the osseous response to implanted natural bone mineral. *Int J Oral Maxillofac Implants* 1997;12:194-199.
294. Roofe PG, Hoecker FE, Voorhees CD. A rapid bone sectioning technic. *Proc Soc Exp Biol Med* 1949;72:619-622.

295. D'Alessandro D, Perale G, Milazzo M, et al. Bovine bone matrix/poly(l-lactic-co-epsilon-caprolactone)/gelatin hybrid scaffold (SmartBone(R)) for maxillary sinus augmentation: A histologic study on bone regeneration. *Int J Pharm* 2017;523:534-544.
296. Friedmann A, Dard M, Kleber BM, Bernimoulin JP, Bosshardt DD. Ridge augmentation and maxillary sinus grafting with a biphasic calcium phosphate: histologic and histomorphometric observations. *Clin Oral Implants Res* 2009;20:708-714.
297. Haas R, Baron M, Donath K, Zechner W, Watzek G. Porous hydroxyapatite for grafting the maxillary sinus: a comparative histomorphometric study in sheep. *Int J Oral Maxillofac Implants* 2002;17:337-346.
298. Saffarzadeh A, Gauthier O, Bilban M, Bagot D'Arc M, Daculsi G. Comparison of two bone substitute biomaterials consisting of a mixture of fibrin sealant (Tisseel) and MBCP (TricOs) with an autograft in sinus lift surgery in sheep. *Clin Oral Implants Res* 2009;20:1133-1139.
299. Kilkenny C, Browne W, Cuthill IC, Emerson M, Altman DG. Animal research: reporting in vivo experiments: the ARRIVE guidelines. *Br J Pharmacol* 2010;160:1577-1579.
300. Lander L. Alveolar Ridge Preservation in the Sheep Model [Thesis, Doctor of Clinical Dentistry]: University of Otago; 2016.
301. Frisken KW, Tagg JR, Laws AJ, Orr MB. Suspected periodontopathic bacteria associated with brokenmouth periodontitis in sheep. *J Periodontal Res* 1988;23:18-21.
302. Ansari MM, Dar KH, Tantray HA, Bhat MM, Dar SH. Efficacy of different therapeutic regimens for acute foot rot in adult sheep. *Journal of Advanced Veterinary and Animal Research* 2014;1:114-118.
303. Liu J. Alveolar bone healing using a novel bone substitute material in a sheep tooth extraction model [Thesis, Doctor of Clinical Dentistry]. Dunedin: University of Otago; 2013.
304. Pertici G. Bone implant matrix and method of preparing the same. In: Google Patents, 2009.
305. Frey M, Ahlers M, Sorg K-H, Huber C. Shaped body with collagen-containing composite material for introduction into a bone defect location. In: Google Patents, 2012.
306. Fawzy El-Sayed KM, Paris S, Becker ST, et al. Periodontal regeneration employing gingival margin-derived stem/progenitor cells: an animal study. *J Clin Periodontol* 2012;39:861-870.
307. Galler KM, Krastl G, Simon S, et al. European Society of Endodontology position statement: Revitalization procedures. *Int Endod J* 2016;49:717-723.
308. Kamitakahara M, Ohtsuki C, Miyazaki T. Review paper: behavior of ceramic biomaterials derived from tricalcium phosphate in physiological condition. *J Biomater Appl* 2008;23:197-212.
309. Wu J, Li B, Lin X. Histological outcomes of sinus augmentation for dental implants with calcium phosphate or deproteinized bovine bone: a systematic review and meta-analysis. *Int J Oral Maxillofac Surg* 2016;45:1471-1477.
310. Aludden HC, Mordenfeld A, Hallman M, Dahlin C, Jensen T. Lateral ridge augmentation with Bio-Oss alone or Bio-Oss mixed with particulate autogenous bone graft: a systematic review. *Int J Oral Maxillofac Surg* 2017;46:1030-1038.
311. Proussaefs P, Lozada J. The "Loma Linda pouch": a technique for repairing the perforated sinus membrane. *Int J Periodontics Restorative Dent* 2003;23:593-598.
312. Donath K, Breuner G. A method for the study of undecalcified bones and teeth with attached soft tissues. The Sage-Schliff (sawing and grinding) technique. *J Oral Pathol* 1982;11:318-326.
313. MacNeal WJ. Tetrachrome blood stain: an economical and satisfactory imitation of Leishman's stain. *J Am Med Assoc* 1922;78:122.
314. Horobin RW, Kiernan JA. *Conn's biological stains: a handbook of dyes, stains and fluorochromes for use in biology and medicine*: BIOS Scientific Publishers; 2002.
315. Schenk RK. Preparation of calcified tissues for light microscopy. *Methods of calcified tissue preparation* 1984;1:1-56.
316. Suvarna KS. Bancroft's Theory and Practice of Histological Techniques. In: Layton C, Bancroft JD, eds. London: London : Elsevier Health Sciences UK, 2012.
317. Cicchetti DV. Guidelines, criteria, and rules of thumb for evaluating normed and standardized assessment instruments in psychology. *Psychol Assess* 1994;6:284.
318. Koole R, Visser WJ, Klein WR, Suiker AM. A comparative investigation on autologous mandibular and iliac crest bone grafts. An experimental study in sheep. *J Craniomaxillofac Surg* 1991;19:133-143.

319. Quteish D, Singrao S, Dolby AE. Light and electron microscopic evaluation of biocompatibility, resorption and penetration characteristics of human collagen graft material. *J Clin Periodontol* 1991;18:305-311.
320. Lu HK, Lee SY, Lin FP. Elastic modulus, permeation time and swelling ratio of a new porcine dermal collagen membrane. *J Periodontol Res* 1998;33:243-248.
321. Ahn J-J, Cho S-A, Byrne G, Kim J-H, Shin H-I. New bone formation following sinus membrane elevation without bone grafting: histologic findings in humans. *The International Journal of Oral & maxillofacial Implants* 2011;26:83.
322. Athanasiou K. Sterilization, toxicity, biocompatibility and clinical applications of polylactic acid/polyglycolic acid copolymers. *Biomaterials* 1996;17:93-102.
323. Kulkarni RK, Pani KC, Neuman C, Leonard F. Polylactic acid for surgical implants. *Arch Surg* 1966;93:839-843.
324. Tokiwa Y, Calabia BP. Biodegradability and biodegradation of poly(lactide). *Appl Microbiol Biotechnol* 2006;72:244-251.
325. Rasal RM, Janorkar AV, Hirt DE. Poly(lactic acid) modifications. *Progress in Polymer Science* 2010;35:338-356.
326. Woodruff MA, Hutmacher DW. The return of a forgotten polymer—polycaprolactone in the 21st century. *Progress in polymer science* 2010;35:1217-1256.
327. Patrício T, Domingos M, Gloria A, D'Amora U, Coelho J, Bártolo P. Fabrication and characterisation of PCL and PCL/PLA scaffolds for tissue engineering. *Rapid Prototyping Journal* 2014;20:145-156.
328. Vert M. Degradable and bioresorbable polymers in surgery and in pharmacology: beliefs and facts. *J Mater Sci Mater Med* 2009;20:437-446.
329. Pitt G, Gratzl M, Kimmel G, Surlis J, Sohindler A. Aliphatic polyesters II. The degradation of poly (DL-lactide), poly (ε-caprolactone), and their copolymers in vivo. *Biomaterials* 1981;2:215-220.
330. Pertici G, Rossi F, Casalini T, Perale G. Composite polymer-coated mineral grafts for bone regeneration: material characterisation and model study. *Annals of Oral & Maxillofacial Surgery* 2014;2.
331. Pertici G, Carinci F, Carusi G, et al. Composite polymer-coated mineral scaffolds for bone regeneration: from material characterization to human studies. *J Biol Regul Homeost Agents* 2014;29:136-148.
332. Schenk RK, Buser D, Hardwick WR, Dahlin C. Healing pattern of bone regeneration in membrane-protected defects: a histologic study in the canine mandible. *Int J Oral Maxillofac Implants* 1994;9:13-29.
333. Yildirim M, Spiekermann H, Biesterfeld S, Edelhoff D. Maxillary sinus augmentation using xenogenic bone substitute material Bio-OssR in combination with venous blood . A histologic and histomorphometric study in humans. *Clin Oral Implants Res* 2000;11:217-229.
334. Hallman M, Lundgren S, Sennerby L. Histologic analysis of clinical biopsies taken 6 months and 3 years after maxillary sinus floor augmentation with 80% bovine hydroxyapatite and 20% autogenous bone mixed with fibrin glue. *Clin Implant Dent Relat Res* 2001;3:87-96.
335. Lindhe J, Cecchinato D, Donati M, Tomasi C, Liljenberg B. Ridge preservation with the use of deproteinized bovine bone mineral. *Clin Oral Implants Res* 2014;25:786-790.
336. Ohayon L. Maxillary sinus floor augmentation using biphasic calcium phosphate: a histologic and histomorphometric study. *Int J Oral Maxillofac Implants* 2014;29:1143-1148.
337. Froum SJ, Wallace SS, Cho SC, Elian N, Tarnow DP. Histomorphometric comparison of a biphasic bone ceramic to anorganic bovine bone for sinus augmentation: 6- to 8-month postsurgical assessment of vital bone formation. A pilot study. *Int J Periodontics Restorative Dent* 2008;28:273-281.
338. Frenken J, Bouwman W, Bravenboer N, Zijdeveld S, Schulten E, Ten Bruggenkate C. The use of Straumann® Bone Ceramic in a maxillary sinus floor elevation procedure: a clinical, radiological, histological and histomorphometric evaluation with a 6-month healing period. *Clin Oral Implants Res* 2010;21:201-208.
339. Antunes AA, Oliveira Neto P, Santis E, Caneva M, Botticelli D, Salata LA. Comparisons between Bio-Oss® and Straumann® Bone Ceramic in immediate and staged implant placement in dogs mandible bone defects. *Clin Oral Implants Res* 2013;24:135-142.
340. Haas R, Baron M, Zechner W, Mailath-Pokorny G. Porous hydroxyapatite for grafting the maxillary sinus in sheep: comparative pullout study of dental implants. *Int J Oral Maxillofac Implants* 2003;18:691-696.

341. Oluwole M, Tan L, White PS. An animal model for training in endoscopic nasal and sinus surgery. *The Journal of Laryngology & Otology* 2007;110:425-428.
342. Whelan J, Pack A, McMillan M. Cardiovascular patch and hydroxylapatite: an alternative GTR technique in sheep. *NZ Dent Journal* 1995;91:142.
343. Mohammed S, Pack ARC, Kardos TB. The effect of transforming growth factor beta one (TGF- β 1) on wound healing, with or without barrier membranes, in a Class II furcation defect in sheep. *J Periodontal Res* 2010;33:335-344.
344. Cole NS. Healing in Class 2 Furcation Defects in Sheep Using Plaster of Paris Alone and in Conjunction with Autogenous Bone: A Research Report Submitted for the Degree of Master of Dental Surgery in Periodontology of the University of Otago, Dunedin, New Zealand [Master of Dental Surgery, Thesis]. Dunedin, New Zealand: University of Otago; 1999.
345. Newman E, Turner AS, Wark JD. The potential of sheep for the study of osteopenia: current status and comparison with other animal models. *Bone* 1995;16:277S-284S.
346. Eitel F, Klapp F, Jacobson W, Schweiberer L. Bone regeneration in animals and in man. A contribution to understanding the relative value of animal experiments to human pathophysiology. *Arch Orthop Trauma Surg* 1981;99:59-64.
347. Felfel RM, Poocha L, Gimeno-Fabra M, et al. In vitro degradation and mechanical properties of PLA-PCL copolymer unit cell scaffolds generated by two-photon polymerization. *Biomed Mater* 2016;11:015011.
348. Pietrzak WS, Kumar M, Eppley BL. The influence of temperature on the degradation rate of LactoSorb copolymer. *J Craniofac Surg* 2003;14:176-183.
349. Haas R, Haidvogel D, Donath K, Watzek G. Freeze-dried homogeneous and heterogeneous bone for sinus augmentation in sheep. Part I: histological findings. *Clin Oral Implants Res* 2002;13:396-404.
350. Barone A, Ricci M, Grassi R, Nannmark U, Quaranta A, Covani U. A 6-month histological analysis on maxillary sinus augmentation with and without use of collagen membranes over the osteotomy window: randomized clinical trial. *Clin Oral Implants Res* 2013;24:1-6.
351. Adeyemo WL, Reuther T, Bloch W, et al. Healing of onlay mandibular bone grafts covered with collagen membrane or bovine bone substitutes: a microscopical and immunohistochemical study in the sheep. *Int J Oral Maxillofac Surg* 2008;37:651-659.
352. Proussaefs P, Lozada J, Kim J, Rohrer MD. Repair of the perforated sinus membrane with a resorbable collagen membrane: a human study. *Int J Oral Maxillofac Implants* 2004;19:413-420.
353. Shlomi B, Horowitz I, Kahn A, Dobriyan A, Chaushu G. The effect of sinus membrane perforation and repair with Lambone on the outcome of maxillary sinus floor augmentation: a radiographic assessment. *Int J Oral Maxillofac Implants* 2004;19:559-562.
354. Favero V, Lang NP, Canullo L, Urbizo Velez J, Bengazi F, Botticelli D. Sinus floor elevation outcomes following perforation of the Schneiderian membrane. An experimental study in sheep. *Clin Oral Implants Res* 2016;27:233-240.

Appendices

Appendix I

Chemical reagents used

Distilled Water (H₂O), purified via reverse osmosis unit (RiOs™ unit, Millipore Intertech, USA)

Xylene, C₆H₄(CH₃)₂, (Ajax Finechem Pty Ltd, New Zealand)

Ethanol, C₂H₅OH, (High grade, Absolute Ethanol, Thermo Fisher Scientific, USA)

10% Natural Buffered Formalin (NBF), (BioLab Ltd, New Zealand)

Methyl methacrylate 99% (MMA), (Sigma Aldrich, USA)

Xylene, C₆H₄(CH₃)₂, (Ajax Finechem Pty Ltd, New Zealand)

Concentrated Hydrochloric Acid (HCl), (100317.2500, Merck, Germany)

Di-Ammonium Oxalate Monohydrate, (1.01190.1000, Merck, Germany)

Phosphate Buffered Saline (PBS), (Gibco™, Invitrogen Corporation, NZ)

3, 3' diaminobenzidine (DAB), (Sigma D3939, Sigma Aldrich, USA)

Equipment used

Mectron® Piezosurgery 2 ultrasonic unit (Henry Schein Shalfoon™, Auckland NZ)

Electrosurgical unit (NeoMed™ 3000A ESU, Solid State Electrosurgery Unit, USA)

Sinus membrane dissectors (Sinus Kit, Osstem™, Korea)

Accutom, cutting machine, (Struers, Ballerup Denmark)

Gendex dental systems, (Monza, Italy)

Tegra-Pol, polishing machine (Struers, Ballerup, Denmark)

Silicon Carbide Paper, Grades 180-4000 (Struers, Ballerup, Denmark)

Incubating/shaking machine (Multitron®, Infors HT, Switzerland)

RiOs™ wall mounted water distillation unit, (Millipore Intertech, USA)

APES (3-aminopropyltriethoxysilane) coated slides (Lab Scientific, Inc., USA).

Materials and medications used in sheep surgery

Medication name	Purpose	Admission	Dose
Thiopentone	General	Intravenous	20 mg/kg
Halothane	General	Inhalation	1-2% (to effect)
Nitrous Oxide	General	Inhalation	1:2 (to effect)
2% Mepivacaine HCL (with 1:100,000 adrenaline)	Local Anaesthetic	Local infiltration	2 x 2.2 ml cartridges around surgical site at the beginning of surgery

0.5% Bupivacaine HCL (with 1:200,000 adrenaline)	Long lasting Local Anaesthetic	Local infiltration	5 ml around surgical site at completion of surgery
Trimethoprim	Antibiotic	Intramuscular	1 ml / 15 kg for 3 days following surgery
Carprofen	Anti- inflammatory agent	Intramuscular	5 ml once/day for 3 days following surgery
0.2% w/v chlorhexidine gluconate solution	Antiseptic	Mouthrinse	rinse once a day with 30ml for 3 days following surgery

Appendix II

Resin for embedding

Ingredients

Methyl methacrylate (Catalogue number M55909, Sigma Aldrich, USA) Benzoyl peroxide (Catalogue number 517909, Sigma Aldrich, USA) Dibutyl phthalate (Catalogue number 524980, Sigma Aldrich, USA) Xylene, (Ajax Finechem Pty Ltd, New Zealand)

Method for MMA I

4 parts Methyl methacrylate

1% Benzoyl peroxide

1 Part Dibutyl phthalate

Method for MMA II

4 parts Methyl methacrylate

0.5% Benzoyl peroxide

1 part Dibutyl phthalate

Method for MMA III

4 parts Methyl methacrylate

1% Benzoyl peroxide

1 part Dibutyl phthalate

MMA Embedding protocol

Immerse specimens, previously dehydrated in ethanol, in xylene for 4 days in fume cupboard on a rotating platform. Change to fresh xylene after 2 days.

Wash specimens in methyl methacrylate (MMA) monomer.

Transfer specimens to MMA I for 2 days in fume cupboard on a rotating platform.

Fill glass jars with MMA III to one-third height, and place in a light-proof plastic container partially filled with water. Leave undisturbed at room temperature for 2-3 days until set.

Immerse specimens in MMA II for 2 days in fume cupboard on a rotating platform.

Retrieve each specimen and its identification tag from the histological cassette. Place the specimen and the tag flat in an individual glass jar with a pre-set MMA III base. Fill the jar with fresh MMA III, and tightly close the lid.

Place glass jars in a half-filled water bath in the light-proof plastic container. Leave undisturbed at room temperature for at least 2 days, until fully set.

Staining with MacNeal's Tetrachrome / Toluidine Blue solution

Solution A

0.5g Methylene blue (Catalogue number 15943 Merck, Germany)

0.8g Azur II (Catalogue number 9211 Merck, Germany)

0.1g Methyl violet 2B (Catalogue number M 0527Sigma Aldrich, USA)

250ml Methanol (Catalogue number 1.06009.6025, Merck, Germany)

250ml Glycerol

Stir with magnetic stirrer until no precipitate seen Leave for 12 hours at 50°C then 3 days at 37°C

Solution B

Toluidine blue in 100ml distilled water + 1.0g borax

Solution A+B

10ml Solution A

5ml Solution B

85ml distilled water

Staining protocol

Place slide in 20% ethanol in Coplin jar

Place Coplin jar in ultrasonic bath for 5 minutes

Replace ethanol with 0.1% formic acid

Place Coplin jar in ultrasonic bath for 5 minutes

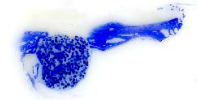
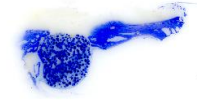
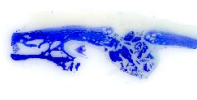
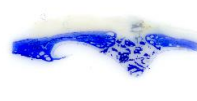
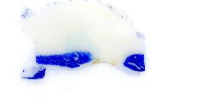

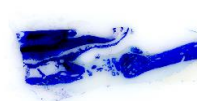
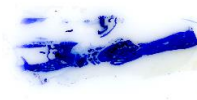
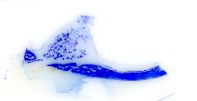
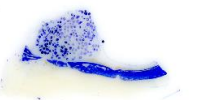
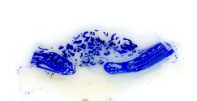
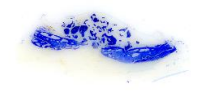
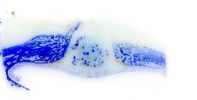
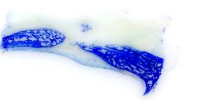
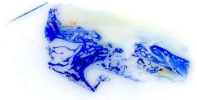
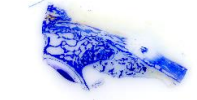
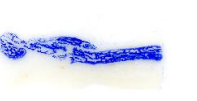
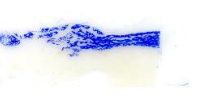
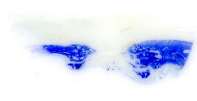
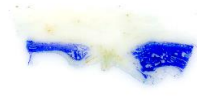
Wash slide with tap water



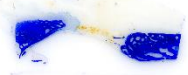



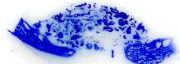
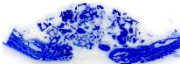
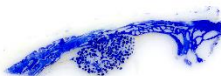

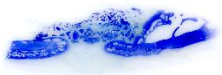
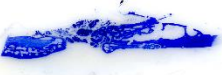
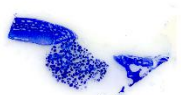
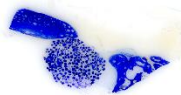
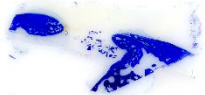
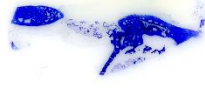

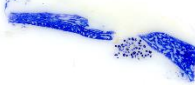
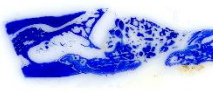
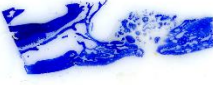
Cover section on slide with Solution A+B for 5 minutes

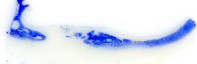

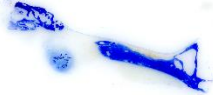
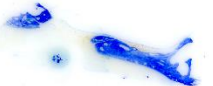
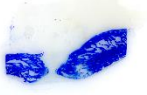
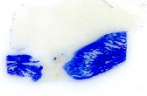
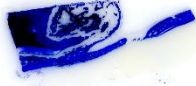
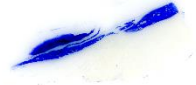


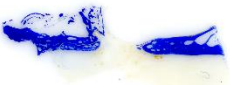
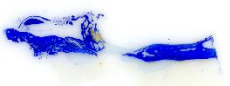
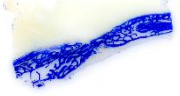
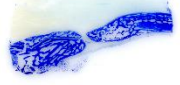
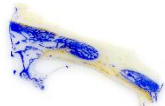
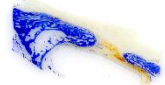


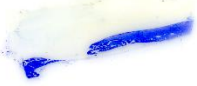

Rinse slide with distilled water for 5 minutes

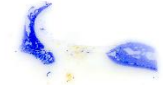
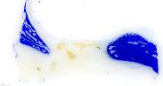
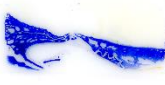






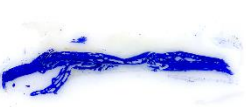

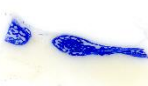


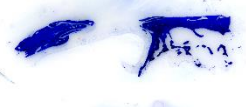



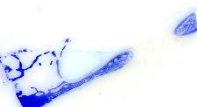

Leave overnight to dry on a benchtop at room temperature

Appendix III – Histologic slides

Sheep	Cone-Oss	Bio-Oss
409	<p>A </p> <p>B </p>	<p>A </p> <p>B </p>
413	<p>A </p> <p>B </p>	<p>A </p> <p>B </p>
414	<p>A </p> <p>B </p>	<p>A </p> <p>B </p>
415	<p>A </p> <p>B </p>	<p>A </p> <p>B </p>
416	<p>A </p> <p>B </p>	<p>A </p> <p>B </p>

Sheep	Cone-Oss	Bio-Oss
417	<p>A </p> <p>B </p>	<p>A </p> <p>B </p>
418	<p>A </p> <p>B </p>	<p>A </p> <p>B </p>
419	<p>A </p> <p>B </p>	<p>A </p> <p>B </p>
420	<p>A </p> <p>B </p>	<p>A </p> <p>B </p>
421	<p>A </p> <p>B </p>	<p>A </p> <p>B </p>

Sheep	Smart-Bone	Cone
409	<p>A </p> <p>B </p>	<p>A </p> <p>B </p>
413	<p>A </p> <p>B </p>	<p>A </p> <p>B </p>
414	<p>A </p> <p>B </p>	<p>A </p> <p>B </p>
415	<p>A </p> <p>B </p>	<p>A </p> <p>B </p>
416	<p>A </p> <p>B </p>	<p>A </p> <p>B </p>

	Smart-Bone	Cone
417	A  B 	A  B 
418	A  B 	A  B 
419	A  B 	A  B 
420	A  B 	A  B 
421	A  B 	A  B 

Appendix IV – Histological data

Histomorphometric data

Sheep	Graft	Site	Total (mm ²)	RG (mm ²)	RG (%)	NB (mm ²)	NB (%)	CT (mm ²)	CT (%)	Max initial gap (mm)	Max resid. gap (mm)	Bridging (mm)	Bridging (%)	Augm. height (mm)	Width of graft (mm)
409	ConeOss	RP3	36.580	13.660	37.3%	3.860	10.6%	19.060	52.1%	7.530	5.080	2.450	32.5%	5.530	6.901
409	ConeOss	RP4	28.461	10.633	37.4%	3.993	14.0%	13.835	48.6%	7.346	4.260	3.086	42.0%	4.900	6.461
413	ConeOss	RA1	0.000	0.000	0.0%	0.000	0.0%	0.000	100.0%	N/A	3.917	N/A	N/A	0.000	0.000
413	ConeOss	RA2	0.000	0.000	0.0%	0.000	0.0%	0.000	100.0%	N/A	4.674	N/A	N/A	0.000	0.000
414	ConeOss	RP6	43.692	3.913	9.0%	0.451	1.0%	39.328	90.0%	9.980	0.620	9.360	93.8%	6.552	6.219
414	ConeOss	RP5	24.974	5.178	20.7%	0.142	0.6%	19.654	78.7%	N/A	1.646	N/A	N/A	6.548	5.784
415	ConeOss	LA5	6.080	0.371	6.1%	0.000	0.0%	5.709	93.9%	7.829	5.092	2.737	35.0%	0.374	5.078
415	ConeOss	LA3	0.000	0.000	0.0%	0.000	0.0%	0.000	100.0%	11.724	6.276	5.448	46.5%	0.000	0.000
416	ConeOss	LP5	0.000	0.000	0.0%	0.000	0.0%	0.000	100.0%	N/A	0.000	N/A	N/A	0.000	0.000
416	ConeOss	LP3	0.000	0.000	0.0%	0.000	0.0%	0.000	100.0%	7.415	1.307	6.108	82.4%	0.000	0.000
417	ConeOss	RA3	0.000	0.000	0.0%	0.000	0.0%	0.000	100.0%	N/A		N/A	N/A	0.000	0.000
417	ConeOss	RA6	0.000	0.000	0.0%	0.000	0.0%	0.000	100.0%	N/A	8.293	N/A	N/A	0.000	0.000
418	ConeOss	RP1	28.520	8.362	29.3%	1.675	5.9%	18.483	64.8%	5.260	2.797	2.463	46.8%	4.792	6.505
418	ConeOss	RP2	31.476	9.068	28.8%	2.377	7.6%	20.031	63.6%	7.460	0.285	7.175	96.2%	4.792	7.924
419	ConeOss	LA6	30.008	8.302	27.7%	3.933	13.1%	18.630	62.1%	N/A	0.000	N/A	100.0%	4.407	7.870
419	ConeOss	LA5	24.913	6.372	25.6%	4.024	16.2%	14.517	58.3%	N/A	0.000	N/A	N/A	3.676	8.134
420	ConeOss	LP1	36.710	15.875	43.2%	1.099	3.0%	22.396	61.0%	N/A	5.078	N/A	N/A	4.642	8.376
420	ConeOss	LP3	33.295	11.036	33.1%	3.029	9.1%	19.230	57.8%	9.692	5.178	4.514	46.6%	4.389	8.337
421	ConeOss	RA3	7.757	1.514	19.5%	0.000	0.0%	6.243	80.5%	N/A	1.421	N/A	N/A	1.244	4.126
421	ConeOss	RA2	8.586	2.219	25.8%	0.000	0.0%	6.367	74.2%	N/A	2.838	N/A	N/A	1.878	5.187

Sheep	Graft	Site	Total (mm ²)	RG (mm ²)	RG (%)	NB (mm ²)	NB (%)	CT (mm ²)	CT (%)	Max initial gap (mm)	Max resid. gap (mm)	Bridging (mm)	Bridging (%)	Augm. height (mm)	Width of graft (mm)
409	BioOss	RA1	22.386	6.277	28.0%	2.758	12.3%	13.351	59.6%	6.490	3.220	3.270	50.4%	4.518	6.949
409	BioOss	RA3	17.542	5.070	28.9%	0.299	1.7%	12.173	69.4%	5.879	3.791	2.088	35.5%	4.285	8.214
413	BioOss	LP4	6.063	0.776	12.8%	1.950	32.2%	3.337	55.0%	7.869	0.000	7.869	100.0%	1.297	5.737
413	BioOss	LP3	8.224	1.039	12.6%	2.187	26.6%	4.998	60.8%	8.469	3.654	4.815	56.9%	0.904	10.057
414	BioOss	RA7	43.824	7.612	17.4%	5.190	11.8%	31.022	70.8%	7.533	3.825	3.708	49.2%	4.921	13.407
414	BioOss	RA3	38.724	6.607	17.1%	3.119	8.1%	28.998	74.9%	5.504	1.925	3.579	65.0%	4.406	10.965
415	BioOss	RP1	22.784	5.052	22.2%	2.757	12.1%	14.975	65.7%	N/A	0.000	N/A	100.0%	3.637	8.360
415	BioOss	RP3	19.354	3.480	18.0%	0.196	1.0%	15.678	81.0%	N/A	0.000	N/A	100.0%	3.238	7.613
416	BioOss	RA3	0.000	0.000	0.0%	0.000	0.0%	0.000	100.0%	9.380	5.241	4.139	44.1%	0.000	0.000
416	BioOss	RA1	0.000	0.000	0.0%	0.000	0.0%	0.000	100.0%	9.579	4.040	5.539	57.8%	0.000	0.000
417	BioOss	LP3	0.000	0.000	0.0%	0.000	0.0%	0.000	100.0%	12.096	9.008	3.088	25.5%	0.000	0.000
417	BioOss	LP5	0.000	0.000	0.0%	0.000	0.0%	0.000	100.0%	9.181	6.365	2.816	30.7%	0.000	0.000
418	BioOss	RA9	75.793	22.309	29.4%	8.117	10.7%	45.367	59.9%	11.293	4.814	6.479	57.4%	5.812	14.549
418	BioOss	RA6	72.286	15.486	21.4%	5.468	7.6%	51.332	71.0%	9.229	6.446	2.783	30.2%	6.106	15.321
419	BioOss	RP1	10.853	3.277	30.2%	0.270	2.5%	7.698	70.9%	8.575	3.410	5.165	60.2%	1.432	12.512
419	BioOss	RP2	36.062	8.198	22.7%	3.110	8.6%	24.754	68.6%	8.576	4.483	4.093	47.7%	4.081	13.586
420	BioOss	LA3	0.000	0.000	0.0%	0.000	0.0%	0.000	100.0%	N/A	7.364	N/A	N/A	0.652	0.000
420	BioOss	LA1	11.598	1.506	13.0%	0.000	0.0%	10.092	87.0%	11.166	6.551	4.615	41.3%	1.890	5.094
421	BioOss	LP5	20.285	3.769	18.6%	2.981	14.7%	17.826	87.9%	7.482	3.035	4.447	59.4%	3.259	10.166
421	BioOss	LP2	45.523	8.652	19.0%	9.763	21.4%	27.108	59.5%	N/A	3.058	N/A	N/A	5.514	11.971

Sheep	Graft	Site	Total (mm ²)	RG (mm ²)	RG (%)	NB (mm ²)	NB (%)	CT (mm ²)	CT (%)	Max initial gap (mm)	Max resid. gap (mm)	Bridging (mm)	Bridging (%)	Augm. height (mm)	Width of graft (mm)
409	Cone	LP5	0.000	0.000	0.0%	0.000	0.0%	0.000	100.0%	N/A	2.000	N/A	N/A	0.000	0.000
409	Cone	LP6	0.000	0.000	0.0%	0.000	0.0%	0.000	100.0%	N/A	4.749	N/A	N/A	0.000	0.000
413	Cone	LA2	0.000	0.000	0.0%	0.000	0.0%	0.000	100.0%	N/A	2.430	N/A	N/A	0.000	0.000
413	Cone	LA1	0.000	0.000	0.0%	0.000	0.0%	0.000	100.0%	N/A	4.131	N/A	N/A	0.000	0.000
414	Cone	LP4	0.000	0.000	0.0%	0.000	0.0%	0.000	100.0%	N/A	3.645	N/A	N/A	0.000	0.000
414	Cone	LP6	0.000	0.000	0.0%	0.000	0.0%	0.000	100.0%	7.562	3.003	4.559	60.3%	0.000	0.000
415	Cone	RA6	0.000	0.000	0.0%	0.000	0.0%	0.000	100.0%	N/A	N/A	N/A	N/A	0.000	0.000
415	Cone	RA2	0.000	0.000	0.0%	0.000	0.0%	0.000	100.0%	N/A	4.348	N/A	N/A	0.000	0.000
416	Cone	RP3	0.000	0.000	0.0%	0.000	0.0%	0.000	100.0%	N/A	4.348	N/A	N/A	0.000	0.000
416	Cone	RP3	0.000	0.000	0.0%	0.000	0.0%	0.000	100.0%	9.480	4.814	4.666	49.2%	0.000	0.000
417	Cone	LA2	0.000	0.000	0.0%	0.000	0.0%	0.000	100.0%	9.692	5.317	4.375	45.1%	0.000	0.000
417	Cone	LA2	0.000	0.000	0.0%	0.000	0.0%	0.000	100.0%	N/A	2.294	N/A	N/A	0.000	0.000
418	Cone	LP1	0.000	0.000	0.0%	0.000	0.0%	0.000	100.0%	N/A	2.754	N/A	N/A	0.000	0.000
418	Cone	LP2	0.000	0.000	0.0%	0.000	0.0%	0.000	100.0%	13.213	6.045	7.168	54.2%	0.000	0.000
419	Cone	RA4	0.000	0.000	0.0%	0.000	0.0%	0.000	100.0%	N/A	5.889	N/A	N/A	0.000	0.000
419	Cone	RA6	0.000	0.000	0.0%	0.000	0.0%	0.000	100.0%	N/A	5.941	N/A	N/A	0.000	0.000
420	Cone	RP3	0.000	0.000	0.0%	0.000	0.0%	0.000	100.0%	N/A	4.574	N/A	N/A	0.000	0.000
420	Cone	RP2	0.000	0.000	0.0%	0.000	0.0%	0.000	100.0%	N/A	2.000	N/A	N/A	0.000	0.000
421	Cone	LA3	0.000	0.000	0.0%	0.000	0.0%	0.000	100.0%	N/A	4.749	N/A	N/A	0.000	0.000
421	Cone	LA4	0.000	0.000	0.0%	0.000	0.0%	0.000	100.0%	N/A	2.430	N/A	N/A	0.000	0.000

Sheep	Graft	Site	Total (mm ²)	RG (mm ²)	RG (%)	NB (mm ²)	NB (%)	CT (mm ²)	CT (%)	Max initial gap (mm)	Max resid. gap (mm)	Bridging (mm)	Bridging (%)	Augm. height (mm)	Width of graft (mm)
409	SmartBone	LA3	0.000	0.000	0.0%	0.000	0.0%	0.000	100.0%	N/A	2.707	N/A	N/A	N/A	N/A
409	SmartBone	LA2	0.000	0.000	0.0%	0.000	0.0%	0.000	100.0%	9.713	0.732	8.981	92.5%	N/A	N/A
413	SmartBone	RP1	0.000	0.000	0.0%	0.000	0.0%	0.000	100.0%	N/A	0.000	N/A	100.0%	N/A	N/A
413	SmartBone	RP2	0.000	0.000	0.0%	0.000	0.0%	0.000	100.0%	N/A	3.881	N/A	N/A	N/A	N/A
414	SmartBone	LA1	0.000	0.000	0.0%	0.000	0.0%	0.000	100.0%	N/A	3.469	N/A	N/A	N/A	N/A
414	SmartBone	LA4	0.000	0.000	0.0%	0.000	0.0%	0.000	100.0%	11.679	7.587	4.092	35.0%	N/A	N/A
415	SmartBone	LP6	0.000	0.000	0.0%	0.000	0.0%	0.000	100.0%	N/A	7.133	N/A	N/A	N/A	N/A
415	SmartBone	LP3	0.000	0.000	0.0%	0.000	0.0%	0.000	100.0%	N/A	0.000	N/A	100.0%	N/A	N/A
416	SmartBone	LA3	0.000	0.000	0.0%	0.000	0.0%	0.000	100.0%	N/A	5.013	N/A	N/A	N/A	N/A
416	SmartBone	LA2	0.000	0.000	0.0%	0.000	0.0%	0.000	100.0%	9.780	2.535	7.245	74.1%	N/A	N/A
417	SmartBone	RP2	0.000	0.000	0.0%	0.000	0.0%	0.000	100.0%	9.869	4.250	5.619	56.9%	N/A	N/A
417	SmartBone	RP5	0.000	0.000	0.0%	0.000	0.0%	0.000	100.0%	N/A	4.271	N/A	N/A	N/A	N/A
418	SmartBone	LA3	7.653	0.135	1.8%	0.457	6.0%	7.061	92.3%	8.281	3.372	4.909	59.3%	1.217	3.743
418	SmartBone	LA6	0.000	0.000	0.0%	0.000	0.0%	0.000	100.0%	N/A	5.013	N/A	N/A	N/A	N/A
419	SmartBone	LP1	0.000	0.000	0.0%	0.000	0.0%	0.000	100.0%	9.780	2.535	7.245	74.1%	N/A	N/A
419	SmartBone	LP2	0.000	0.000	0.0%	0.000	0.0%	0.000	100.0%	9.869	4.250	5.619	56.9%	N/A	N/A
419	SmartBone	LP2	0.000	0.000	0.0%	0.000	0.0%	0.000	100.0%	N/A	4.271	N/A	N/A	N/A	N/A
420	SmartBone	RA5	0.000	0.000	0.0%	0.000	0.0%	0.000	100.0%	12.377	6.805	5.572	45.0%	N/A	N/A
420	SmartBone	RA6	0.000	0.000	0.0%	0.000	0.0%	0.000	100.0%	N/A	6.742	N/A	N/A	N/A	N/A
421	SmartBone	RP3	0.000	0.000	0.0%	0.000	0.0%	0.000	100.0%	10.614	0.478	10.136	95.5%	N/A	N/A

Inter-examiner agreement

Principal examiner, March 2017

Sheep	Graft	Site	Whole graft	Total (mm2)	Graft (mm2)	Graft (%)	New Bone (mm2)	New bone (%)	CT (mm2)	CT (%)
409	BioOss	RA3	17.501	3.005	0.634	21.1%	0.000	0.0%	2.371	78.9%
409	ConeOss	RP4	29.021	7.166	3.060	42.7%	0.830	11.6%	3.276	45.7%
414	ConeOss	RP6	43.78	8.160	2.158	26.4%	0.000	0.0%	6.002	73.6%
414	BioOss	RA3	38.694	4.610	0.540	11.7%	0.041	0.9%	4.029	87.4%
416	BioOss	RA3	0.000	0.000	0.000	0.0%	0.000	0.0%	0.000	0.0%
416	ConeOss	LP5	0.000	0.000	0.000	0.0%	0.000	0.0%	0.000	0.0%
418	BioOss	RA9	75.695	4.748	0.267	5.6%	0.080	1.7%	4.401	92.7%
418	ConeOss	RP1	28.45	4.800	0.271	5.6%	0.423	8.8%	4.106	85.5%
420	BioOss	LA3	0.000	0.000	0.000	0.0%	0.000	0.0%	0.000	0.0%
420	ConeOss	LP1	36.551	8.278	2.338	28.24%	0.031	0.37%	5.909	71.38%

Principal examiner, May 2017

Sheep	Graft	Site	Whole graft	Total (mm2)	Graft (mm2)	Graft (%)	New Bone (mm2)	New bone (%)	CT (mm2)	CT (%)
409	BioOss	RA3	17.542	3.074	0.567	18.4%	0.000	0.0%	2.507	81.6%
409	ConeOss	RP4	28.461	6.966	2.972	42.7%	1.001	14.4%	2.993	43.0%
414	ConeOss	RP6	43.692	8.169	2.100	25.7%	0.000	0.0%	6.069	74.3%
414	BioOss	RA3	38.724	4.650	0.615	13.2%	0.051	1.1%	3.984	85.7%
416	BioOss	RA3	0.000	0.000	0.000	0.0%	0.000	0.0%	0.000	0.0%
416	ConeOss	LP5	0.000	0.000	0.000	0.0%	0.000	0.0%	0.000	0.0%
418	BioOss	RA9	75.793	4.595	0.255	5.5%	0.074	1.6%	4.266	92.8%
418	ConeOss	RP1	28.52	4.913	0.280	5.7%	0.399	8.1%	4.234	86.2%
420	BioOss	LA3	0.000	0.000	0.000	0.0%	0.000	0.0%	0.000	0.0%
420	ConeOss	LP1	36.71	8.343	2.339	28.04%	0.022	0.26%	5.982	71.70%

Independent examiner

Sheep	Graft	Site	Whole graft	Total (mm2)	Graft (mm2)	Graft (%)	New Bone (mm2)	New bone (%)	CT (mm2)	CT (%)
409	BioOss	RA3	17.555	3.244	0.601	18.5%	0.000	0.0%	2.643	81.5%
409	ConeOss	RP4	25.773	6.808	3.990	58.6%	0.807	11.9%	2.011	29.5%
414	ConeOss	RP6	41.635	8.871	2.550	28.7%	0.000	0.0%	6.321	71.3%
414	BioOss	RA3	36.81	5.711	0.822	14.4%	0.099	1.7%	4.790	83.9%
416	BioOss	RA3	0.000	0.000	0.000	0.0%	0.000	0.0%	0.000	0.0%
416	ConeOss	LP5	0.000	0.000	0.000	0.0%	0.000	0.0%	0.000	0.0%
418	BioOss	RA9	66.896	4.831	0.100	2.1%	0.645	13.4%	4.086	84.6%
418	ConeOss	RP1	27.763	4.307	0.341	7.9%	0.431	10.0%	3.535	82.1%
420	BioOss	LA3	0.000	0.000	0.000	0.0%	0.000	0.0%	0.000	0.0%
420	ConeOss	LP1	36.469	8.047	3.013	37.44%	0.034	0.42%	5.000	62.13%

Appendix V – Radiograph of the resin-embedded specimens

